

# THE EFFECT OF DOOR ANGLE ON FIRE INDUCED FLOW THROUGH A DOORWAY

By

L. R. CLARK

**Supervised by**

**Dr C. M. Fleishmann**

A research project report presented as partial fulfilment of the requirements for the  
degree of Master of Engineering in Fire Engineering

Department of Civil Engineering

University of Canterbury

Christchurch, New Zealand

2002



# **Abstract**

This report investigates the effect of including a partially closed door in a doorway on the fire-induced flow through the doorway.

This was investigated through a series of full-scale fire experiments. These were performed in two rooms that conformed to ISO 9705 standard connected by a single rectangular doorway. A comprehensive series of temperature, gas speed and gas concentration measurements were taken throughout these compartments. In the doorway a door was installed and the effect of placing this door at 20, 30, 40 and 60 degrees was investigated. The compartment was subjected to a series of small-scale steady state fires; the heat release rate of these fires was altered between 60, 120 and 180kW. The configuration of the compartments vent to the atmosphere was also altered.

It was found that the addition of the doorway caused a change to the speed and temperature profile seen across the width of the doorway. The speed profile was seen to decrease across the width of the doorway. The neutral plane height was observed to change across the width of the doorway. The addition of the doorway also impacted on the behaviour of the flame within the compartment. The effect of the doorway on the system was seen to diminish as the door angle was increased.

A significant discrepancy between temperature measurements made by aspirated and bare wire thermocouples was observed. This was particularly true in measurements made in the lower layer of the fire compartment.



# Acknowledgements

A big thank you to the following people who made the last year and this research report possible.

- The New Zealand Fire Service commission both for their support of the program and for the personal funding this year.
- Dr Charley Fleischmann for the support during the project and particularly the time spent at McLeans Island
- Tony Parkes for the time taken away from his own work and studies to help with the experiments at McLeans Island.
- Luke Rutherford and Judith Shulz for the amount of time and effort in the experimental setup
- Andy and Mike for the time and effort put into the program and the help during the year
- The remaining M.E.F.E students for making the year as enjoyable as it was.
- My Family for the support
- Lisa for everything



# Table of Contents

<b>ABSTRACT.....</b>	<b>III</b>
<b>ACKNOWLEDGEMENTS .....</b>	<b>V</b>
<b>TABLE OF CONTENTS .....</b>	<b>VII</b>
<b>LIST OF FIGURES .....</b>	<b>XI</b>
<b>LIST OF TABLES .....</b>	<b>XVII</b>
<b>NOMENCLATURE.....</b>	<b>XIX</b>
<b>1 INTRODUCTION .....</b>	<b>1</b>
1.1    Impetus for Research .....	1
1.2    Research Purpose .....	2
1.3    Outline of Report .....	2
<b>2 FIRE INDUCED VENT FLOWS.....</b>	<b>3</b>
2.1 General Concepts .....	3
2.2 Modelling of flow behaviour .....	4
2.2.1 Ideal behaviour .....	4
2.2.2 The Fire Situation .....	6
2.2.3 Flow Coefficients.....	7
<b>3 EXPERIMENTAL SET UP .....</b>	<b>9</b>
3.1 Site Details .....	9
3.2 Room Construction .....	9
3.3 Fire Details.....	10
3.4 Temperature Measurements.....	12
3.4.1 Barewire Thermocouples .....	12
3.4.2 Aspirated thermocouples .....	15
3.5 Inter-compartment Door .....	15
3.6 Instrumentation in the doorway .....	16
3.6.1 Bi-directional probes.....	16
3.6.2 Bare wire Thermocouples.....	17
3.6.3 Aspirated Thermocouples .....	18
3.6.4 Sample lines .....	18
3.7 Front Opening .....	19

3.7.1 Configuration .....	19
3.7.2 Instrumentation.....	20
3.8 Experiments performed .....	21
<b>4 FULLY OPEN DOOR .....</b>	<b>23</b>
4.1 Introduction .....	23
4.2 Burner in Centre of compartment.....	23
4.2.1 Description of Experiments.....	23
4.2.2 60kW Fire.....	23
4.2.3 120kW Fire.....	25
4.2.4 180 kW Fire.....	27
4.3 Burner on walls of compartment.....	29
4.3.1 Description of experiments .....	29
4.3.2 Burner in corner .....	29
4.3.3 Burner on back wall .....	31
4.4 Mass flow rate calculation.....	33
4.5 Aspirated Thermocouple comparison .....	35
4.6 Discussion .....	35
4.6.1 Speed Profiles.....	35
4.6.2 Effect of Burner location.....	38
4.6.3 Mass flow predictions .....	39
4.6.4 Temperature profiles .....	41
4.6.5 Errors.....	42
<b>5. PARTIALLY CLOSED DOOR.....</b>	<b>45</b>
5.1 Introduction .....	45
5.2 Front Opening Fully Open .....	45
5.2.1 20° Open Door .....	45
5.2.2 30° Open Door .....	47
5.2.3 40° Open Door .....	49
5.2.4 60° Open Door .....	51
5.3 Front opening as door.....	53
5.3.1 20° Open Door .....	53
5.3.2 30° Open Door .....	55
5.3.3 40° Open Door .....	57
5.4 Aspirated Thermocouple comparison .....	59
5.5 Qualitative observations.....	60
5.5.1 Introduction.....	60
5.5.2 Wind blown plume .....	60
5.5.3 Flame behaviour.....	60
5.6 Discussion .....	61
5.6.1 Speed profiles.....	61
5.6.2 Fire plume behaviour .....	61
5.6.3 Temperature Profiles .....	63



5.6.4 Repeatability of results .....	65
5.6.5 Mass flow rate predictions .....	66
5.6.5 Errors in speed measurements .....	67
<b>6 CONCLUSIONS .....</b>	<b>69</b>
<b>7 RECOMMENDATIONS.....</b>	<b>71</b>
<b>REFERENCES.....</b>	<b>73</b>
<b>APPENDIX A.....</b>	<b>75</b>
A.1 Burner in Centre of Compartment .....	75
A.1.1 60kW Fire Size .....	75
A.1.2 120kW Fire Size .....	77
A.1.3 180kW Fire Size .....	78
A.2 Burner on Walls of Compartment.....	80
A.2.1 Burner in Corner .....	80
A.2.2 Burner on Back Wall .....	81
<b>APPENDIX B .....</b>	<b>83</b>
B.1 Front opening fully open.....	83
B.1.1 Door at 20° .....	83
B.1.2 Door at 30° .....	85
B.1.3 Door at 40° .....	86
B.1.4 Door at 60° .....	88
B.2 Front opening as door.....	89
B.2.1 Door at 20° .....	89
B.2.2 Door at 30° .....	91
B.2.3 Door at 40° .....	92



# List of Figures

Figure 2.1 Pressure profile in compartment during initial fire growth.....	3
Figure 2.2 Pressure profile in compartment after initial growth phase .....	4
Figure 2.3 Pressure Differences for Idealised Compartment.....	5
Figure 2.4 Pressure Gradients in Real Compartment .....	6
Figure 3.1 Fire test room dimensions .....	10
Figure 3.2 Burner and Igniter .....	10
Figure 3.3 Burner locations within fire compartment.....	11
Figure 3.4 Thermocouple tree guides .....	13
Figure 3.5 Thermocouple tree locations and designations .....	14
Figure 3.6 Location of door in compartments .....	16
Figure 3.7 Doorway as used in experiments, Bi-directional probes at 100mm from open door edge.....	17
Figure 3.8 Measurement locations within doorway.....	19
Figure 3.9 Variation in front opening configuration.....	20
Figure 4.1 Temperature profile in doorway, burner in centre of compartment, 60kW fire size, front opening and door fully open .....	24
Figure 4.2 Doorway speed profile for outflow section, burner in centre of compartment, 60kW fire size, front opening and door fully open.....	24
Figure 4.3 Doorway speed profile for inflow section, burner in centre of compartment, 60kW fire size, front opening and door fully open.....	25
Figure 4.4 Temperature profile in doorway, burner in centre of compartment, 120kW fire size, front opening and door fully open.....	26
Figure 4.5 Doorway speed profile for outflow section, burner in centre of compartment, 120kW fire size, front opening and door fully open.....	26
Figure 4.6 Doorway speed profile for inflow section, burner in centre of compartment, 120kW fire size, front opening and door fully open.....	27
Figure 4.7 Temperature profile in doorway, burner in centre of compartment, 180kW fire size, front opening and door fully open.....	27
Figure 4.8 Doorway speed profile for outflow section, burner in centre of compartment, 180kW fire size, front opening and door fully open.....	28

Figure 4.9 Doorway speed profile for inflow section, burner in centre of compartment, 180kW fire size, front opening and door fully open .....	29
Figure 4.10 Temperature profile in doorway, burner in corner of compartment, 120kW fire size, front opening and door fully open .....	30
Figure 4.11 Doorway speed profile for outflow section, burner in corner of compartment, 120kW fire size, front opening and door fully open .....	30
Figure 4.12 Doorway speed profile for inflow section, burner in corner of compartment, 120kW fire size, front opening and door fully open .....	31
Figure 4.13 Temperature profile in doorway, burner on back wall of compartment, 120kW fire size, front opening and door fully open .....	32
Figure 4.14 Doorway speed profile for outflow section, burner in corner of compartment, 120kW fire size, front opening and door fully open .....	32
Figure 4.15 Doorway speed profile for inflow section, burner in corner of compartment, 120kW fire size, front opening and door fully open .....	33
Figure 4.16. Pressure distribution across doorway .....	36
Figure 4.17, Pressure differential readings in doorway, 120kW fire size, burner in centre, door and front opening fully open, smoothed data .....	37
Figure 4.18 Effect of temperature distribution on neutral plane prediction .....	39
Figure 4.19 Standard deviation in average pressure differential, outflow section, run 643	
Figure 4.20 Standard deviation in average pressure differential, inflow section, run 6..	44
Figure 5.1 Temperature profile in Doorway, 120kW fire, Burner in centre of compartment, Door at 20°, Front opening fully open .....	45
Figure 5.2 Doorway speed profile for outflow section, 120kW fire, burner in centre, 20° door angle, front opening fully open .....	46
Figure 5.3 Doorway speed profile for inflow section, 120kW fire, burner in centre, 20° door angle, front opening fully open .....	47
Figure 5.4 Temperature profile in Doorway, 120kW fire, Burner in centre of compartment, Door at 30°, Front opening fully open .....	47
Figure 5.5 Doorway speed profile for outflow section, 120kW fire, burner in centre, 30° door angle, front opening fully open .....	48
Figure 5.6 Doorway speed profile for inflow section, 120kW fire, burner in centre, 30° door angle, front opening fully open .....	49
Figure 5.7 Temperature profile in Doorway, 120kW fire, Burner in centre of compartment, Door at 40°, Front opening fully open .....	49

Figure 5.8 Doorway speed profile for outflow section, 120kW fire, burner in centre, 40° door angle, front opening fully open .....	50
Figure 5.9 Doorway speed profile for inflow section, 120kW fire, burner in centre, 40° door angle, front opening fully open .....	51
Figure 5.10 Temperature profile in Doorway, 120kW fire, burner in centre of compartment, door at 40°, front opening fully open .....	51
Figure 5.11 Doorway speed profile for outflow section, 120kW fire, burner in centre, 60° door angle, front opening fully open.....	52
Figure 5.12 Doorway speed profile for inflow section, 120kW fire, burner in centre, 60° door angle, front opening fully open .....	53
Figure 5.13 Temperature profile in doorway, 120kW fire, burner in centre of compartment, door at 20°, front opening as door .....	53
Figure 5.14 Doorway speed profile for outflow section, 120kW fire, burner in centre, 20° door angle, front opening as door .....	54
Figure 5.15 Doorway speed profile for inflow section, 120kW fire, burner in centre, 20° door angle, front opening as door .....	55
Figure 5.16 Temperature profile in doorway, 120kW fire, burner in centre of compartment, door at 30°, front opening as door .....	55
Figure 5.17 Doorway speed profile for outflow section, 120kW fire, burner in centre, 30° door angle, front opening as door .....	56
Figure 5.18 Doorway speed profile for inflow section, 120kW fire, burner in centre, 30° door angle, front opening as door .....	57
Figure 5.19 Temperature profile in doorway, 120kW fire, burner in centre of compartment, door at 40°, front opening as door .....	57
Figure 5.20 Doorway speed profile for outflow section, 120kW fire, burner in centre, 40° door angle, front opening as door .....	58
Figure 5.21 Doorway speed profile for inflow section, 120kW fire, burner in centre, 40° door angle, front opening as door .....	59
Figure 5.22 Direction of flame tilt observed in relation to fire compartment system ....	60
Figure 5.23 Points in compartment for Benoulli's analysis.....	62
Figure A.1 Doorway temperature measurements for duration of experiment, 60kW fire in centre of compartment, fully open door, front opening fully open .....	75

Figure A.2 Doorway pressure differential measurements for duration of experiment, 60kW fire in centre of compartment, fully open door, front opening fully open, 120s smoothed data .....	76
Figure A.3 Doorway temperature measurements for duration of experiment, 120kW fire in centre of compartment, fully open door, front opening fully open.....	77
Figure A.4 Doorway pressure differential measurements for duration of experiment, 120kW fire in centre of compartment, fully open door, front opening fully open, 120s smoothed data .....	77
Figure A.5 Doorway temperature measurements for duration of experiment, 180kW fire in centre of compartment, fully open door, front opening fully open.....	78
Figure A.6 Doorway pressure differential measurements for duration of experiment, 180kW fire in centre of compartment, fully open door, front opening fully open, 120s smoothed data .....	79
Figure A.7 Doorway temperature measurements for duration of experiment, 120kW fire in corner of compartment, fully open door, front opening fully open .....	80
Figure A.8 Doorway pressure differential measurements for duration of experiment, 120kW fire in corner of compartment, fully open door, front opening fully open, 120s smoothed data .....	80
Figure A.9 Doorway temperature measurements for duration of experiment, 120kW fire on back wall, fully open door, front opening fully open.....	81
Figure A.10 Doorway pressure differential measurements for duration of experiment, 120kW fire on back wall, fully open door, front opening fully open, 120s smoothed data .....	82
Figure B.1 Doorway temperature measurements for duration of experiment, 120kW fire in centre of compartment, door at 20°, front opening fully open.....	83
Figure B.2 Doorway pressure differential measurements for duration of experiment, 120kW fire in centre of compartment, door 20° open, front opening fully open, 120s smoothed data .....	84
Figure B.3 Doorway temperature measurements for duration of experiment, 120kW fire in centre of compartment, door at 30°, front opening fully open.....	85
Figure B.4 Doorway pressure differential measurements for duration of experiment, 120kW fire in centre of compartment, door 30° open, front opening fully open, 120s smoothed data .....	85

Figure B.5 Doorway temperature measurements for duration of experiment, 120kW fire in centre of compartment, door at 40°, front opening fully open .....	86
Figure B.6 Doorway pressure differential measurements for duration of experiment, 120kW fire in centre of compartment, door 40° open, front opening fully open, 120s smoothed data.....	87
Figure B.7 Doorway temperature measurements for duration of experiment, 120kW fire in centre of compartment, door at 60°, front opening fully open .....	88
Figure B.8 Doorway pressure differential measurements for duration of experiment, 120kW fire in centre of compartment, door 60° open, front opening fully open, 120s smoothed data.....	88
Figure B.9 Doorway temperature measurements for duration of experiment, 120kW fire in centre of compartment, door at 20°, front opening as door .....	89
Figure B.10 Doorway pressure differential measurements for duration of experiment, 120kW fire in centre of compartment, door 20° open, front opening as door, 120s smoothed data .....	90
Figure B.11 Doorway temperature measurements for duration of experiment, 120kW fire in centre of compartment, door at 30°, front opening as door .....	91
Figure B.12 Doorway pressure differential measurements for duration of experiment, 120kW fire in centre of compartment, door 30° open, front opening as door, 120s smoothed data .....	91
Figure B.13 Doorway temperature measurements for duration of experiment, 120kW fire in centre of compartment, door at 40°, front opening as door .....	92
Figure B.14 Doorway pressure differential measurements for duration of experiment, 120kW fire in centre of compartment, door 40° open, front opening as door, 120s smoothed data .....	93





# List of Tables

Table 2.1 Comparison of published flow coefficients.....	7
Table 3.1 Thermocouple Tree Locations.....	12
Table 3.2 Thermocouple heights within thermocouple trees.....	13
Table 3.3 Location of aspirated thermocouples.....	15
Table 3.4 Vertical error in bi-directional probe placement in doorway. ....	17
Table 3.5 Location of bi-directional probes in front opening.....	21
Table 3.7 Summary of experiments performed. ....	22
Table 4.1 Experimental mass flow predictions and neutral plane heights.....	34
Table 4.2 Comparison of temperature prediction for aspirated and bare wire thermocouples, 120kW fire size, burner in centre.....	35
Table 4.3 Comparison of mass flow rate predictions with other studies.....	40
Table 5.1 Comparison of temperature measurements for aspirated and bare wire thermocouples for run 1.....	59
Table 5.2 Comparison of maximum upper layer temperatures for fully open front opening experiments.....	64
Table A.1 Comparison of temperature measurements for aspirated and bare wire thermocouples, 60kW fire in centre of compartment, fully open door, front opening fully open.....	76
Table A.2 Comparison of temperature measurements for aspirated and bare wire thermocouples, 120kW fire in centre of compartment, fully open door, front opening fully open.....	78
Table A.3 Comparison of temperature measurements for aspirated and bare wire thermocouples, 180kW fire in centre of compartment, fully open door, front opening fully open.....	79
Table A.4 Comparison of temperature measurements for aspirated and bare wire thermocouples, 120kW fire in corner of compartment, fully open door, front opening fully open.....	81
Table A.5 Comparison of temperature measurements for aspirated and bare wire thermocouples, 120kW fire on back wall, fully open door, front opening fully open .....	82

Table B.1 Comparison of temperature measurements for aspirated and bare wire thermocouples, 120kW fire in centre of compartment, door 20° open, front opening fully open.....	84
Table B.2 Comparison of temperature measurements for aspirated and bare wire thermocouples, 120kW fire in centre of compartment, door 30° open, front opening fully open.....	86
Table B.3 Comparison of temperature measurements for aspirated and bare wire thermocouples, 120kW fire in centre of compartment, door 40° open, front opening fully open.....	87
Table B.4 Comparison of temperature measurements for aspirated and bare wire thermocouples, 120kW fire in centre of compartment, door 60° open, front opening fully open.....	89
Table B.5 Comparison of temperature measurements for aspirated and bare wire thermocouples, 120kW fire in centre of compartment, door 20° open, front opening as door .....	90
Table B.6 Comparison of temperature measurements for aspirated and bare wire thermocouples, 120kW fire in centre of compartment, door 30° open, front opening as door .....	92
Table B.7 Comparison of temperature measurements for aspirated and bare wire thermocouples, 120kW fire in centre of compartment, door 40° open, front opening as door .....	93

# Nomenclature

$\theta$	Door angle.	( $^{\circ}$ )
$\rho$	Ambient Density	( $\text{kg/m}^3$ )
$a$	Door width	(m)
$B$	Door height	(m)
$C$	Flow coefficient	(-)
$H_L$	Height of upper layer above floor of compartment	(m)
$H_N$	Height of neutral plane above floor in compartment	(m)
$m_{in}$	Mass flow rate of air entering compartment	( $\text{kg/s}$ )
$m_{out}$	Mass flow rate of air leaving compartment	( $\text{kg/s}$ )
$m_{fuel}$	Mass flow rate of fuel burnt in the compartment	( $\text{kg/s}$ )
$p$	ambient pressure	(Pa)
$\Delta p$	Pressure Differential	(Pa)
$u$	speed	( $\text{m/s}$ )
$z$	Height above floor	(m)



# **1 Introduction**

## **1.1 Impetus for Research**

The movement of smoke through a building is one of the major concerns in the provision of life safety to occupants. It is acknowledged that the smoke represents the most significant hazard to the life safety of occupants (Hall 2000). It is therefore necessary for a clear understanding of the dynamics of smoke movement.

One of the critical areas in smoke movement is the flow of smoke through vents in the system. If we do not adequately understand this behaviour then we cannot adequately understand the movement of smoke through the system. One of the major tools utilised for this modelling is the zone model. The reason for this is also the most significant drawback, the simplicity of implementing a model. In order to streamline the calculation time required these models rely on calculation of fire conditions through empirical calculations. This method is fine for the modelling of simple structures or scenarios. As these are close to the scale of the fire experiments that the correlations are derived from. However this represents a limited number of scenarios.

It is common in the use of these models that the user must adapt their scenario to fit the limitations of the model being used. This can lead to results that no longer represent the system in question. This also requires a high degree of knowledge by the user on fire situations and the limitations of these zone models. This is often not the case.

It is therefore beneficial to produce zone models with as much flexibility in model parameters as possible. This requires experiments to be performed to investigate the effect of changing as many parameters within a fire situation as possible. This is the basis for this research report. The field of fire-induced flows has been covered in detail with investigations looking at the effect of changing the size, shape and positioning of the doorway. However, previous research in this field has focused on fully open vents only. The effect of the addition of a door to this vent has been largely overlooked.

This has meant that the modelling of a door in a doorway has been restricted to either closed or fully open, this does not represent the full range of scenarios possible. For

example if a scenario required the modelling of a doorway that was chocked half open this would be unable to be adequately modelled in a zone model.

The use of CFD modelling which predicts fire behaviour from first principles will eliminate some of these problems, as the scope for modelling is much broader. However at the present time the required computer power to model these scenarios is a major limitation to their use.

## **1.2 Research Purpose**

The purpose of this research project was to investigate the effect of adding a door to the fire induced flow through a vent. This was investigated through a series of full-scale fire tests. The primary variable that was altered was the angle of the door leaf relative to the system.

## **1.3 Outline of Report**

The second chapter of this report provides a brief introduction to fire induced flows, the mechanisms within a fire that causes them, and how they are modelled in fire situations.

The third chapter of this report provides a full description of the test facility that was used to perform the full-scale fire tests. This includes a description of the instrumentation present in the compartments and the experiments performed.

The fourth chapter describes the results obtained when no door is present in the system. This section acts as a benchmark to see whether the results obtained from these experiments are consistent with other work performed in the field.

The fifth chapter of the report describes the results obtained when a door is added to the system and the deviation from the behaviour observed in the previous sections.

The final two chapters present the conclusions that can be drawn from this series of experiments and the recommendations for further research in this field.

## 2 Fire Induced Vent flows

### 2.1 General Concepts

The motion of fluids is governed by pressure differences. Any fluid will move from a place of high pressure to that of low pressure. This is the governing factor for fire induced flows in a compartment. The energy released by the fire causes pressure gradients to be formed both within the compartment and between the compartment and the ambient surroundings. This leads to the flow of gases within the fire system.

This motion can be describe in two phases. The first phase occurs after the initial ignition of the fire. The energy released by the fire causes a heating of the air within the compartment. This causes an expansion of the air that leads to an increase in pressure above ambient at all points within the compartment. This results in a net outflow of gas from the compartment at all heights. This is illustrated in figure 2.1 below.

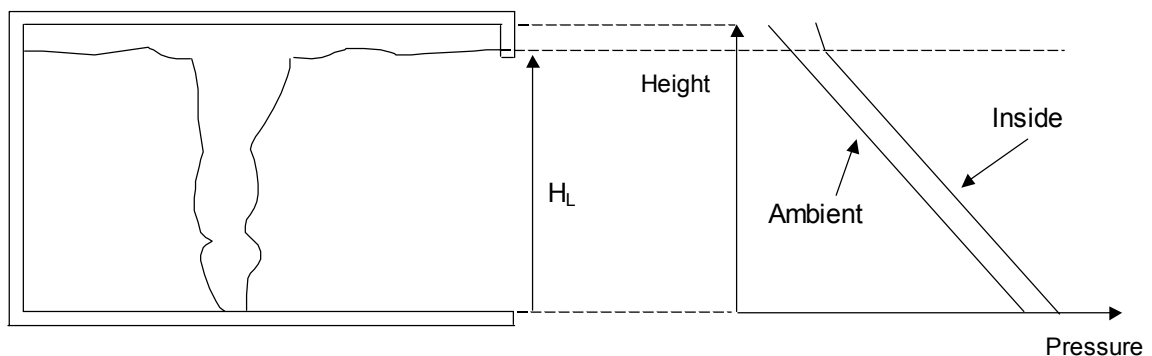


Figure 2.1 Pressure profile in compartment during initial fire growth

The second phase of the vent flow behaviour occurs when the hot upper layer within the compartment falls below the height of the opening. At this stage some of the gases in the hot layer will flow out through the vent. The flow of these hot gases out of the compartment soon exceeds the increase in volume due to expansion. This results in a negative pressure relative to ambient in the lower layer of the compartment. This results in air being pulled into room from the ambient surroundings. This is illustrated in Figure 2.2 below.

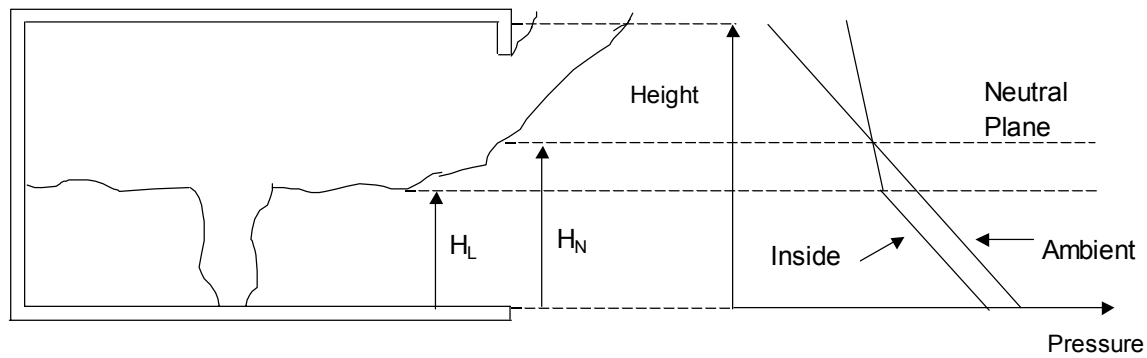


Figure 2.2 Pressure profile in compartment after initial growth phase

As a result of this there is two distinct gas motions in the system. Hot gas from the upper layer in the fire compartment is expelled from the top of the vent and cool air is pulled into the compartment through the bottom of the vent. At a height in the doorway there will be no net pressure difference between the compartment and the ambient surroundings. At this point there is no driving force for motion and there will be no resultant air movement. This area is called the neutral plane and represents the boundary between the two gas flows. This second phase of behaviour holds for fires where two distinct layers are present within the compartment.

It is important to note that there is a relationship between the inlet and outlet flow from the compartment. This can be expressed as:

$$\dot{m}_{out} = \dot{m}_{in} + \dot{m}_{fuel} \quad (2.1)$$

This result is obtainable by considering the compartment as a closed system. No mass can be created or lost in the system; therefore the total mass entering the compartment must equal the total mass leaving the compartment.

## 2.2 Modelling of flow behaviour

### 2.2.1 Ideal behaviour

A relationship for flow through a doorway can be obtained by considering Bernoulli's equation. First consider the situation where a uniform pressure gradient acts across a rectangular doorway. If we consider two points at identical heights the first inside the



doorway and the second in the doorway plane. This situation is illustrated in Figure 2.3 below.

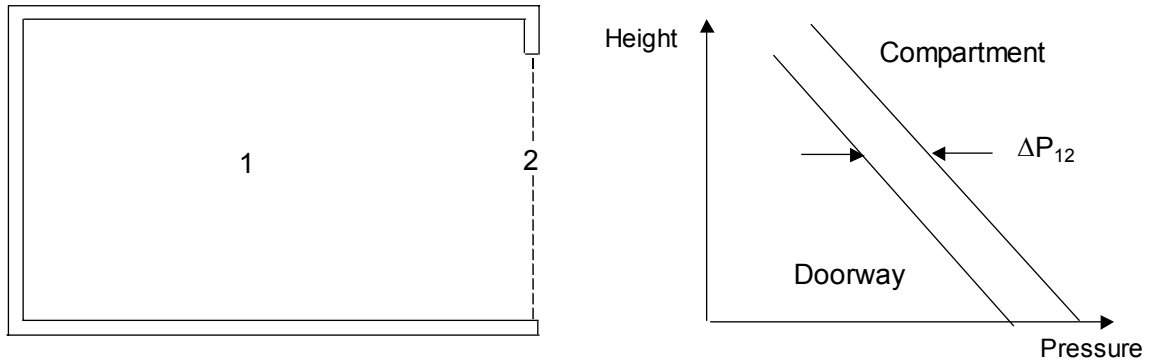


Figure 2.3 Pressure Differences for Idealised Compartment

Bernoulli's equation states:

$$p_1 + \frac{1}{2} \rho_1 u_1^2 + \rho_1 g h_1 = p_2 + \frac{1}{2} \rho_2 u_2^2 + \rho_2 g h_2 \quad (2.2)$$

If we assume that point 1 is at rest and that the two points are at the same height and temperature then this simplifies to:

$$u_2 = \sqrt{\frac{2(p_1 - p_2)}{\rho_2}} \quad (2.3)$$

$$\text{or} \quad \rho_2 u_2 = \sqrt{2 \rho_2 \Delta p_{12}} \quad (2.4)$$

For a plane rectangular opening this flow should be consistent at all widths, and the pressure difference is not a function of height. Therefore the mass flow rate of gas through the compartment can be described as:

$$\dot{m} = CA \sqrt{2 \rho \Delta p} \quad (2.5)$$

Where A is the area of the opening and C is a flow coefficient. The flow coefficient is used to correct discrepancies caused by taking this hydraulic approach for calculating the mass flow rate.

## 2.2.2 The Fire Situation

There are some important differences between the idealised case presented above and the case present in fire situations.

- There are two flows present, an inflow below the neutral plane and an outflow above the neutral plane.
- The pressure gradient is not constant and is a function of the height in the doorway.
- The temperature is not constant and is a function of the height in the doorway.

This situation is shown in figure 2.4 below.

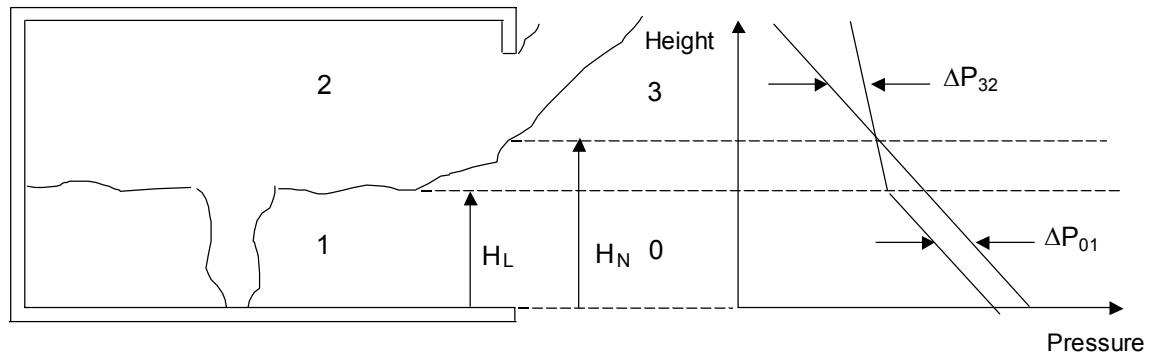


Figure 2.4 Pressure Gradients in Real Compartment

Therefore, a simple solution is not possible in fire situations and equation 4 must be modified and integrated above and below the neutral plane. The resultant mass flow expressions are:

For Outflow

$$\dot{m}_{out} = aC \int_{H_N}^B [2\rho_2(z)\Delta p_{32}(z)]dz \quad (2.6)$$

For Inflow

$$\dot{m}_{in} = aC \int_0^{H_N} [2\rho_0(z)\Delta p_{01}(z)]dz \quad (2.7)$$

Where  $a$  is the width of the doorway and  $B$  is the total height of the doorway.

Many researchers have proposed methods for dealing with this integral. Emmons (1995) suggests four approaches depending on the type of measurements taken in the experiments and the level of accuracy required. The most common approach is to express the pressure and density as a function of temperature and reduce the integral to only one variable. A variety of correlations are available for this case for example those presented by Kawagoe (1958) and Rockett (1976).

### 2.2.3 Flow Coefficients

The value chosen for the flow coefficient can also be critical in fire situations. For this reason it has been investigated by a number of sources. A summary of some of these results is shown in table 2.1 below.

Table 2.1 Comparison of published flow coefficients

<i>Inflow Coefficient</i>	<i>Outflow Coefficient</i>	<i>Determination Method</i>	<i>Author</i>
0.7	0.7	Pipe Flow Technology	Kawagoe (1958)
0.68	0.68	Kerosene/ Water Model	Prahl and Emmons (1975)
0.68	0.73	Full Scale Fire Experiments	Steckler et al (1984)
0.68	0.68	Full Scale Fire Experiments	Nakaya et al (1986)

It is generally accepted to use a coefficient value of 0.68 for both inflow and outflow configurations in fire situations.



## **3 Experimental Set Up**

This section represents a précis view of the equipment and facilities used for the experiments performed. A more comprehensive description is provide in the report by Luke Rutherford (2002).

### **3.1 Site Details**

The experiments were performed at the Universities facility in McLeans Island. This facility consists of two rooms built to comply to the ISO-9750 standard. These rooms are joined by the means of a single doorway. The rooms are contained in a large building that prevents a negative interaction with ambient conditions such as wind and rain. The combustion gases are vented to the atmosphere through an open flue, without forced expulsion.

### **3.2 Room Construction**

The rooms had floor dimensions of 2.4m x 3.6m and were 2.4m high. Between the rooms there was a doorway measuring 0.8m wide by 2.01m high. The dimensions of the rooms are shown in Figure 2.1 below.

The rooms were constructed of 12.5mm Gib Fyrelite® branded fire rated gypsum plasterboard. This was attached to steel studs. In order to protect the gypsium from thermal degradation all exposed surfaces were insulated using Triton Kaowool ceramic fibreboard. This insulation has a maximum service temperature of 1260°C.

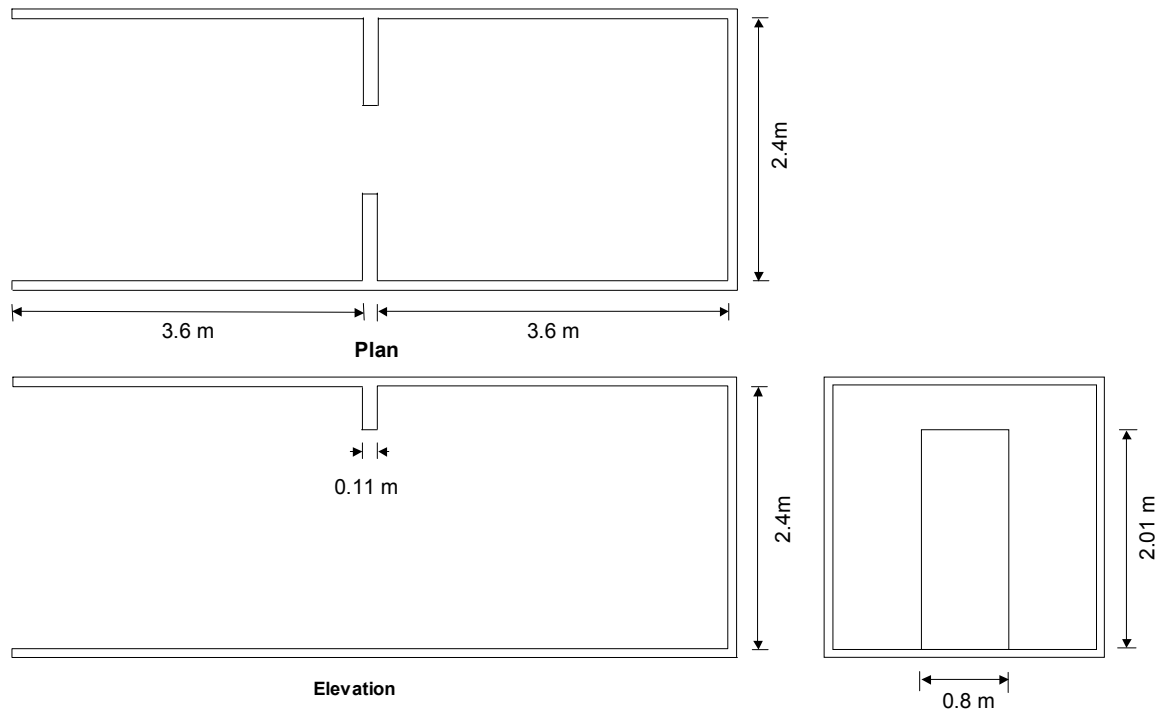


Figure 3.1 Fire test room dimensions

### 3.3 Fire Details

The fire source for these experiments was a single gas burner with LPG as the fuel source. The burner had dimensions of 0.3m x 0.3m and the top surface was 0.3m above the floor surface. The burner and igniter is shown in figure 3.2 Below.



Figure 3.2 Burner and Igniter

The fire size was controlled through the use of a mass flow controller. The fuel was obtained from cylinders on site whose mass was measured at the beginning and conclusion of each run as a check on the fire size.

The fire was ignited through the use of a pilot flame that fired across the burner surface that was ignited by an electric arc. The pilot flame and arc were immediately switched off once full ignition of the burner had occurred.

To ensure that ignition occurred over the full surface of the burner the gas was forced to diffuse through a layer of small stones of 200mm total depth. This ensured a buoyancy driven flame rather than a diffusion flame.

Three burner positions were used during the tests. The burner was positioned in the centre of the fire compartment, flush on the centre of the back wall of the fire compartment and in the back right hand corner of the fire compartment. These locations are shown in Figure 3.3 below.

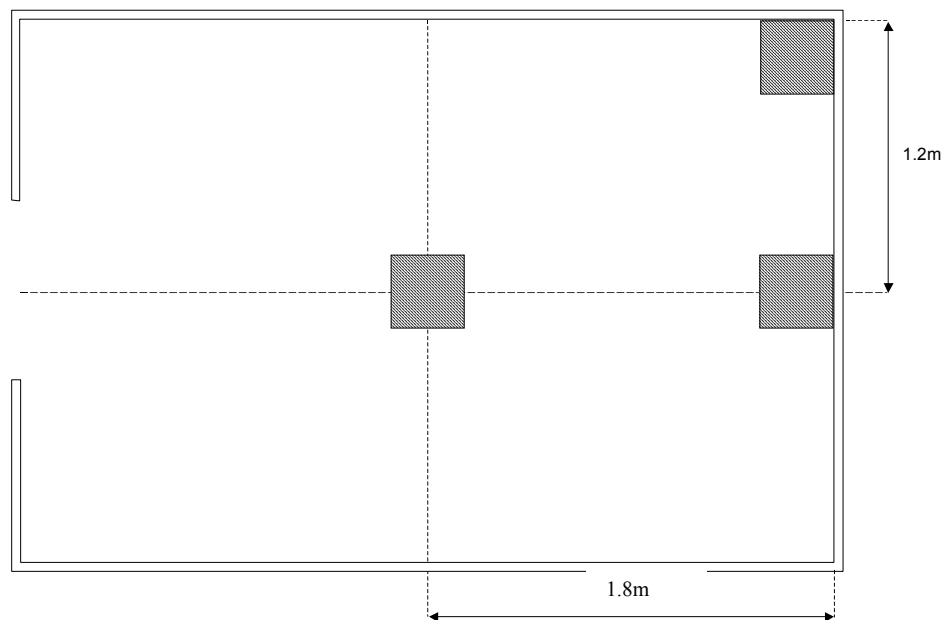


Figure 3.3 Burner locations within fire compartment

### 3.4 Temperature Measurements

Two types of temperature measurement were utilised in the compartment. The majority of the temperature measurements were made using bare wire thermocouples. Aspirated Thermocouples were placed in some locations within the compartment, to check the magnitude of the error in temperature predictions due to the effects of radiation.

#### 3.4.1 Barewire Thermocouples

All the bare wire thermocouples used in the compartment were standard glass insulated Type K bare bead 24 gauge.

#### Room Trees

The majority of the temperature measurements were made on a series of thermocouple trees located on the centre line of each compartment. Their locations and designations are summarised in table 3.1 below.

Table 3.1 Thermocouple Tree Locations	
<i>Tree Designation</i>	<i>Location</i>
1	100mm from rear wall, fire compartment
2	900mm from rear wall, fire compartment
3	1800mm from rear wall, fire compartment
4	2700mm from rear wall, fire compartment
5	900mm from rear wall, adjacent compartment
6	1800mm from rear wall, adjacent compartment
7	2700mm from rear wall, adjacent compartment

There were 16 thermocouples within each thermocouple tree. Their heights are summarised in Table 3.2 below.



Table 3.2 Thermocouple heights within thermocouple trees

Thermocouple Designation	1	2	3	4	5	6	7	8
Height below Ceiling (mm)	0	50	100	200	300	400	600	800
Thermocouple Designation	9	10	11	12	13	14	15	16
Height below Ceiling (mm)	1000	1200	1400	1600	1800	2000	2200	2400

Thermocouples 1 and 16 were attached to the back of a metal plate. These thermocouples were used as an indication of the surface temperature of the compartment in these locations.

The room thermocouples were positioned by the use of guides. These consisted of a central stainless steel tube that was 20mm in diameter. This was attached to the ceiling of the compartment and acted as conduit for the thermocouple wire. From this central tube 14 separate “branches” were constructed. These were constructed of 2mm stainless steel tubing and were welded to the central tube. Each branch was bent 90° away from the central tube at the required height for the thermocouple. The thermocouples were threaded through these branches so that the bead was situated at least 10mm from end of the tube. This arrangement is shown in Figure 3.4 below.



Figure 3.4 Thermocouple tree guides

The purpose of this arrangement was two fold; the first was that it allowed the thermocouples to be rigidly set in place so that their position in the compartment could be accurately reported. The second was that the conduit provided protection for the majority of the thermocouple, this that meant that it was not necessary to use high temperature thermocouple wire. The position of the thermocouples within the compartment would be accurate to  $\pm 5\text{mm}$ .

### Corner Trees

In each of the rooms a thermocouple tree was placed in one of the rear corners in the room. In the fire compartment the thermocouples were located 110mm off the sidewall and 100mm from the rear wall. In the adjacent compartment the thermocouples were located 100mm from the sidewall and 100mm from the rear wall. In both cases the thermocouples were spaced vertically at 150mm intervals from 100mm below the ceiling to 2350mm below the ceiling.

The corner tree thermocouples were introduced into the compartment through the side wall. They were held in place by a stainless steel bracket that was fastened to the exterior of the compartment. The thermocouple bead extended 10mm beyond the bracket.

### Door and front Opening Thermocouple Trees

Two additional trees were located in the doorway and front opening. The positions of these thermocouples are discussed in sections 3.6.2 and 3.7.1. The location of all the thermocouple trees is shown in figure 3.5 below.

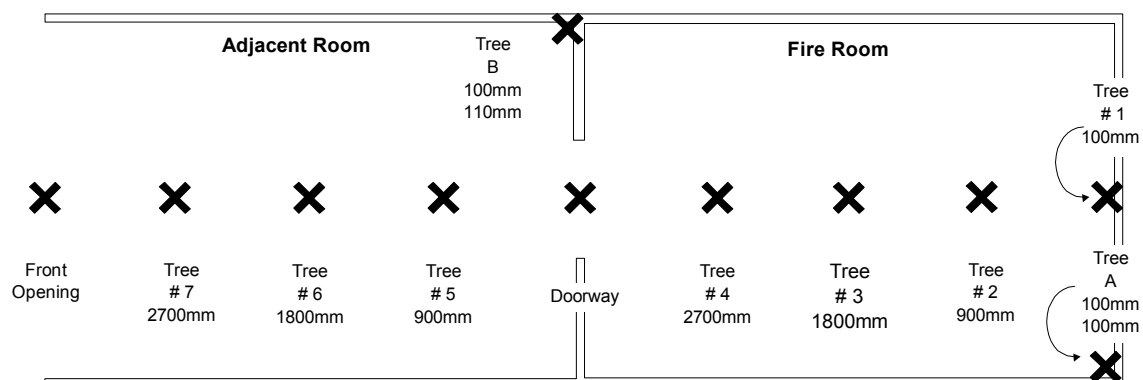


Figure 3.5 Thermocouple tree locations and designations

### 3.4.2 Aspirated thermocouples

Twelve Aspirated thermocouples were placed within the compartment. Six were placed within the doorway; their locations are discussed in detail in section 3.6.3. The remaining six aspirated thermocouples were placed within the fire compartment. They were attached to field trees in the room at the same height as an existing bare wire thermocouple. Their locations are summarised in table 3.3 below.

Table 3.3 Location of aspirated thermocouples

<i>Aspirated Thermocouple designation</i>	<i>Location</i>
1	Field Tree #2, 200mm below ceiling
2	Field Tree #2, 1400mm below ceiling
3	Field Tree #2, 2000mm below ceiling
4	Field Tree #4, 200mm below ceiling
5	Field Tree #4, 1400mm below ceiling
6	Field Tree #4, 2000mm below ceiling

### 3.5 Inter-compartment Door

The door between the two rooms was constructed using one sheet of 12.5mm fire rated gypsum plasterboard. The door measured 2.0m high by 0.8m wide. To protect the gypsum from thermal degradation the door was completely covered in ceramic fibreboard.

Due to the instrumentation in the doorway the door was required to be hinged on the front wall of the fire compartment rather than within the doorframe. The door opened into the fire compartment. The door angle ( $\theta$ ) was set by the use of chocks, so that there was no free movement possible for the door. The positioning of the door is shown in Figure 3.6 below.

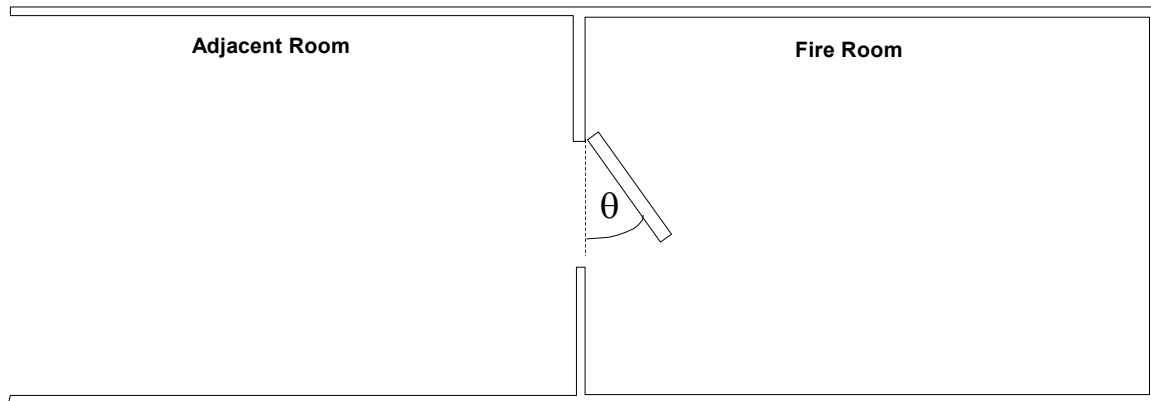


Figure 3.6 Location of door in compartments

During the experiments four door angles were investigated; 20, 30, 40 and 60 degrees..

### 3.6 Instrumentation in the doorway

#### 3.6.1 Bi-directional probes

The speed of the gases entering and leaving the fire compartment was measured by the use of bi-directional probes. There were eight bi-directional probes positioned vertically throughout the doorway.

In order to increase the resolution of measurements for calculation purposes these bi-directional probes were moved across the width of the doorway. This was however limited to a total travel distance of 500mm of the 800mm width of the doorway by the length of the bidirectional probes. For this reason measurements were taken at 100mm increments from 100mm from the open door edge. In total this gives a matrix of 40 velocity measurements across the doorway. The doorway with the bi-directional probes in the first position is shown in figure 3.7 below.



Figure 3.7 Doorway as used in experiments, Bi-directional probes at 100mm from open door edge

The act of sliding the bi-directional probes prevented their height from being rigidly controlled. Therefore there was a slight discrepancy in the measurement height as the probes were moved across the width of the door. This is summarised in table 3.3 below.

Table 3.4 Vertical error in bi-directional probe placement in doorway.

<i>Probe No</i>	<i>Minimum Height below Soffit (m)</i>	<i>Maximum Height below Soffit (m)</i>
1	0.105	0.120
2	0.350	0.360
3	0.605	0.615
4	0.850	0.855
5	1.100	1.110
6	1.365	1.385
7	1.610	1.615
8	1.860	1.870

### 3.6.2 Bare wire Thermocouples

One bare wire thermocouple was attached to each of the bidirectional probes used within the doorway. These were attached 50mm closer to the open edge of the doorway

than the centre of the probe head. This offset was to prevent interference of the measurements taken by either device due to the presence of the other device. Care was taken so that the bead of the thermocouple was not in contact with the bi-directional probe.

### **3.6.3 Aspirated Thermocouples**

Six aspirated Thermocouples were placed throughout the doorway to investigate the likely magnitude of the error in the use of bare wire thermocouples within the doorway. These were positioned 150mm from the closed door edge, and at 250mm intervals from 150mm below the soffit, with measurements omitted at 900mm and 1150mm below the soffit.

### **3.6.4 Sample lines**

Eight sample lines were placed in the doorway. They were located 100mm from the closed door edge. They were positioned vertically at 250mm intervals starting at 150mm from the soffit. A complete summary of the position of all measurements within the doorway is shown in figure 3.8 below.

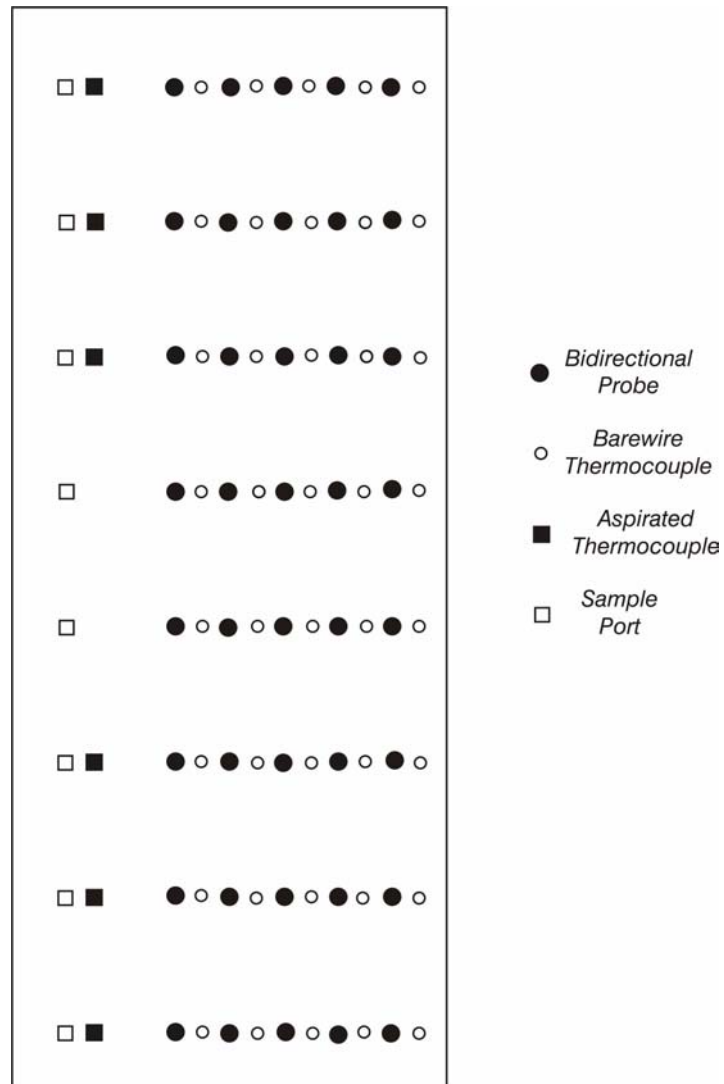


Figure 3.8 Measurement locations within doorway.

## 3.7 Front Opening

### 3.7.1 Configuration

Three configurations were used in the front opening for the experiments. These were the front opening being fully open, a soffit over the full width of the opening and a second doorway being installed in the front opening. The dimensions of these scenarios are summarised in Figure 3.9 below.

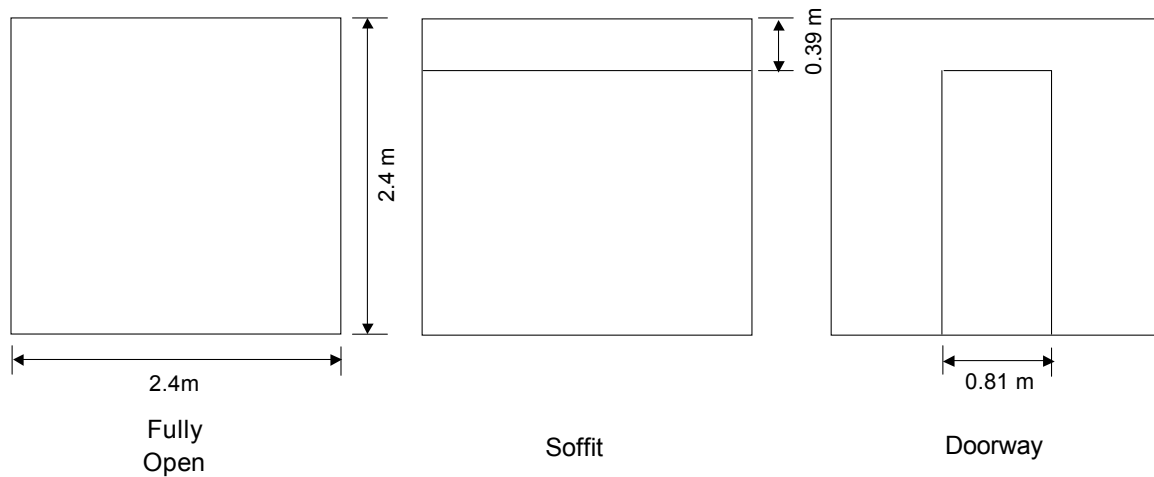


Figure 3.9 Variation in front opening configuration.

### 3.7.2 Instrumentation

The instrumentation in the front opening was similar to that in the doorway between compartments. There was a vertical array of bi-directional probes that measured the pressure differential across the doorway, attached to these were bare wire thermocouples that were attached 50mm away from the centre of the measurement head.

These probes could be moved across the opening in a similar manner to the probes that were placed in the doorway. However they were only moved in the experiments where the front opening was configured as a doorway. For all the other experiments the probes were stationary in the centre of the opening. When the probes were moved readings, were recorded at 100mm intervals from 100 to 500mm across the width of the doorway.

The heights of the bi-directional probes is summarised in table 3.5 below. It should be noted that in the case where the probes were moved that the range of heights over the probes path is stated rather than an exact height.



Table 3.5 Location of bi-directional probes in front opening

<i>Front Opening Configuration</i>	<i>Fully Open</i>	<i>Soffit</i>	<i>Doorway</i>	
<i>Probe No.</i>	<i>Height below Ceiling (m)</i>	<i>Height below Soffit (m)</i>	<i>Minimum Height below Soffit (m)</i>	<i>Maximum Height below Soffit (m)</i>
9	0.250	0.075	0.075	0.080
10	0.475	0.325	0.325	0.330
11	0.735	0.585	0.580	0.590
12	0.980	0.830	0.830	0.830
13	1.235	1.085	1.080	1.090
14	1.490	1.340	1.340	1.350
15	1.761	1.611	1.600	1.620
16	2.000	1.850	1.840	1.855

Four sample ports were also placed in the front opening when it was configured as a doorway. These were located 100mm from the edge of the door at heights of 0.075, 0.325, 0.585 and 0.830m below the soffit.

### 3.8 Experiments performed

Table 3.7 below provides a full summary of all the experiments performed at McLeans Island during the testing period.

Table 3.7 Summary of experiments performed.

<i>Test</i>	<i>Fire Size (kW)</i>	<i>Burner Location</i>	<i>Door Orientation</i>	<i>Front Opening Configuration</i>
1	120	Centre	20°	Open
2	120	Centre	60°	Open
3	120	Centre	40°	Open
4	120	Centre	30°	Open
5	120	Centre	Open	Open
6	60	Centre	Open	Open
7	180	Centre	Open	Open
8	60	Corner	Open	Open
9	120	Corner	Open	Open
10	180	Corner	Open	Open
11	60	Wall	Open	Open
12	120	Wall	Open	Open
13	180	Wall	Open	Open
14	60	Centre	Open	Soffit
15	120	Centre	Open	Soffit
16	180	Centre	Open	Soffit
17	60	Centre	Open	Door
18	120	Centre	Open	Door
19	180	Centre	Open	Door
20	120	Centre	40°	Door
21	120	Centre	30°	Door
22	120	Centre	20°	Door

## **4 Fully Open Door**

### **4.1 Introduction**

The purpose of this section is to present the results obtained from the series of experiments performed without the door being in position. This will give a frame of reference for the data involving the door and allow comparisons with other experiments performed. This section will cover experiments numbers 5,6,7,9 and 12 as specified in the preceding chapter. The data presented in this section represents average data as taken during the experiments, the raw data from the experiments can be found in the Appendix A of this report.

### **4.2 Burner in Centre of compartment**

#### **4.2.1 Description of Experiments**

This section will look at three experiments all performed with an identical room configuration. The burner was positioned in the centre of the room, the front opening was fully open and the doorway between the compartments was fully open. The only variable between the three experiments was the heat release rate. Three heat release rates were used 60kW, 120kW and 180kW.

#### **4.2.2 60kW Fire**

The temperature distribution within the doorway is shown in figure 4.1 below. It can be seen that there is a clear transition between the hot and cold zones in the doorway. In the lower layer or inflow zone the temperatures are near constant, whereas for the outflow zone they increase with increasing height in the compartment. There seems to be close agreement in the temperature profile across the doorway, with the exception of the measurements that took place at 0.05 from the open door edge.

The speed profile for outflow section of the doorway is shown in figure 4.2 below. It can be seen that at all heights, the speed is at a maximum at the edge of the doorway, and is at a minimum in the centre of the doorway.

The speed profile for the inflow section of the doorway is shown in figure 4.3 below.

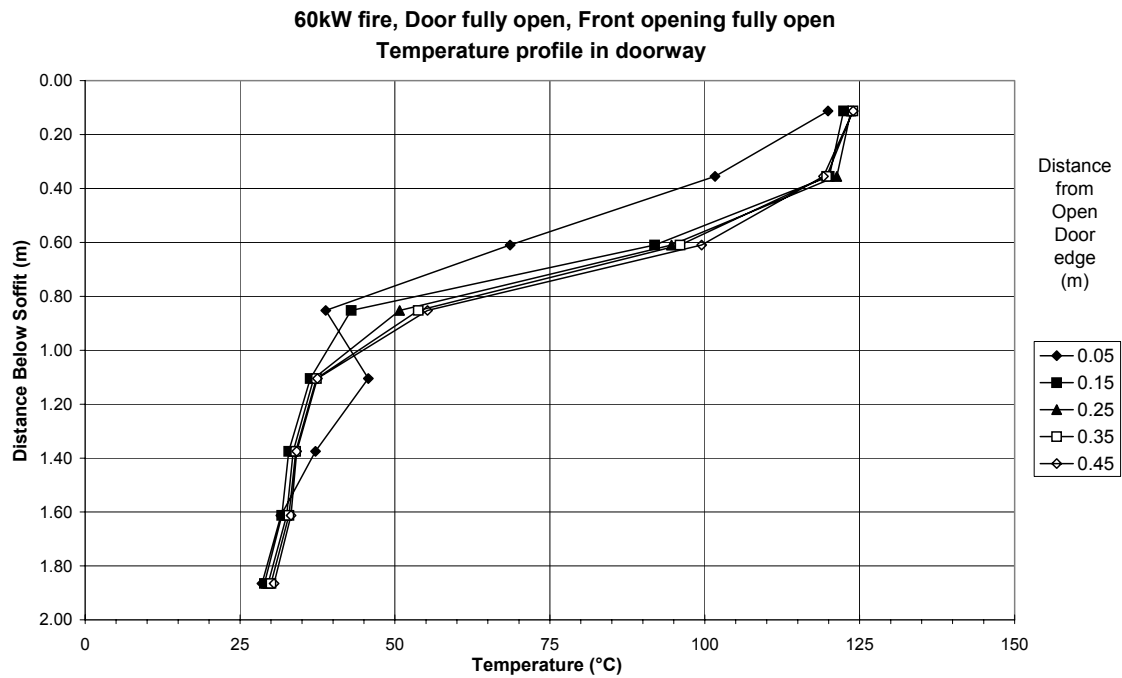


Figure 4.1 Temperature profile in doorway, burner in centre of compartment, 60kW fire size, front opening and door fully open

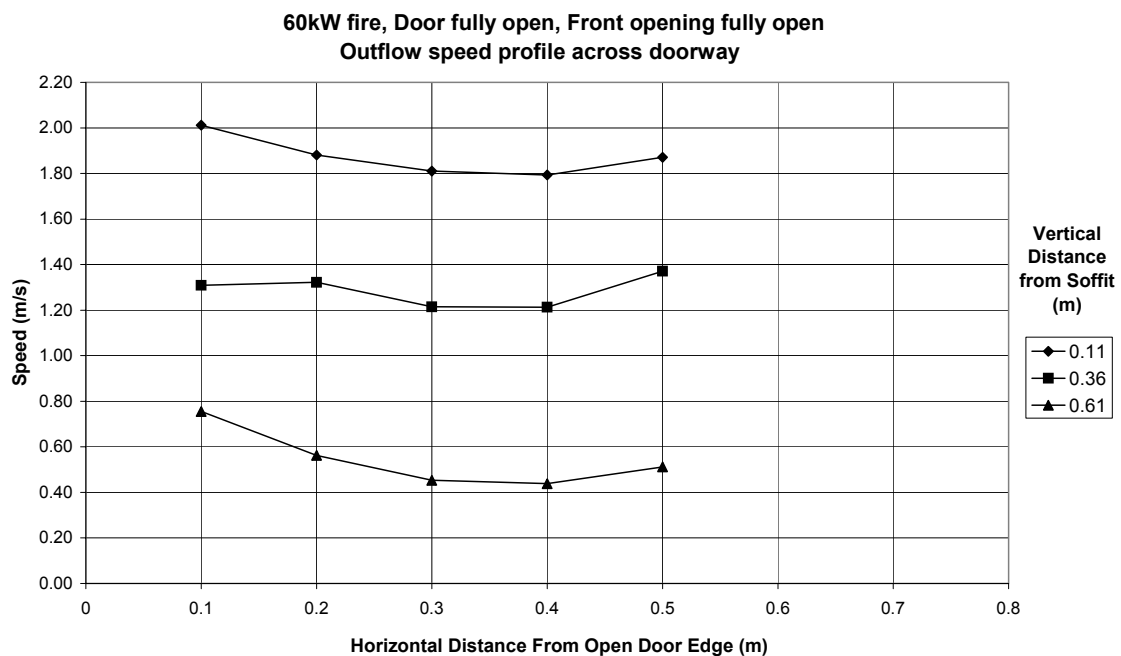


Figure 4.2 Doorway speed profile for outflow section, burner in centre of compartment, 60kW fire size, front opening and door fully open

Again it can be seen that for the majority of measurement positions the speed is at a maximum at the edge of the doorway and reduces across the width of the doorway. The exception to this is the measurement at 1.11m below the soffit which increases across the width of the doorway.

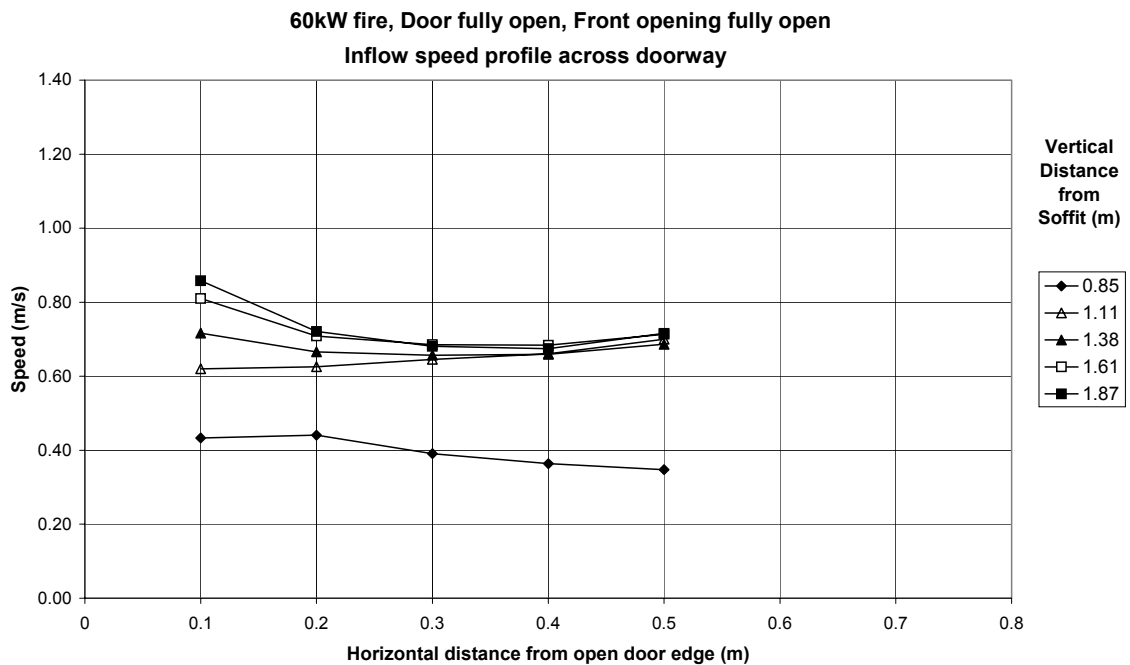


Figure 4.3 Doorway speed profile for inflow section, burner in centre of compartment, 60kW fire size, front opening and door fully open

### 4.2.3 120kW Fire

The temperature distribution is shown in figure 4.4 below. Again the transition from the outflow to inflow regimes can be seen through the transition between the lower inflow layer that is of almost constant temperature, and the upper outflow layer that shows an increasing temperature with height. Again the results are consistent across the width of the doorway except for the measurement taken at 0.05m from the door edge.

The speed profile for the outflow section is shown in figure 4.5 below. Again it can be seen that the speed is maximum at the door edge and reduces across the width of the doorway.

The speed profile for the inflow section is shown in figure 4.6 below. With the exception of two uppermost measurement positions the speed is again seen to be maximum at the door edge and reduce across the width of the doorway. The upper most

measurement is essentially constant across the width of the doorway. The measurement at 1.1m below the soffit increases across the width of the doorway.

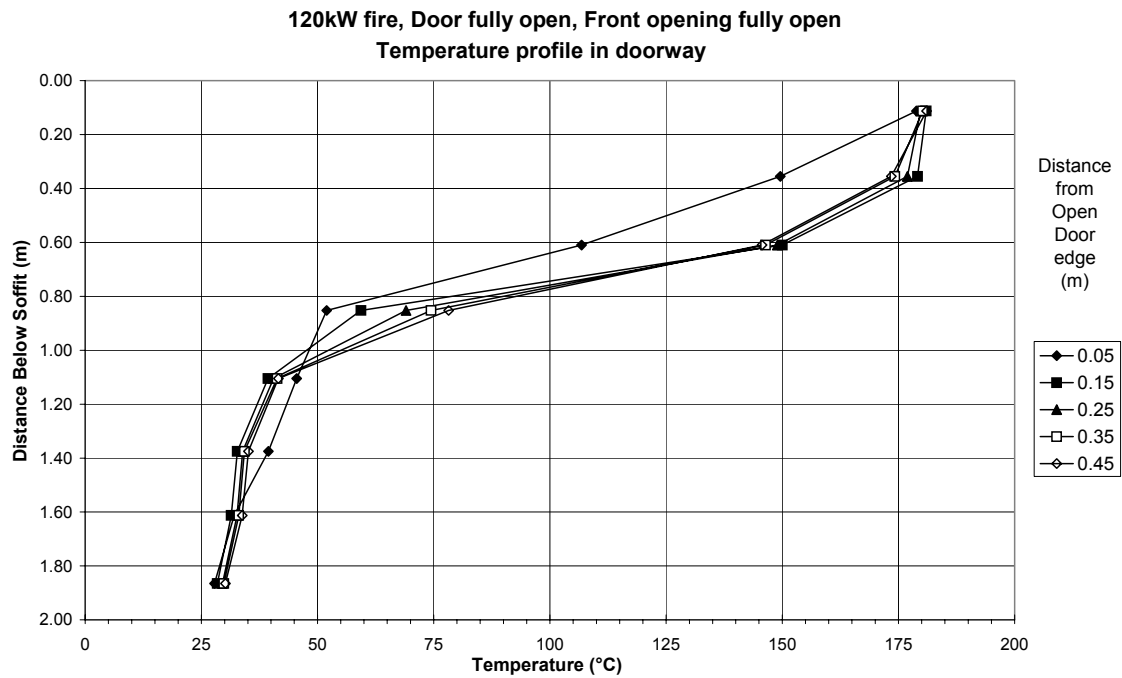


Figure 4.4 Temperature profile in doorway, burner in centre of compartment, 120kW fire size, front opening and door fully open

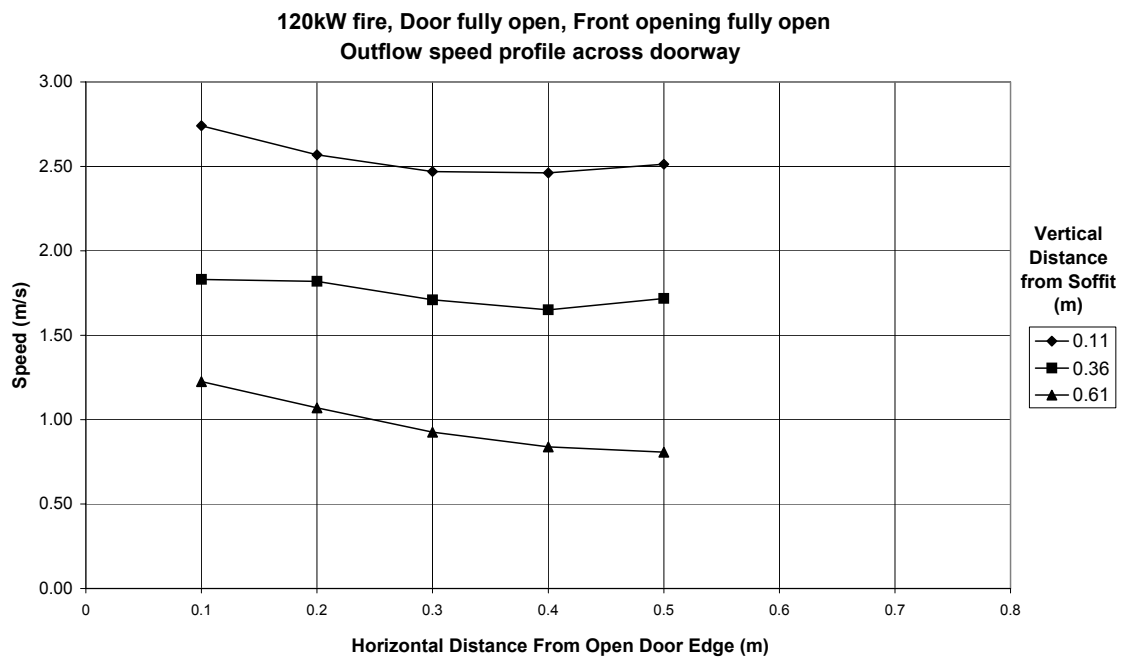


Figure 4.5 Doorway speed profile for outflow section, burner in centre of compartment, 120kW fire size, front opening and door fully open

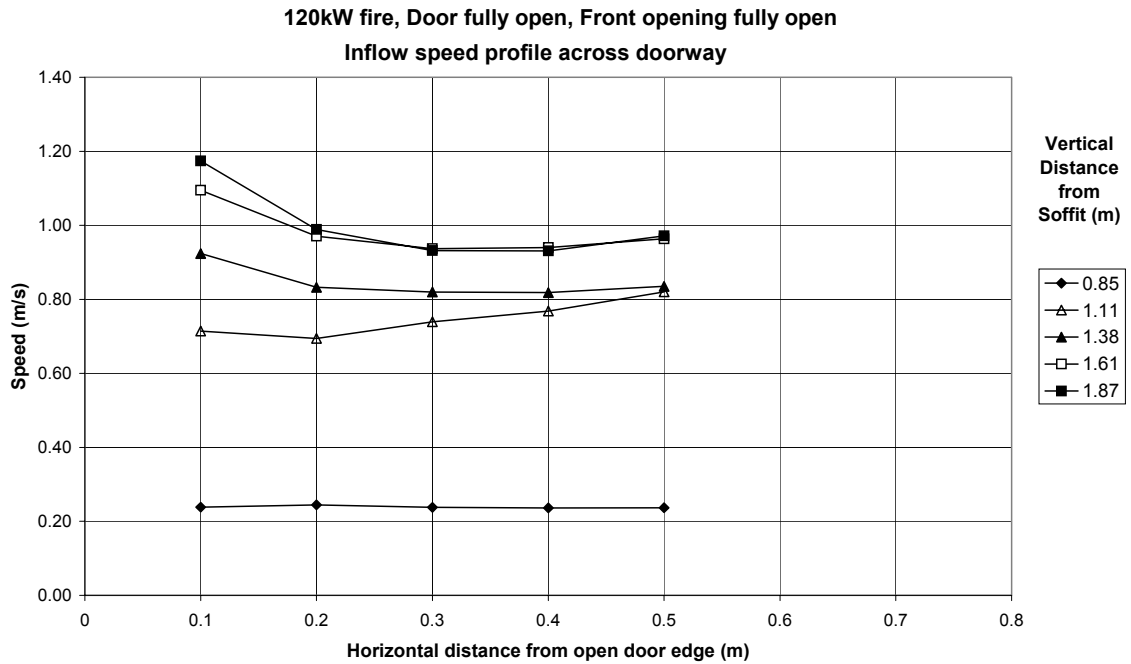


Figure 4.6 Doorway speed profile for inflow section, burner in centre of compartment, 120kW fire size, front opening and door fully open

#### 4.2.4 180 kW Fire

The temperature profile in the doorway is shown in figure 4.6 below. A clear distinction can be seen between the inflow and outflow sections of the doorway.

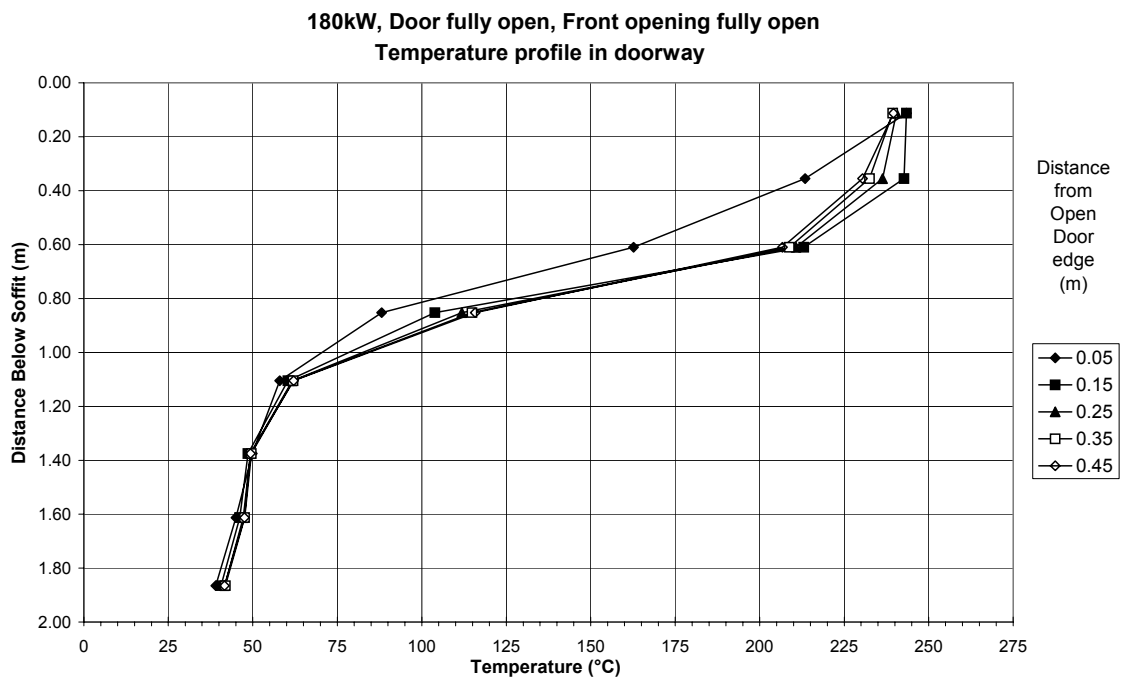


Figure 4.7 Temperature profile in doorway, burner in centre of compartment, 180kW fire size, front opening and door fully open

Again the temperature profile is relatively constant across the doorway with the exception of the measurement at a distance of 0.05m from the open door edge.

The speed profile for the outflow section of the doorway is shown in figure 4.8 below. Again the predominate trend is that the speed is maximum at the door edge and falls to a minimum near the centre of the doorway. The exception is the data at 0.85 m below the soffit in this case the speed increases across the width of the doorway.

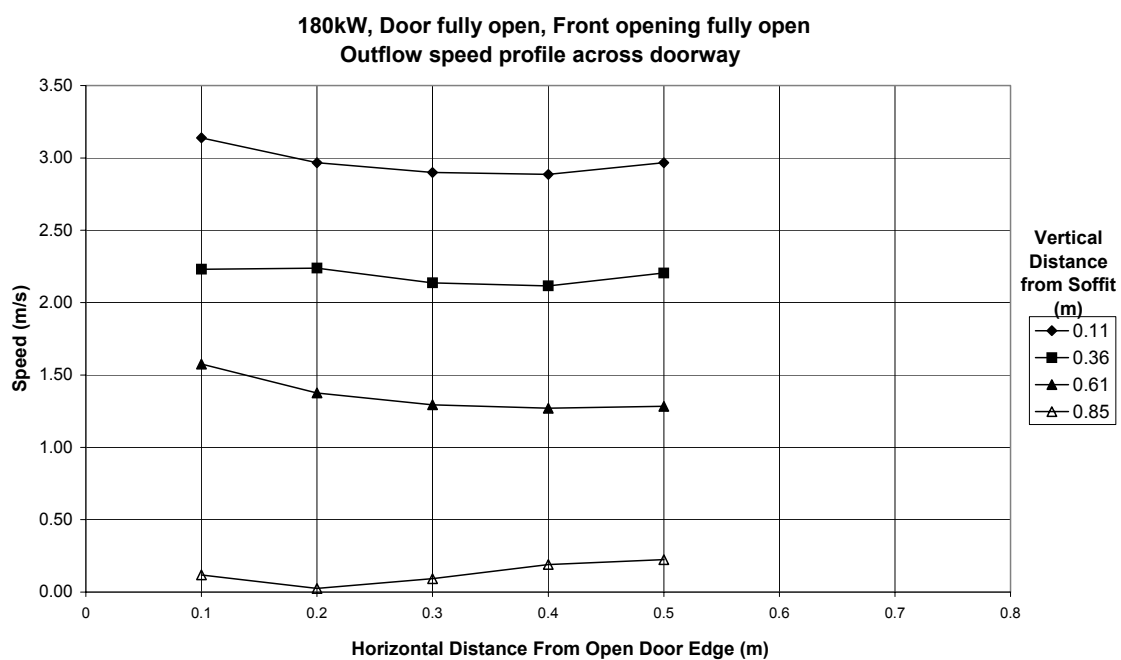


Figure 4.8 Doorway speed profile for outflow section, burner in centre of compartment, 180kW fire size, front opening and door fully open

The speed profile for the inflow section is shown in figure 4.9 below. The majority of the data exhibits the trend that the maximum speed occurs at the door edge and decreases to a minimum at the centre of the doorway. The data series at a height of 1.11m however displays a speed which increases across the width of the doorway. The speed is seen to increase with increasing height from the soffit.



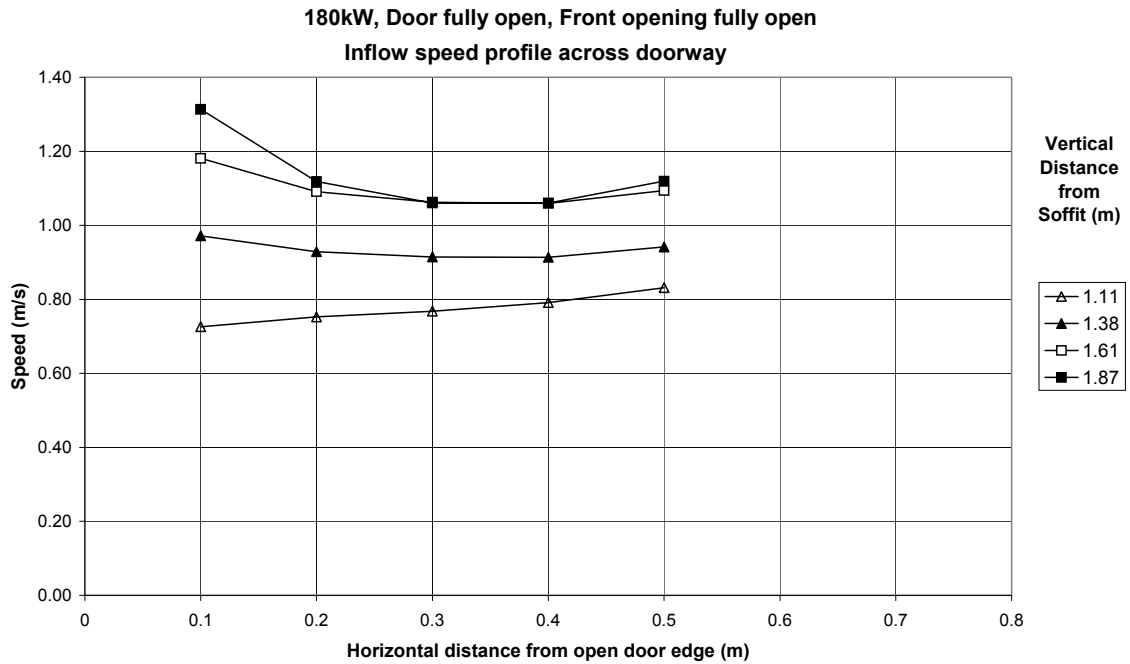


Figure 4.9 Doorway speed profile for inflow section, burner in centre of compartment, 180kW fire size, front opening and door fully open

## 4.3 Burner on walls of compartment

### 4.3.1 Description of experiments

This section describes two experiments where the burner was moved from its location in the centre of the fire compartment. The first involves the burner in the back corner of the fire compartment and the second the burner in the centre of the back wall. The fire size was 120kW for both of these experiments and both the doorway and front opening were fully open.

### 4.3.2 Burner in corner

The temperature distribution within the doorway is shown in figure 4.10 below. It can be seen that temperature in the lower zone is no longer as constant as it was in the burner in centre cases. It is more difficult to see a clear transition between the zone behaviour. Again the behaviour is consistent across the width of the doorway with the exception of the measurement taken at 0.05m from the door edge.

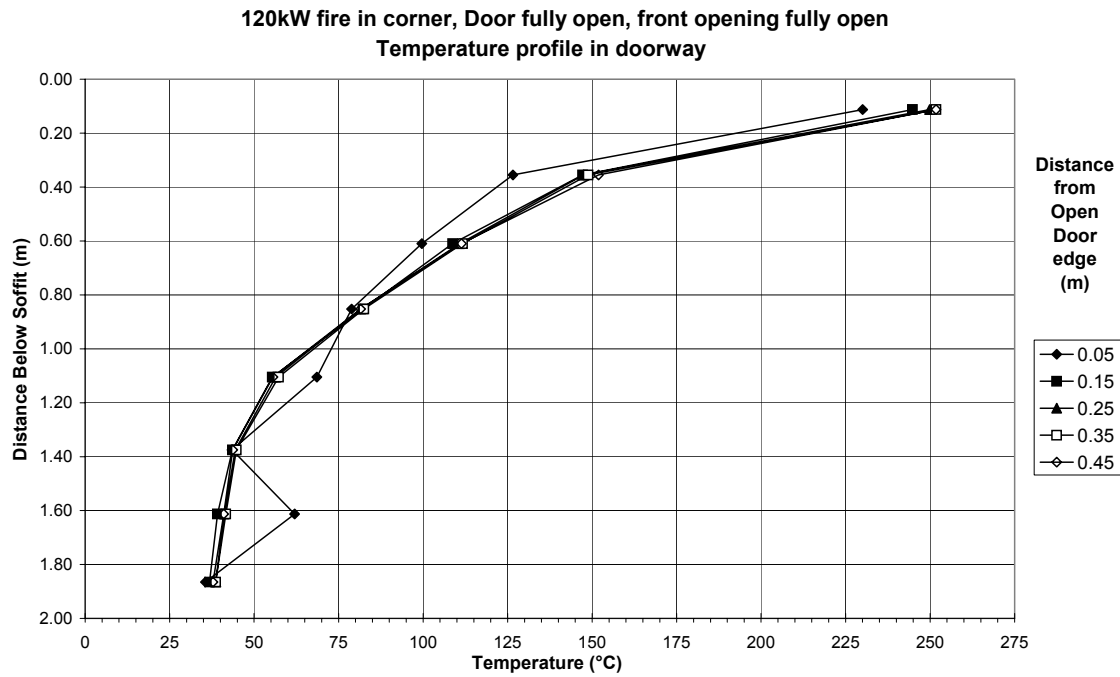


Figure 4.10 Temperature profile in doorway, burner in corner of compartment, 120kW fire size, front opening and door fully open

The speed profile for the outflow section is shown in figure 4.11 below.

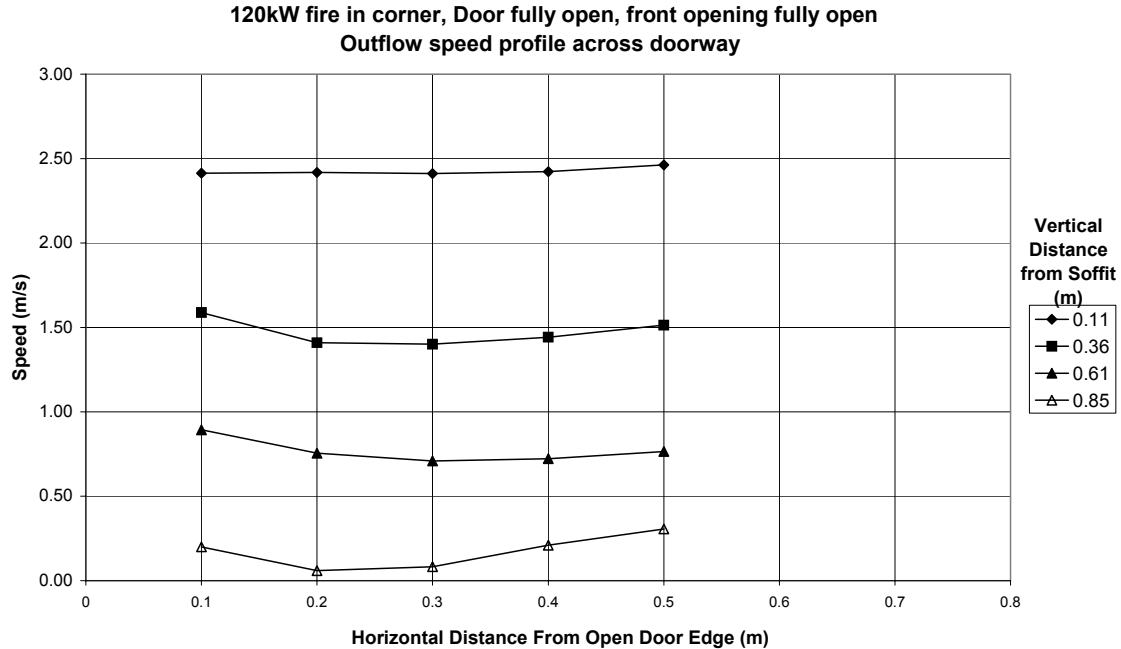


Figure 4.11 Doorway speed profile for outflow section, burner in corner of compartment, 120kW fire size, front opening and door fully open

The speed is seen to be maximum at the edge of the doorway, and minimum near the centre of the doorway. It can be seen however the measurement at 0.11m below the

soffit is constant across the majority of the doorway. The measurement at 0.85m below soffit also initially follows this trend but then climbs to a maximum at the measurement made at 0.5m from the door edge.

The speed profile for the inflow section of the doorway is shown in figure 4.11 below.

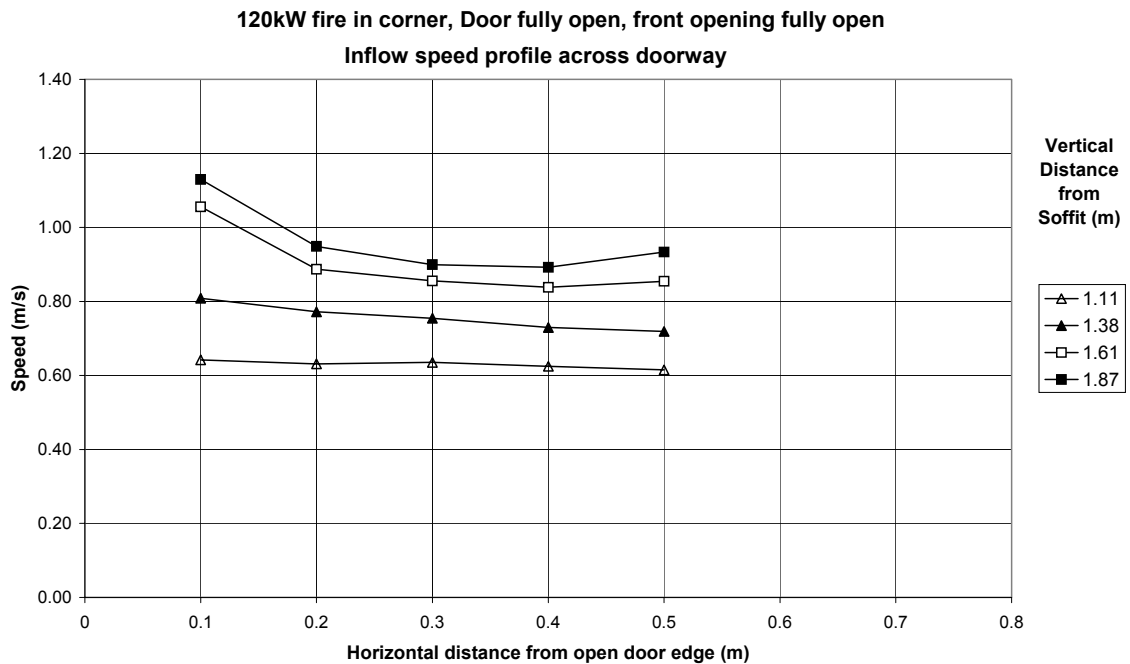


Figure 4.12 Doorway speed profile for inflow section, burner in corner of compartment, 120kW fire size, front opening and door fully open

Again the speed can be seen to be at a maximum at the edge of the doorway falling to a minimum near the centre of the doorway. In this case the behaviour is consistent at all measurement heights. The speed is seen to increase with increasing height from the soffit.

#### 4.3.3 Burner on back wall

Figure 4.13 below shows the temperature distribution in the doorway. It can be seen that the temperature profile is consistent across the width of the doorway with the exception of the measurement at 0.05m from the door edge. There is again more variation in the temperature in the lower zone than in the case of the burner in the centre of the compartment.

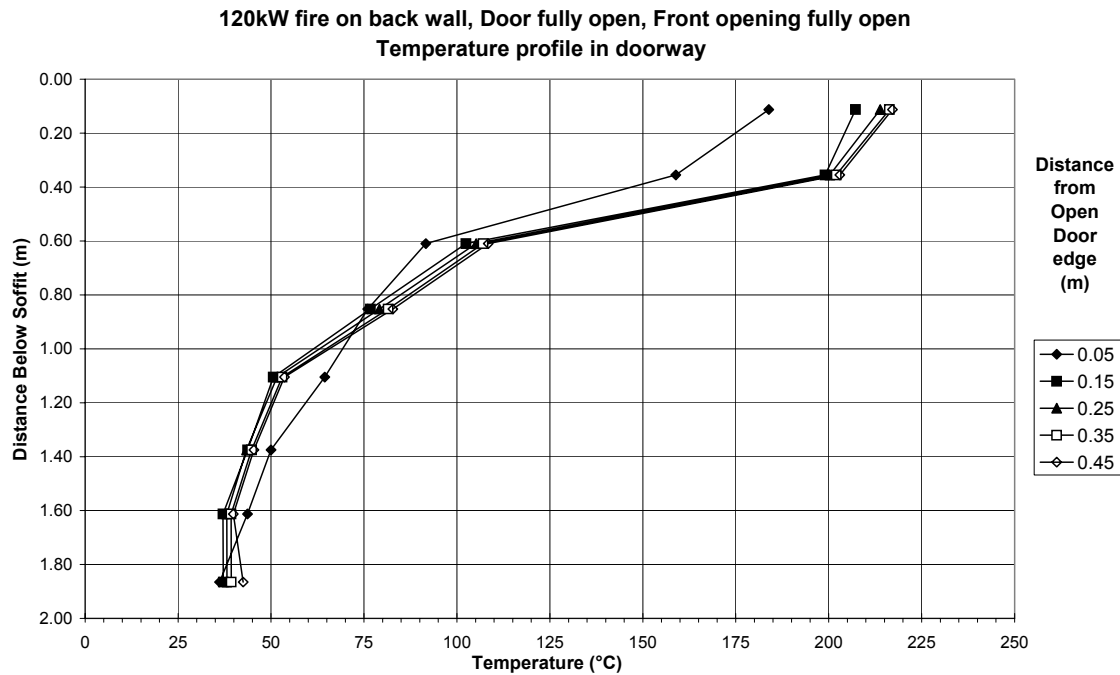


Figure 4.13 Temperature profile in doorway, burner on back wall of compartment, 120kW fire size, front opening and door fully open

The speed profile for the outflow section is shown in figure 4.14 below.

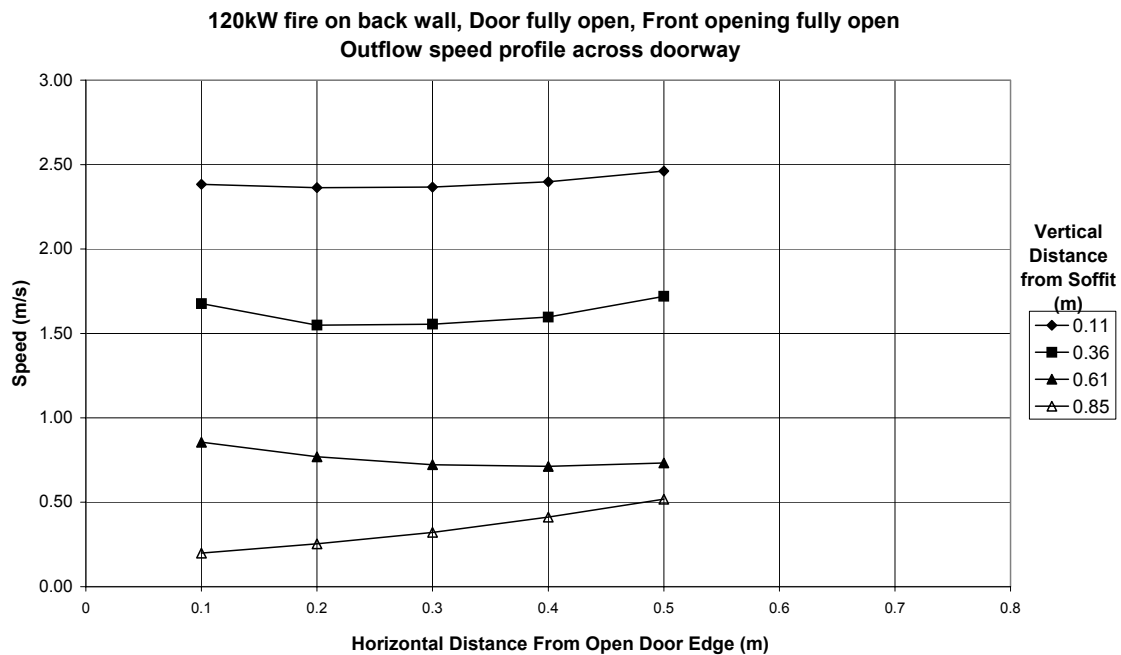


Figure 4.14 Doorway speed profile for outflow section, burner in corner of compartment, 120kW fire size, front opening and door fully open

In this case the behaviour is more mixed. At all heights apart from 0.61m below the centre the speed is measured as a maximum at a distance of 0.5m from the open door

edge. The behaviour at different heights also varies; the lowest measurement at 0.85m below the soffit appears to have a linear increase across the width of the doorway. Whereas the remaining measures show the behaviour as seen previously where there the measurement starts at a maximum value and falls to a minimum before rising again. The speed is seen to increase with decreasing height from the soffit.

The speed profile for the inflow region of the doorway is shown in figure 4.14 below.

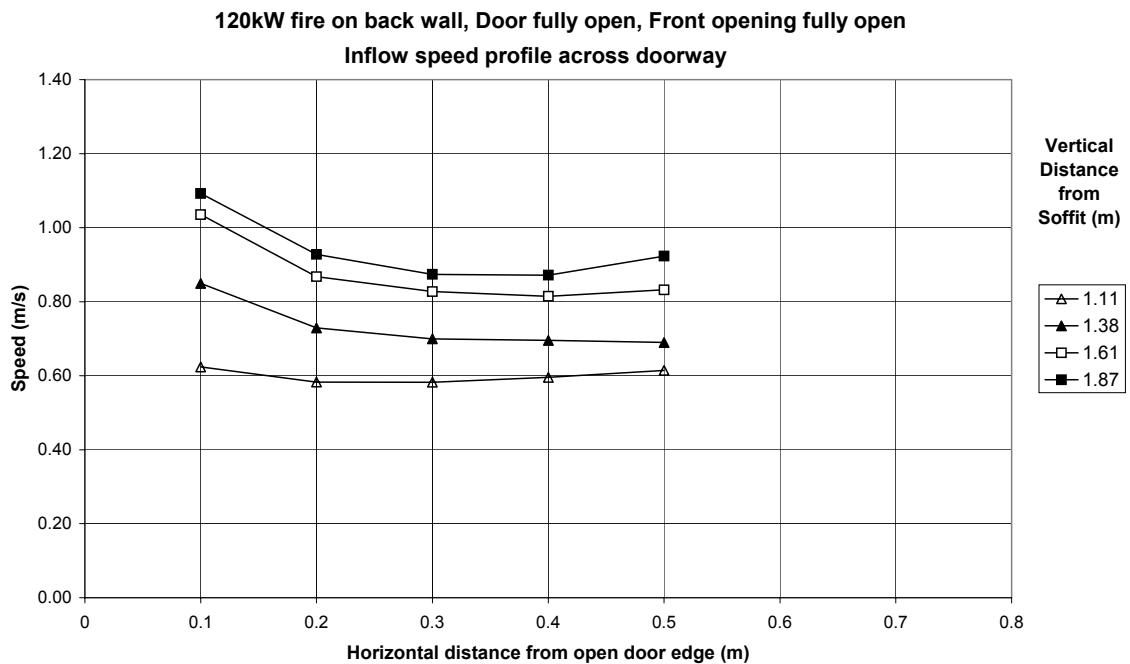


Figure 4.15 Doorway speed profile for inflow section, burner in corner of compartment, 120kW fire size, front opening and door fully open

In this case the behaviour is much more standard over the height of the doorway. The speed is at a maximum at the position closest to the door edge, falling to a minimum near the centre of the doorway before rising again. It can also be seen that the speed measured increases with distance from the soffit.

## 4.4 Mass flow rate calculation

This section deals with the calculation of the mass flow rate from the speed and temperature data taken in the experiment. This is based on the two following relationships

$$\dot{m}_{in} = \int_0^{Hn} \int_0^a \rho u da db \quad (4.1)$$

$$\dot{m}_{out} = \int_{Hn}^B \int_0^a \rho u da db \quad (4.2)$$

Where the mass flow rate is found by integrating the mass velocity over the area of either the inflow or outflow section.

This integration was performed numerically based on the measurements taken during the experiment. This gave a set of 80 integration points. The integration requires knowledge of the neutral plane height. The quoted neutral plane height was numerically determined by minimising the difference between the two mass flow rates. Due to the measurement limitations velocities were not measured across the whole doorway, for this reason the mass flows quoted in this section are taken from an integration performed over half the width of the door then doubled. This assumes a symmetrical flow, but this should be present in the rums where the door is not installed.

The results of this calculation for the experiments discussed in this section are shown in table 4.1 below.

Table 4.1 Experimental mass flow predictions and neutral plane heights

<i>Fire Size (kW)</i>	<i>Fire Location</i>	<i>Mass Flowrate</i>		<i>Neutral Plane Height (m)</i>
		<i>Inflow (kg/s)</i>	<i>Outflow (kg/s)</i>	
60	Centre	0.72	0.72	1.17
120	Centre	0.90	0.90	1.21
180	Centre	0.92	0.92	1.06
120	Corner	0.74	0.74	0.99
120	Wall	0.77	0.77	1.07

Two trends are obvious from this data: that as the fire size increases so does the fire induced mass flow rate; and that the flow is maximised by having the burner in the centre of the compartment. The trend in the neutral plane height is less obvious. There is no clear correlation between neutral plane height and the flow rate observed through the doorway.

## 4.5 Aspirated Thermocouple comparison

A comparison between the temperature measurements taken with the aspirated and bare wire thermocouples for run 5 is shown in table 4.2 below. The data for the remaining are in Appendix A of this report.

Table 4.2 Comparison of temperature prediction for aspirated and bare wire thermocouples, 120kW fire size, burner in centre

<i>Height below Soffit (m)</i>	<i>Aspirated Thermocouple (°C)</i>	<i>Bare Wire Thermocouple (°C)</i>	<i>Difference (°C)</i>	<i>%Difference</i>
0.11	192.0	180.3	10.3	6.5
0.36	190.1	174.5	21.9	9.0
0.61	157.2	146.9	23.6	7.0
1.38	19.9	74.1	40.7	-73.1
1.61	19.2	41.2	24.4	-53.4
1.87	20.0	34.4	16.0	-42.1

Two clear trends can be seen: for the measurements above the neutral plane height the aspirated thermocouple over predicts the temperature in comparison to the bare wire thermocouple; for the measurements below the neutral plane, the aspirated thermocouples under predict the temperature in comparison to the bare wire thermocouple.

## 4.6 Discussion

### 4.6.1 Speed Profiles

A clear trend in all of the data is that the speed measured in the experiments increased as the distance from the neutral plane increased. This was seen to occur for both the inflow and outflow section of the doorway. This is due to the variation in pressure distribution over the doorway. This is illustrated in Figure 4.16 below.

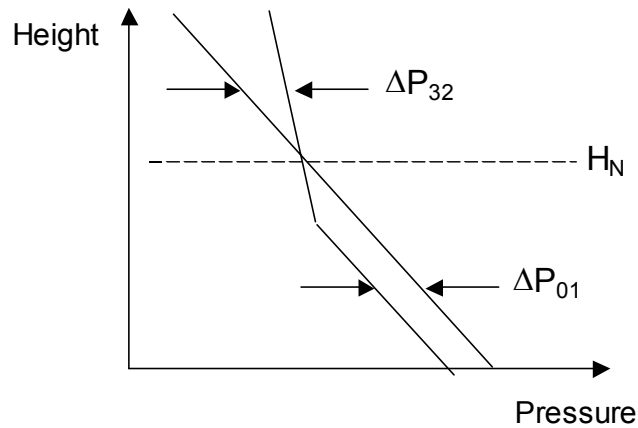


Figure 4.16. Pressure distribution across doorway

It can be seen that both pressure differentials fall to zero at the neutral plane and increase with distance from the neutral plane. This leads to the minimum speed being recorded in the area surrounding the neutral plane.

It was also observed that the speed profiles showed a common trend across most of the data recorded. This was that the speed measured was at a maximum near the door edge and fell to a minimum near the centre of the doorway. This effect has also been observed in experiments performed at the National Bureau of Statistics (NBS) (Steckler 1984). In this series of experiments the speed profile was seen to be parabolic with the maximum at the edge of the doorway and the minimum at the centre of the doorway.

The experimental data shows that the measurements in the outflow section are less likely to show this trend. A possible reason for this is that the speeds in the doorway are higher resulting in a more turbulent flow that would disturb the usual flow pattern. This turbulence is illustrated in figure 4.17 that shows the pressure transducer measurements surrounding the neutral plane for run 5, the remaining runs can be seen in Appendix A of this report.





Figure 4.17, Pressure differential readings in doorway, 120kW fire size, burner in centre, door and front opening fully open, smoothed data.

It can be seen that the data for the outflow section (negative pressure differential readings) show more variability in the data than those in the inflow section. This is still evident even after a significant smoothing of the data, suggesting that this is more than short-term spikes in the measurements taken.

It is also interesting to note that at all heights significant variation is seen in the measurement made at 100mm from the door edge. This is likely due to vortices shedding from the streamline flow caused by the door edge. This will result in eddy currents being formed, and therefore, localised instability in the pressure differential reading observed.

The airflow near the neutral plane is also of interest. The speed distribution at the heights nearest the predicted neutral plane height did not seem to follow the same trends as the rest of the data. This is to be expected to some degree due to the nature of the neutral plane. It will be a region of localised turbulence due to the nature of the shear boundary that is developed. This turbulence will prevent the formation of a stable flow pattern. This is demonstrated by the variation in trend seen in the speed profile near the neutral plane. Take for instance the speed measurement taken at the height of 0.85m

below the soffit for runs 5, 6 and 7 (see figures 4.3, 4.6 and 4.8). In run 5 the speed decreases across the width of the doorway, in run 6 it is very stable across the width of the doorway and in run 7 it increases across the width of the doorway.

#### **4.6.2 Effect of Burner location**

The temperature profiles observed in the doorway are consistent with the results that were obtained in phase 1 of the McLeans Island experiments (Nielson 2000). That is that the two-layer behaviour evident when the fire is located in the centre of the compartment is not seen when the fire is moved to the walls of the compartment. For instance the temperature profile in the doorway for run 6 (see figure 4.4) shows a much clearer transition between the lower layer of nearly constant temperature and the upper layer. This contrasts with the profiles seen in runs 9 and 12 (see figures 4.10, 4.13) where the shape of the temperature distribution is much less angular and suggests that there may not be clear two-layer behaviour in the fire compartment.

It is also interesting that the predicted neutral plane height was significantly lower in the two cases where the burner was moved to the wall. This is another indication that the temperature profile in the fire compartment is different in each case. As the neutral plane is determined as where the pressure differential is zero across the doorway. Altering the temperature differential within the compartment will alter this point. This is illustrated in figure 4.18 below. This figure shows two pressure differentials within a system. The only difference between the two is at which height the inside pressure deviates significantly from ambient levels. It can be seen that the case where the pressure distribution changes earlier, results in a lower neutral plane.

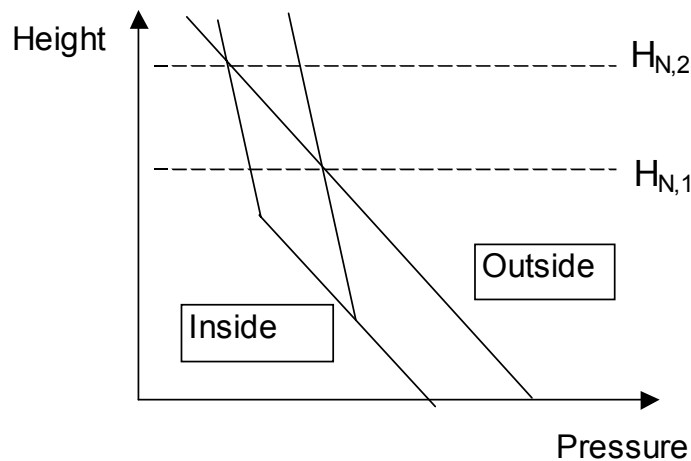


Figure 4.18 Effect of temperature distribution on neutral plane prediction

It is important to however state that a lower neutral plane does not necessarily result in a greater total mass flow rate being observed across the doorway. In these experiments the flow rate in the centre case was larger than the wall case that was larger than the corner case (0.92, 0.77 and 0.74 kg/s respectively). However the predicted neutral plane height was reversed (1.21, 1.07 and 0.99m respectively). This result is again consistent with work performed at the NBS (Steckler 1982).

#### 4.6.3 Mass flow predictions

It can be seen from table 4.1 that the prediction of mass flow rate for the inflow and outflow are in all cases equal. This is the expected result due to the mass input of fuel being small. This however is a contrived result as the neutral plane height estimation was altered so that this occurred. This was necessary due to no visual record being taken which would allow a direct input of an experimental neutral plane height.

However care was taken so that the neutral plane prediction was consistent with the experimental results. Take for example the temperature distribution found in the doorway for run 5 (see figure 4.4) the predicted neutral plane height occurs at 1.21m above the floor (0.8m below soffit). This corresponds to the region with the greatest gradient between temperature measurements. This is consistent with methods of predicting neutral plane height from temperature data. (Emmons 1997)

It is useful to compare the mass flow rate predicted in these experiments with those measured by other researchers. For this reason two other experiments will be compared.

The data found at the NBS (Steckler 1982), and that at the Building research institute in Japan (Nakaya 1986). Both of these experiments are consistent with this research as moveable bi-directional probes were used in the doorway to allow for a matrix of speed calculations. Pertinent results are summarised in table 4.3 below.

Table 4.3 Comparison of mass flow rate predictions with other studies

	<i>Fire Size</i> (kW)	$A_o H_o^{1/2}$ ( $m^{5/2}$ )	<i>Mass Flow rate</i> <i>Outflow (kg/s)</i>	$m/ A_o H_o^{1/2}$ (kg/s/ $m^{5/2}$ )
Steckler	62.9	1.83	0.58	0.32
Current research	60	2.27	0.72	0.32
Steckler	105.3	1.83	0.63	0.34
Nakaya	100	1.19	0.50	0.42
Current research	120	2.27	0.90	0.39
Steckler	158	1.83	0.70	0.38
Nakaya	200	1.80	0.75	0.42
Current research	180	2.27	0.92	0.41

Difficulties exist in these comparisons due to differences in fire size and room geometry. For this reason the results from this study appear to be higher than those of the other two researchers, however the opening used in this study is significantly larger than that used in these studies. If the data is normalised by dividing the mass flow rate observed by the ventilation factor, then the results obtained across the three experiments are similar. This is a crude method of judgement however as it does not account for the variation in heat release rate observed in each experiment, and it would be more beneficial to compare like experiments to like. Unfortunately due to time constraints no identical experimental runs were performed in this study to test the reproducibility of the results.

It should also be noted that the compartment used in the NBS experiments vented straight to the ambient conditions. This is of interest as in the two room case as seen in the current research and the BRI experiments will lead to slight differences in the flow behaviour. This is due to a hot upper layer being present in the adjacent compartment. This will mean that there will be a change in the gradient in the pressure profile in the

adjacent compartment in this case. The effect of this change in behaviour will depend on the fire conditions and the size of this layer.

#### **4.6.4 Temperature profiles**

The temperature profile measured across the doorway was in general consistent across the width of the doorway. The one clear outlier from this trend is the temperature measurements that were taken at 0.05m from the door edge. The temperature profile at this point often exhibited quite different behaviour. From looking at the data it would appear that this could be determined as a instrumentation problem, however it should be realised that this data is the result of measurements taken with eight individual thermocouples, and that these instruments were used to measure the location at all the other positions in the doorway.

As mentioned in the previous section a greater variability was also shown in the pressure transducer reading when the bi-directional probes were at this position. This suggests that the temperature measurements are also effected by the local turbulence observed at this position.

The temperature measurement was however taken quite close to the doorway and it is possible that the wall acted as a shield for part of the thermocouples length, this could have caused a temperature gradient over the 100mm closest to the bead of the thermocouple and this influenced the results obtained.

As the speed measured in the doorway is a function of the pressure differential and temperature measured in the doorway, this variability in temperature reading could affect the speed that is calculated. However, it should be pointed out that the speed is proportional to the density in the doorway, which is assumed to be an inverse function of the absolute temperature in these conditions. This means that the speed calculation is not strongly sensitive to the temperature measurement. For this reason it was not thought necessary to discard any of this temperature data.

An interesting comparison is that between the bare wire, and aspirated thermocouples that were placed in the doorway. It is known that bare wire thermocouples over predict

the temperature in room fire conditions due to radiative heat transfer from the hot upper layer. It has been found that this effect is most profound in the lower layer (Lou 1997). For this reason six aspirated thermocouples were placed in the doorway to try to measure the magnitude of this effect. It can be seen from Table 4.2 that there were clear differences between the two methods for temperature measurement. In the lower layer the aspirated thermocouples measure behaviour that mimics that predicted by theory. That is that there is a layer of constant near ambient temperature in the lower layer. The bare wire thermocouples show an increasing temperature with height; whilst the temperatures are near ambient they are not as steady as aspirated thermocouple values. It should also be noted that the discrepancy in prediction increases with proximity to the upper layer.

An interesting result is that the aspirated thermocouple measurements are higher than the bare wire in the upper layer. This suggests that there is some mode of heat loss occurring from the bead in the upper layer. This could again be a radiative-based process.

Overall the level of the discrepancy between the two values is of concern. The Percentage discrepancies of 40-70% in the lower layer shows that the radiation effects present in the doorway are significant and should be taken into consideration in future planning of similar experiments. The difficulty lies in the feasibility of using large numbers of aspirated thermocouples in experimental situations.

#### **4.6.5 Errors**

For data recorded in the doorway there are two major sources of error. These are errors in the placement of measurement equipment, and error due to the method of taking data.

The error present in the location of measurement equipment has been minimised as much as possible. However, it is difficult to be certain as to probe placement where the measurement equipment is moved dynamically during the experiment. However the quoted maximum error in vertical placement of probes in the doorway of  $\pm 0.01\text{m}$  is far from excessive. The error in the horizontal placement would be similar to the value quoted above.

The majority of the data that has been reported in this section is an averaged value from the raw data taken. This is necessary due to the large volume of data collected. It is necessary to realise that these values are not absolute and that there is scatter present in the raw data. A good measure of the level of scatter in the data is to look at the standard deviation of the data over the range that the data is taken. An example of this is shown for the pressure differential readings for run 6 shown in figures 4.19 And 4.20 below.

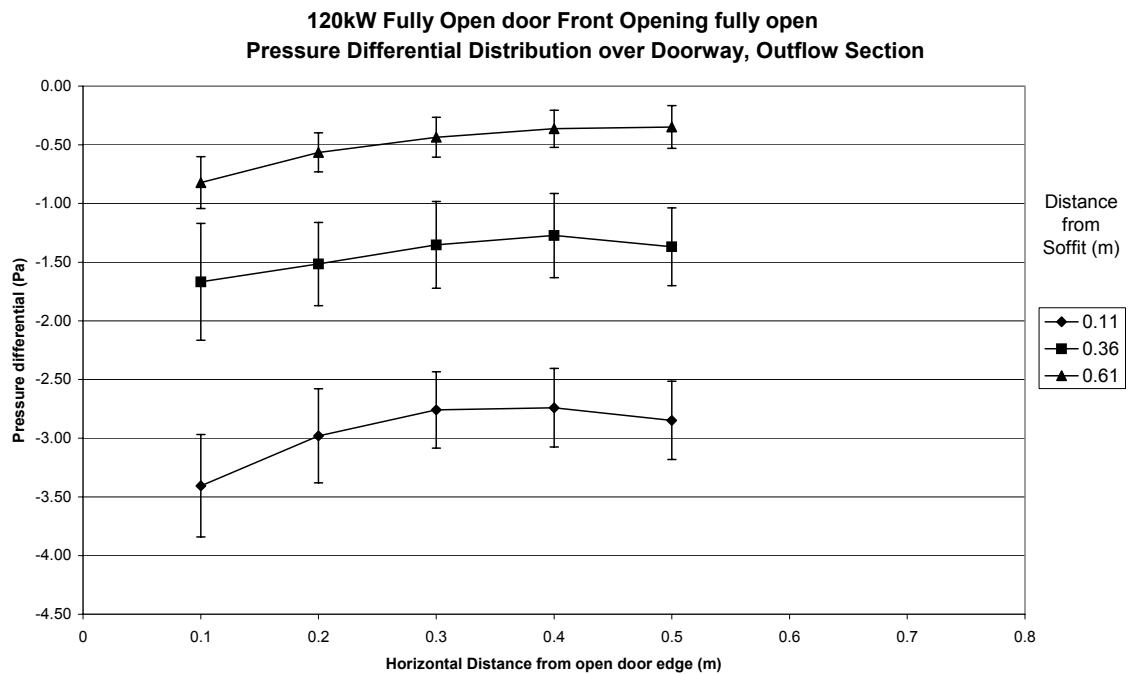


Figure 4.19 Standard deviation in average pressure differential, outflow section, run 6

It can be seen that although a one standard deviation range covers a wide range of values, that this level is reasonably consistent across all measurements and would not effect the trends reported.

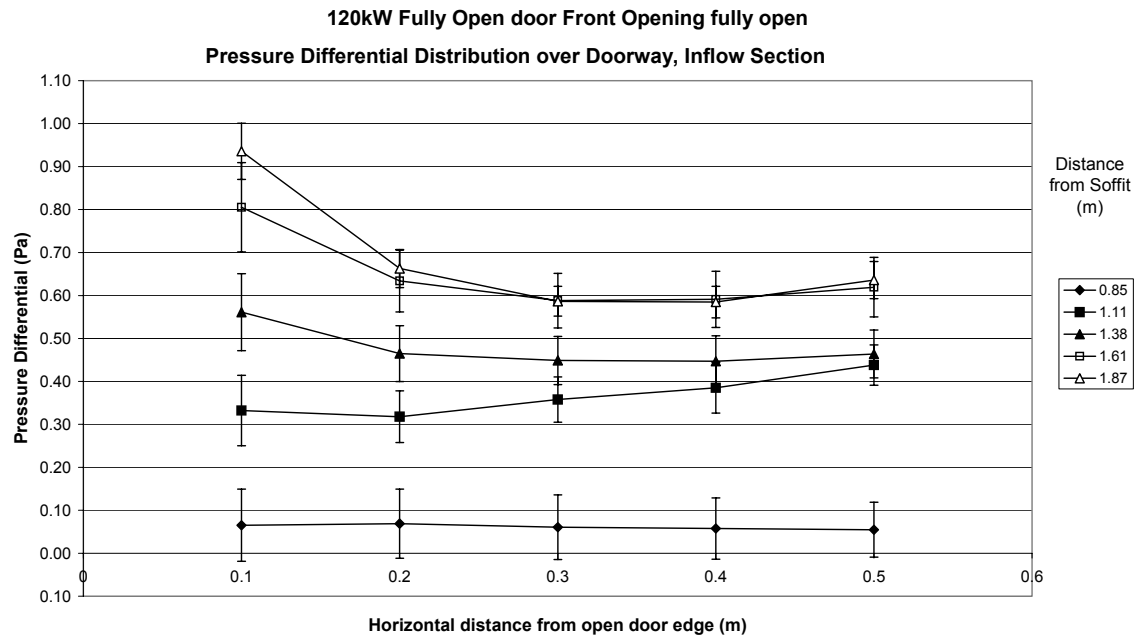


Figure 4.20 Standard deviation in average pressure differential, inflow section, run 6



## 5. Partially Closed Door

### 5.1 Introduction

This section deals with the experiments performed with a door present and partially opened into the doorway. All these runs were performed with a fire size of 120kW and with the burner in the centre of the compartment. Two variables were altered, the angle of the door leaf and the configuration of the front opening. The front opening was either fully open or a second doorway. The data presented in this section represents average data as taken during the experiments, the raw data from the experiments can be found in Appendix B of this report

### 5.2 Front Opening Fully Open

#### 5.2.1 20° Open Door

Figure 5.1 shows the temperature distribution within the doorway.

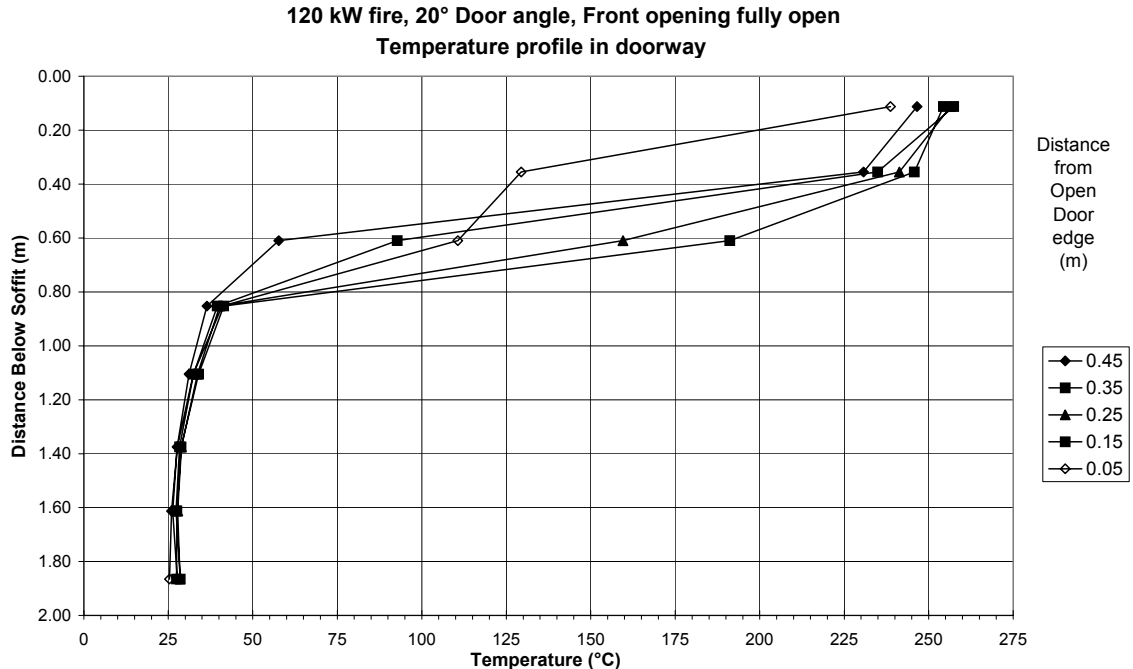


Figure 5.1 Temperature profile in Doorway, 120kW fire, Burner in centre of compartment, Door at 20°, Front opening fully open

It can be seen that there is a near constant temperature in the lower layer portion of the doorway as has been seen previously. However the behaviour in the transition to the

upper layer is interesting. By looking at the measurements made at 0.61 m below the soffit it can be seen that there is a temperature gradient across the width of the doorway at this point, with the temperature decreasing with width across the doorway. Again the data recorded at 0.05m from the open door edge is seen to differ from the general trends.

The speed profile for the outflow section is shown in figure 5.2 below.

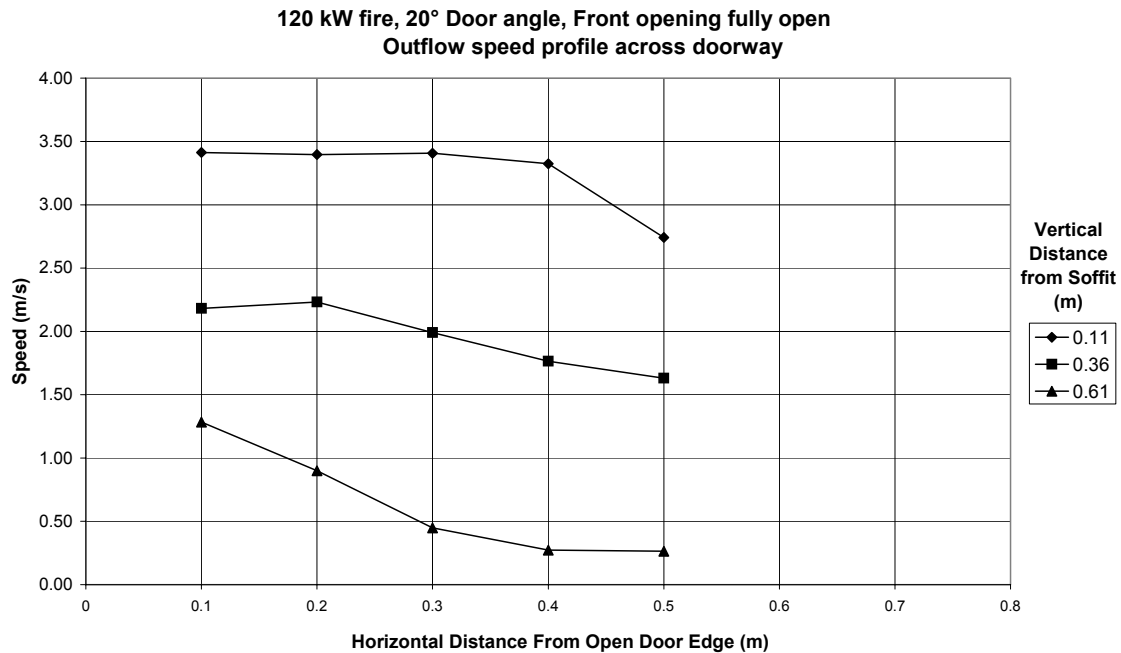


Figure 5.2 Doorway speed profile for outflow section, 120kW fire, burner in centre, 20° door angle, front opening fully open

In this case the speed distribution appears to vary with height and no clear correlation is seen in the measured data. However in all cases the speed is at a minimum at the measurement taken at 0.5m from the door edge and at a maximum near the door edge.

The speed profile for the inflow section is shown in figure 5.3 below. Here the speed is clearly decreasing across the width of the doorway at all measurement heights. In both the inflow and outflow cases the speed is seen to increase with increasing distance from the neutral plane.

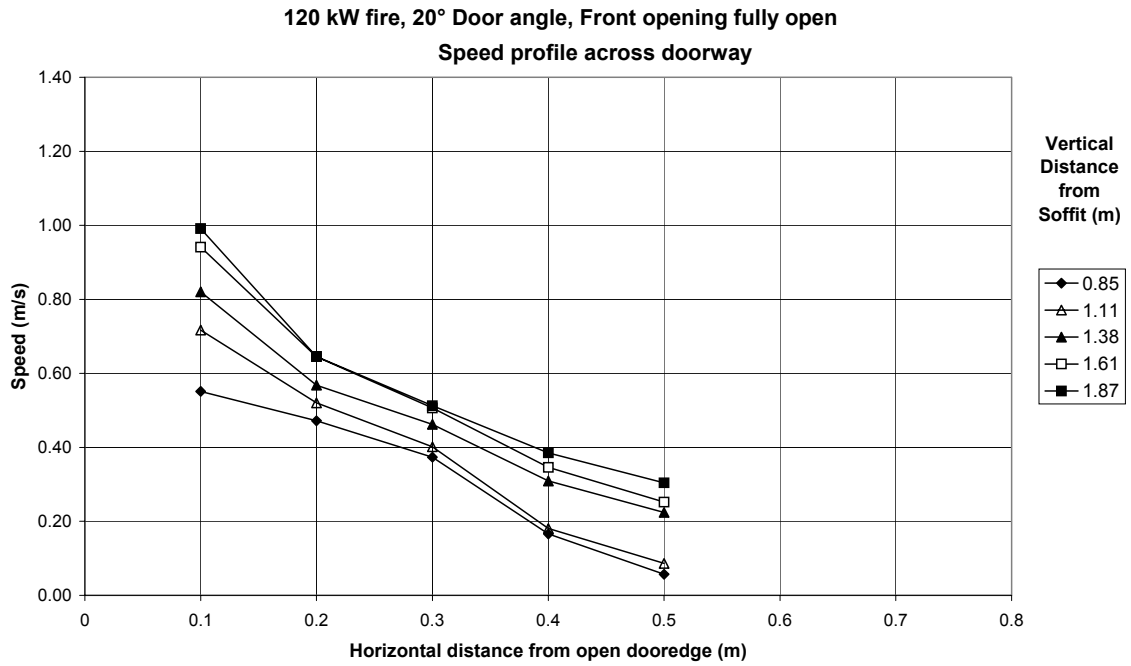


Figure 5.3 Doorway speed profile for inflow section, 120kW fire, burner in centre, 20° door angle, front opening fully open

### 5.2.2 30° Open Door

The temperature profile in the doorway is shown in figure 5.4 below.

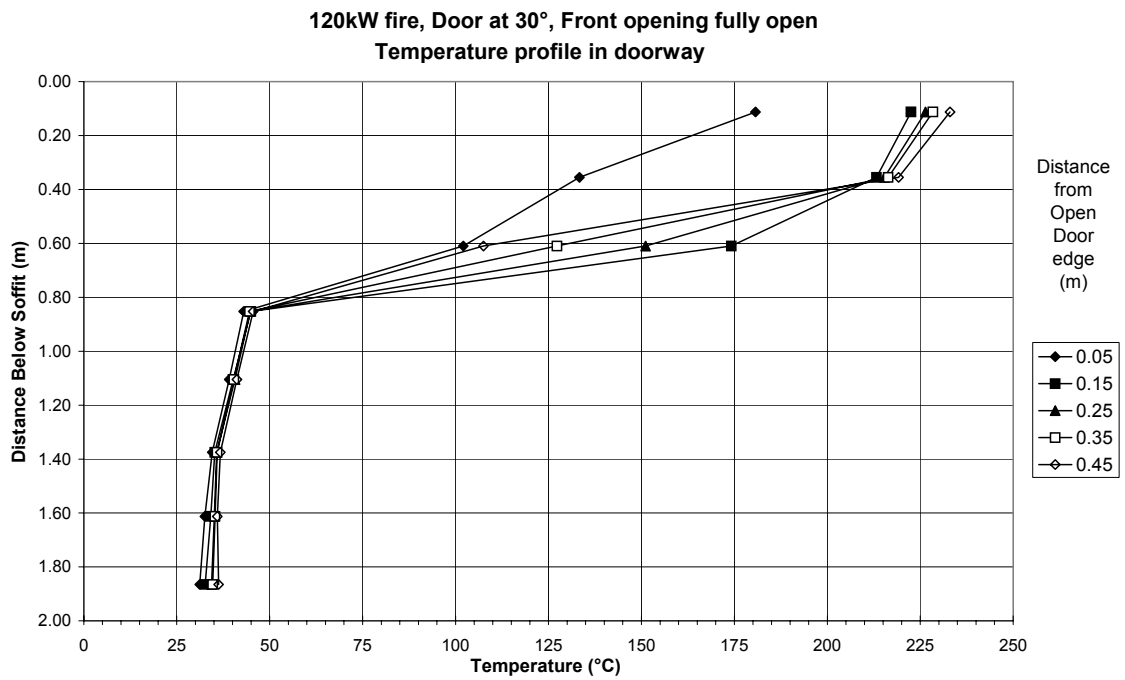


Figure 5.4 Temperature profile in Doorway, 120kW fire, Burner in centre of compartment, Door at 30°, Front opening fully open

Similar behaviour can be seen here as with the 20° open run. Again a temperature gradient is seen across the width of the doorway at the measurement taken at 0.61m below the soffit. The measurement taken at 0.05m from the open door edge again exhibits different behaviour from the rest of the data.

The speed distribution for the outflow section is shown in figure 5.5 below.

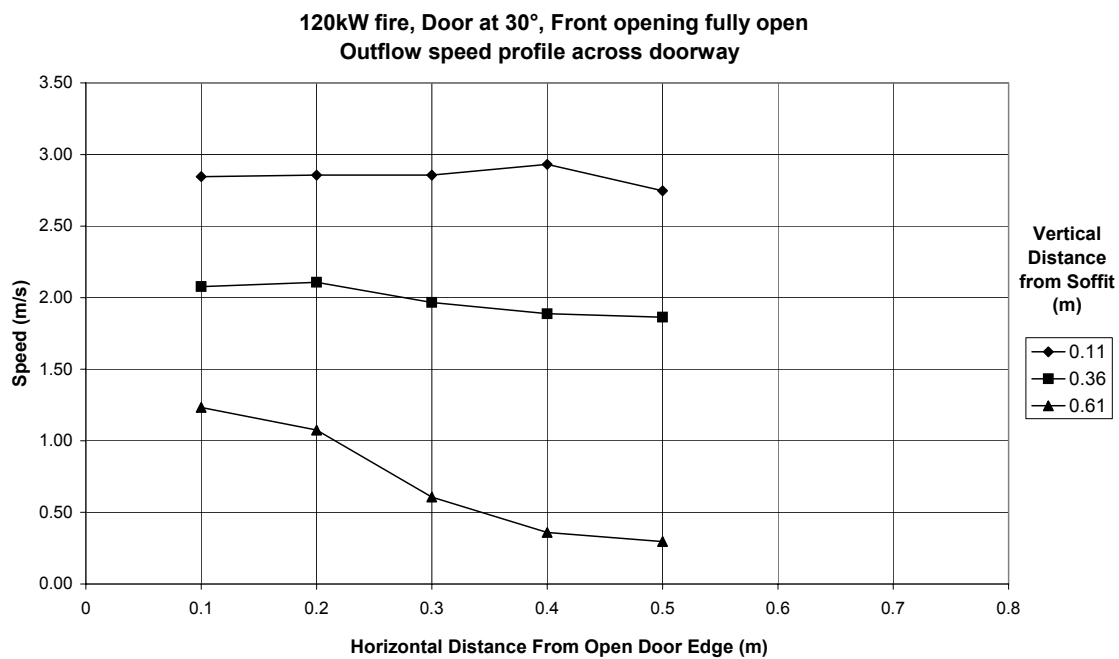


Figure 5.5 Doorway speed profile for outflow section, 120kW fire, burner in centre, 30° door angle, front opening fully open

Again the speed increases with increasing distance from the neutral plane. However there appears to be no clear correlation for the speed profile across the width of the doorway.

The speed distribution for the inflow section is shown in figure 5.6 below. It can be seen that in general the speed falls across the width of the doorway, but increases with distance from the neutral plane. There appear to be two outliers in this data however, the measurement at 0.85m below the soffit at which the speed increases across the width of the doorway, and the data at 1.87m below the soffit where the speed falls at a much greater rate for the rest of the measurements.

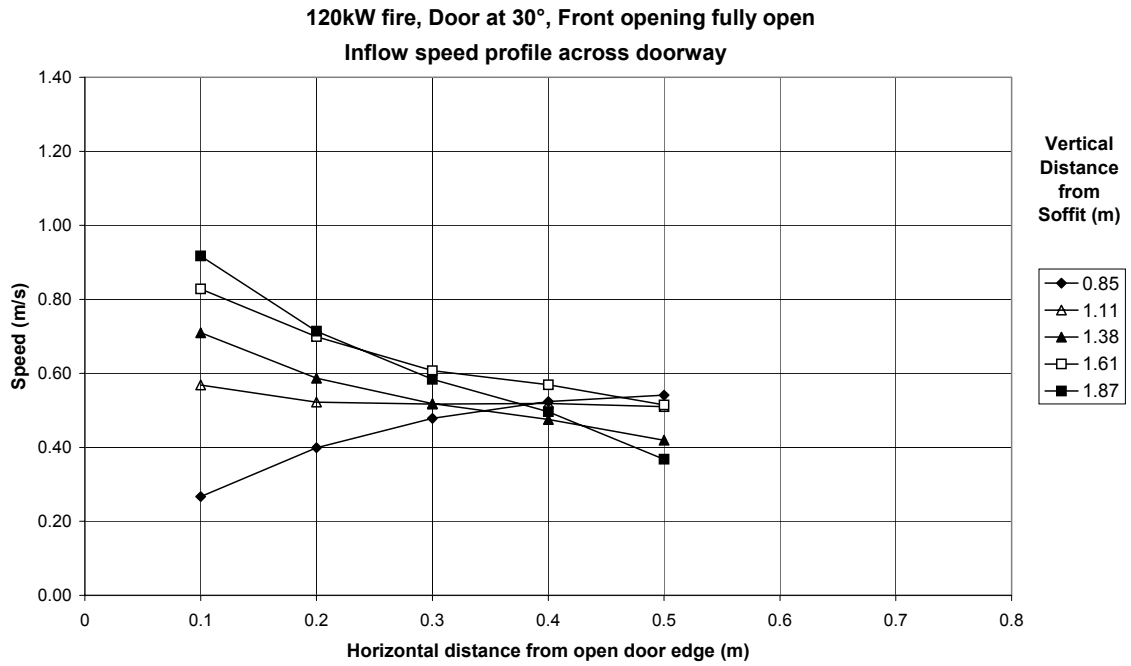


Figure 5.6 Doorway speed profile for inflow section, 120kW fire, burner in centre, 30° door angle, front opening fully open

### 5.2.3 40° Open Door

The temperature profile in the doorway is shown in figure 5.7 below.

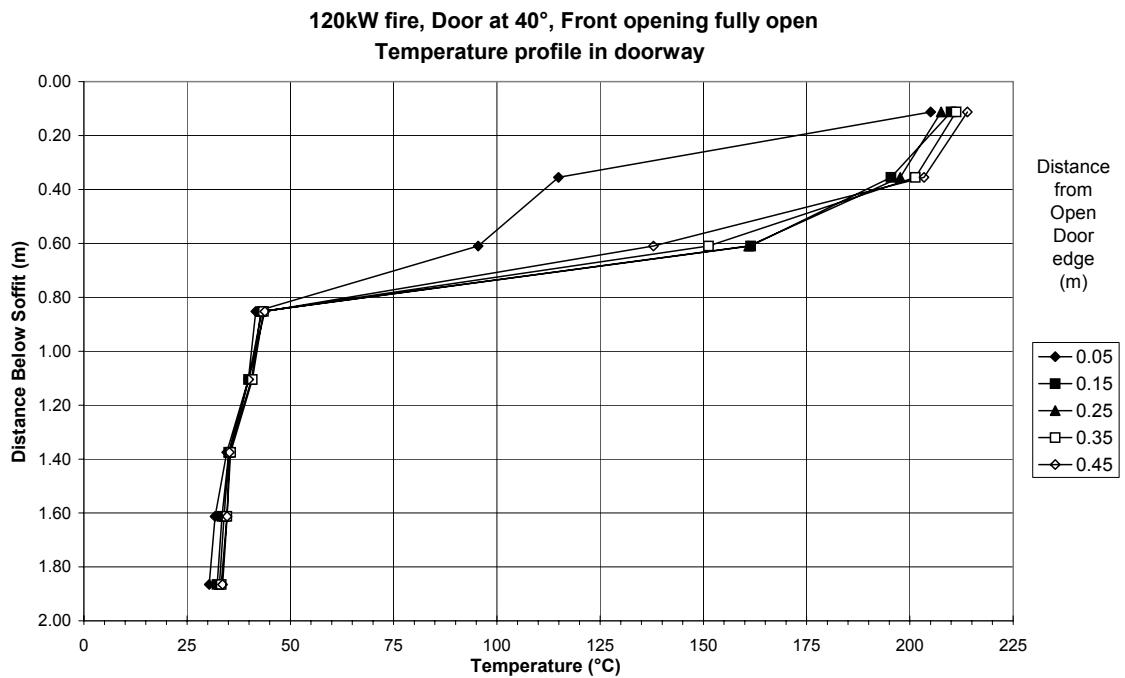


Figure 5.7 Temperature profile in Doorway, 120kW fire, Burner in centre of compartment, Door at 40°, Front opening fully open

It can be seen that for the measurement below the neutral plane are near constant in temperature. There again appears to be a temperature gradient across the doorway at a height of 0.61m below the soffit. The measurement at 0.05m from the door edge appears to differ from the general trend in the data.

The speed distribution for the inflow section is shown in figure 5.8 below.

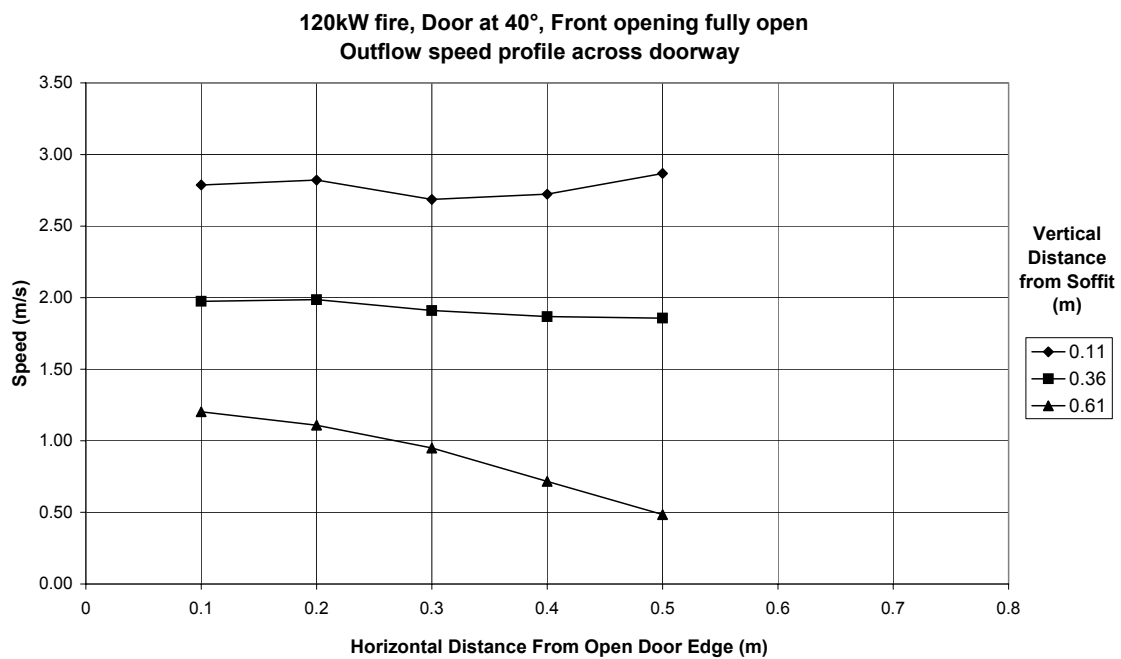


Figure 5.8 Doorway speed profile for outflow section, 120kW fire, burner in centre, 40° door angle, front opening fully open

Again the speed measured increases with height above the neutral plane. There again appears to be no correlation between the speed measured and the position relative to the edge of the doorway.

The speed profile for the inflow section is shown in figure 5.9 below. It can be seen that in this case there is no clear correlation for the speed in terms of either the height below the neutral plane or the distance from the open door edge.

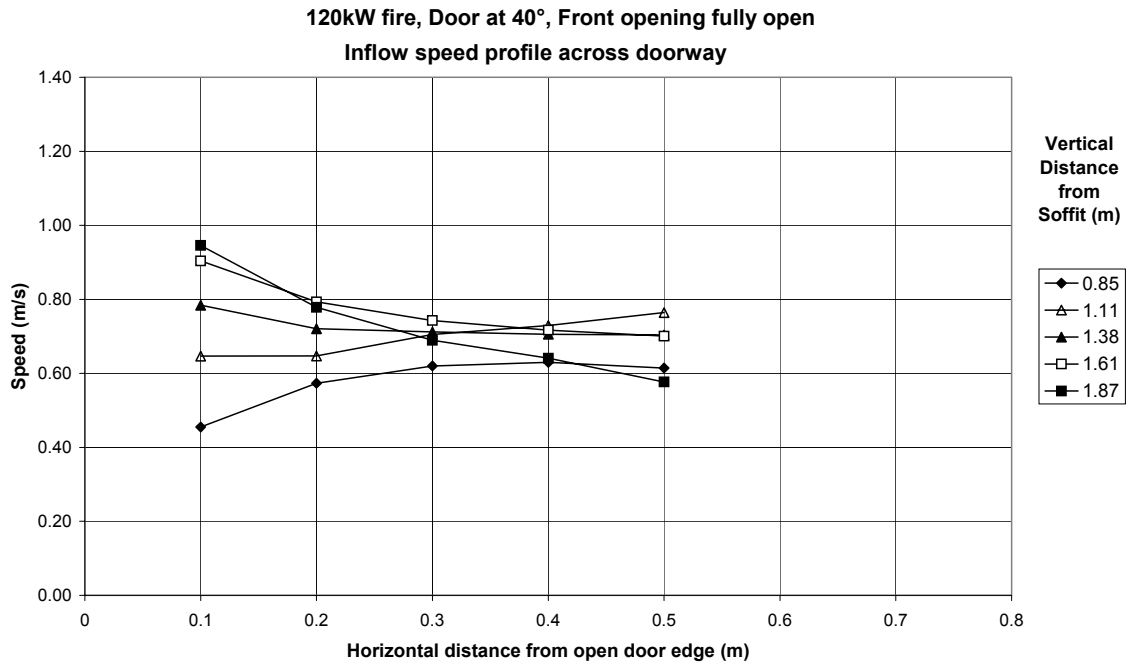


Figure 5.9 Doorway speed profile for inflow section, 120kW fire, burner in centre, 40° door angle, front opening fully open

#### 5.2.4 60° Open Door

The temperature profile in the doorway is shown in figure 5.10 below.

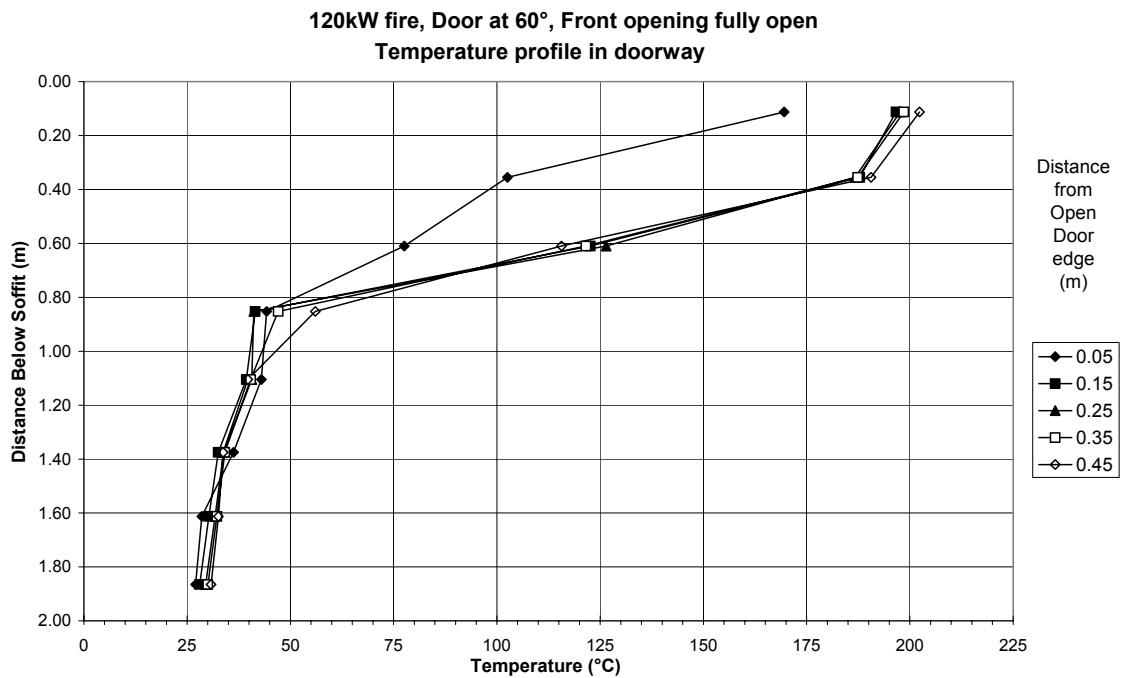


Figure 5.10 Temperature profile in Doorway, 120kW fire, burner in centre of compartment, door at 40°, front opening fully open

It can be seen that the temperature profile is consistent across the width of the doorway. The exception to this is the measurement taken at 0.05m from the door edge that does not follow the trend. There appears to be a slight temperature gradient at a height of 0.85m below the soffit with the temperature decreasing across the width of the doorway.

The speed profile for the outflow section is shown in figure 5.11 below.

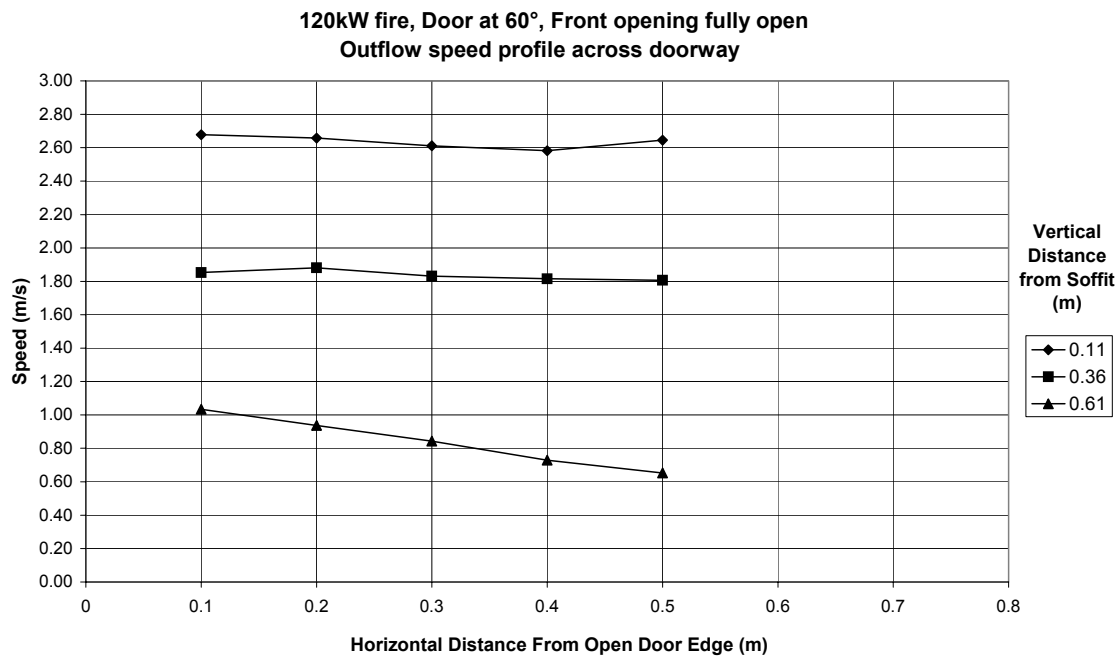


Figure 5.11 Doorway speed profile for outflow section, 120kW fire, burner in centre, 60° door angle, front opening fully open

It can be seen that at the heights nearest the soffit, the speed seen is fairly constant across the doorway. However at the measurement height of 0.61m below the soffit, the temperature decreases across the width of the doorway. It is important to note one measurement at a height of 0.85m below the soffit that reads as an outflow value.

The speed profile for the inflow section is shown in figure 5.12 below. It can be seen that for the majority of the measurement locations the speed is at a maximum at the edge of the doorway and then falls to a minimum near the centre. There are two exceptions, the measurement at 1.11m below the soffit increases across the width of the doorway, and the measurements at 0.85m first increase then decrease eventually changing flow direction entirely.



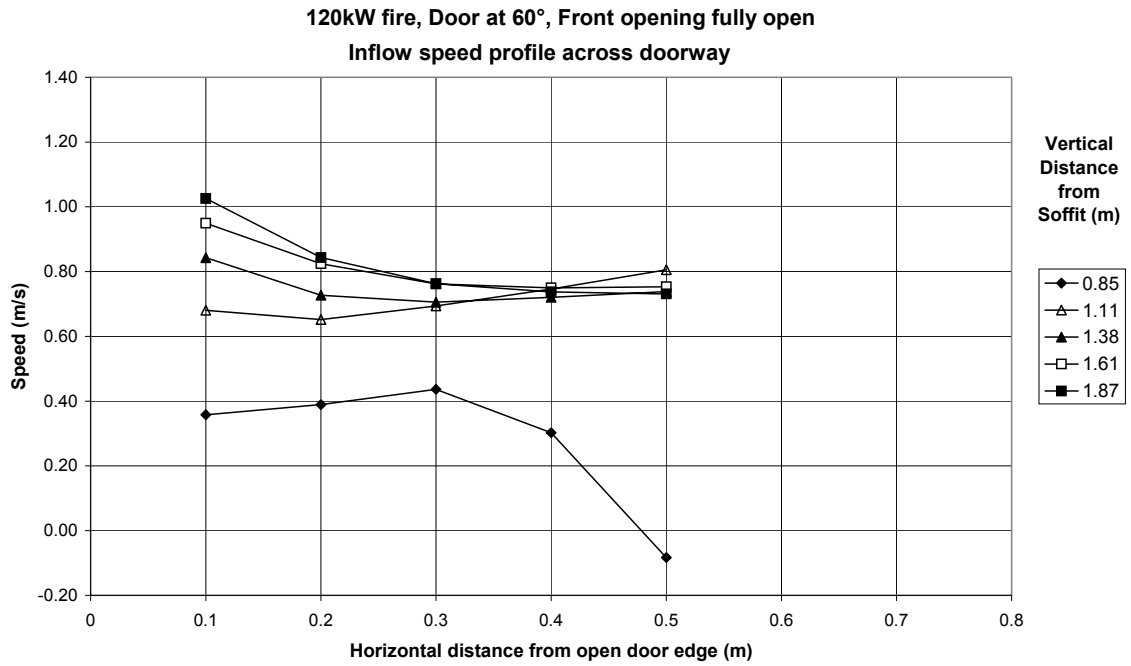


Figure 5.12 Doorway speed profile for inflow section, 120kW fire, burner in centre, 60° door angle, front opening fully open

## 5.3 Front opening as door

### 5.3.1 20° Open Door

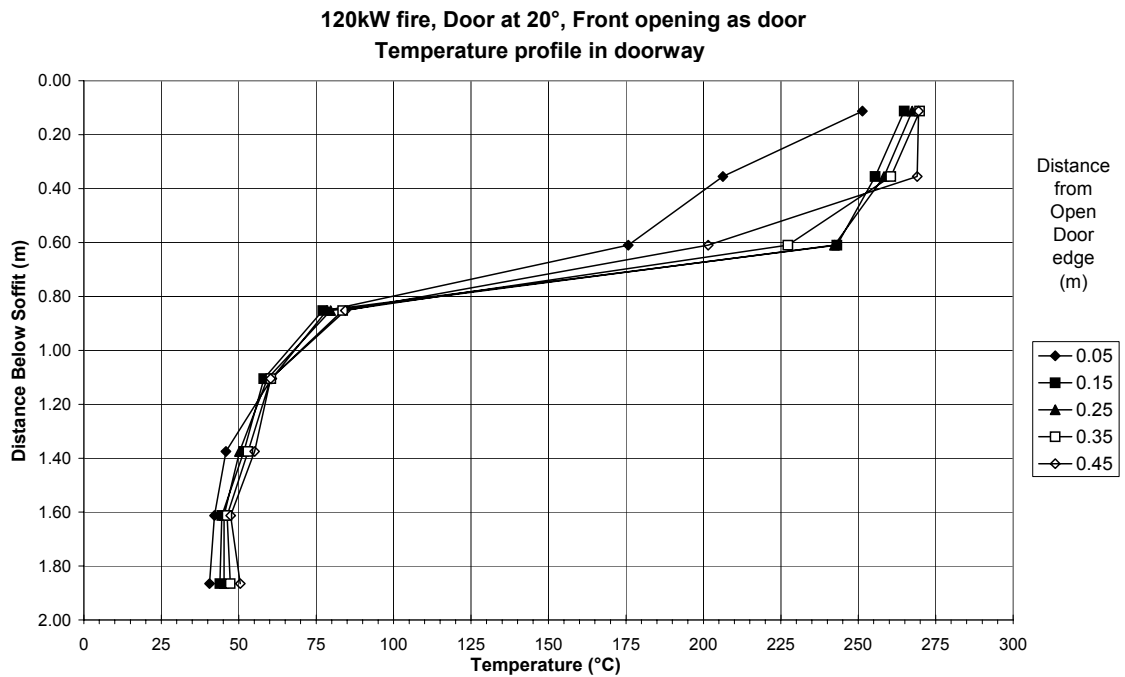


Figure 5.13 Temperature profile in doorway, 120kW fire, burner in centre of compartment, door at 20°, front opening as door

The temperature profile in the doorway is shown in figure 5.13 above. The temperature profile for this experiment shows a less constant lower layer temperature. Again there appears to be a temperature gradient across the doorway at a height of 0.61m below the soffit where the temperature decreases across the width of the doorway.

The speed profile for the outflow section is shown in figure 5.14 below.

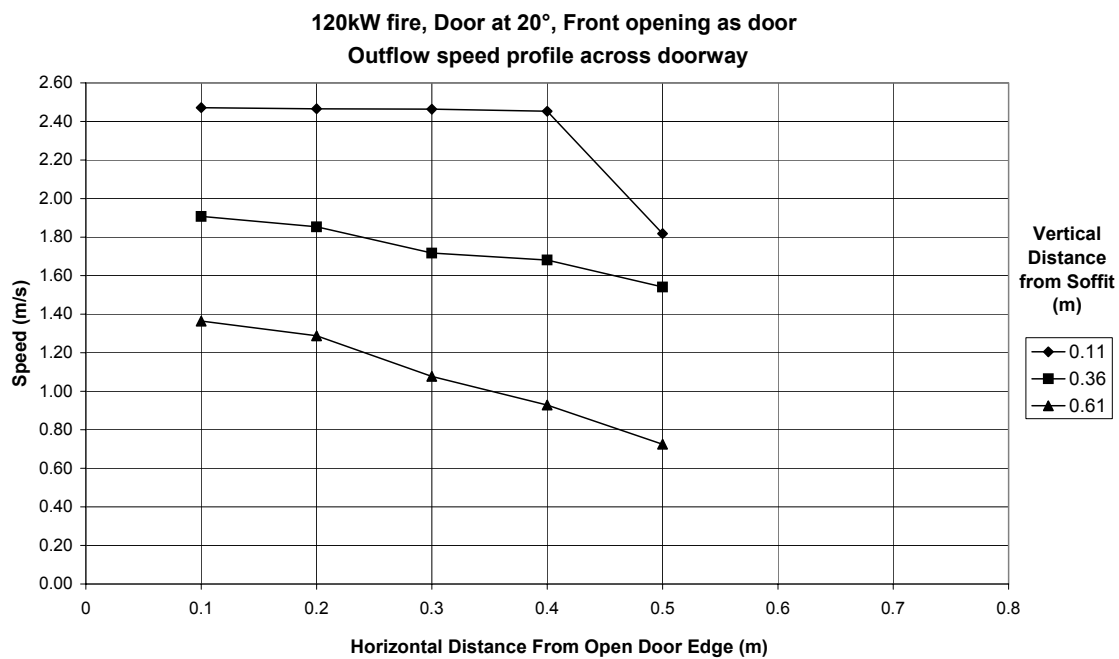


Figure 5.14 Doorway speed profile for outflow section, 120kW fire, burner in centre, 20° door angle, front opening as door

Here the speed in the doorway is seen to decrease across the width of the doorway. The exception is the measurement at 0.11m below the soffit that is constant for all but the final measurement at 0.5m from the open door edge.

The speed profile for the inflow section is shown in figure 5.15 below. It can be seen that the general trend for this data is that the speed falls across the width of the doorway. The exception is the measurement at 0.85m below the soffit where the speed falls across the width of the doorway.

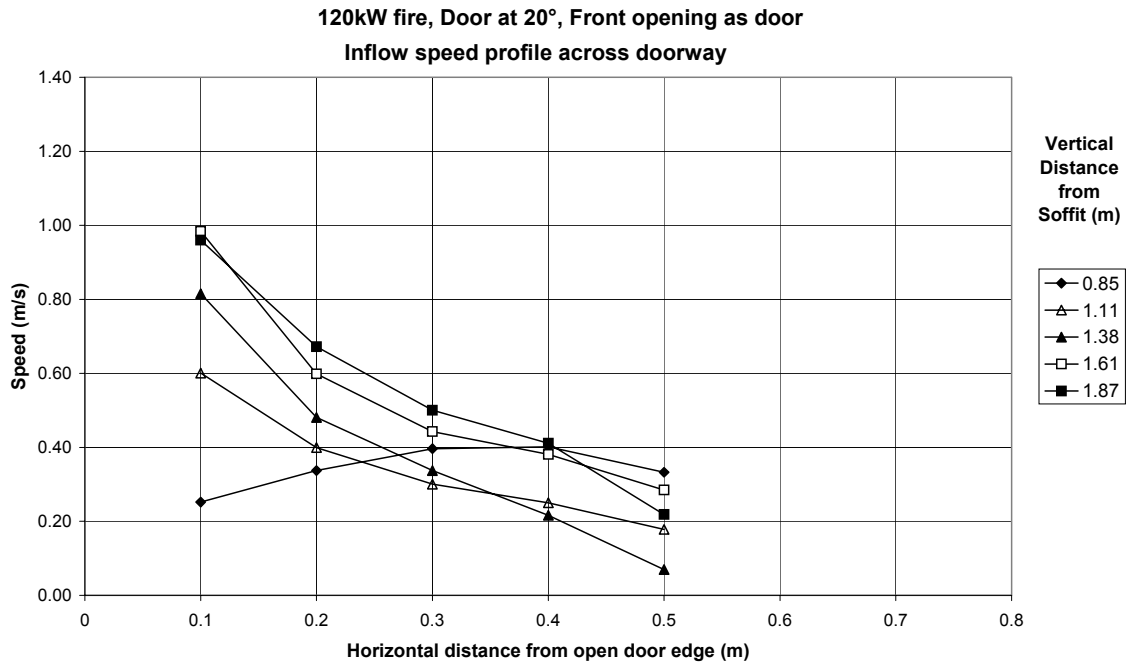


Figure 5.15 Doorway speed profile for inflow section, 120kW fire, burner in centre, 20° door angle, front opening as door

### 5.3.2 30° Open Door

The temperature profile across the doorway is shown in figure 5.16 below.

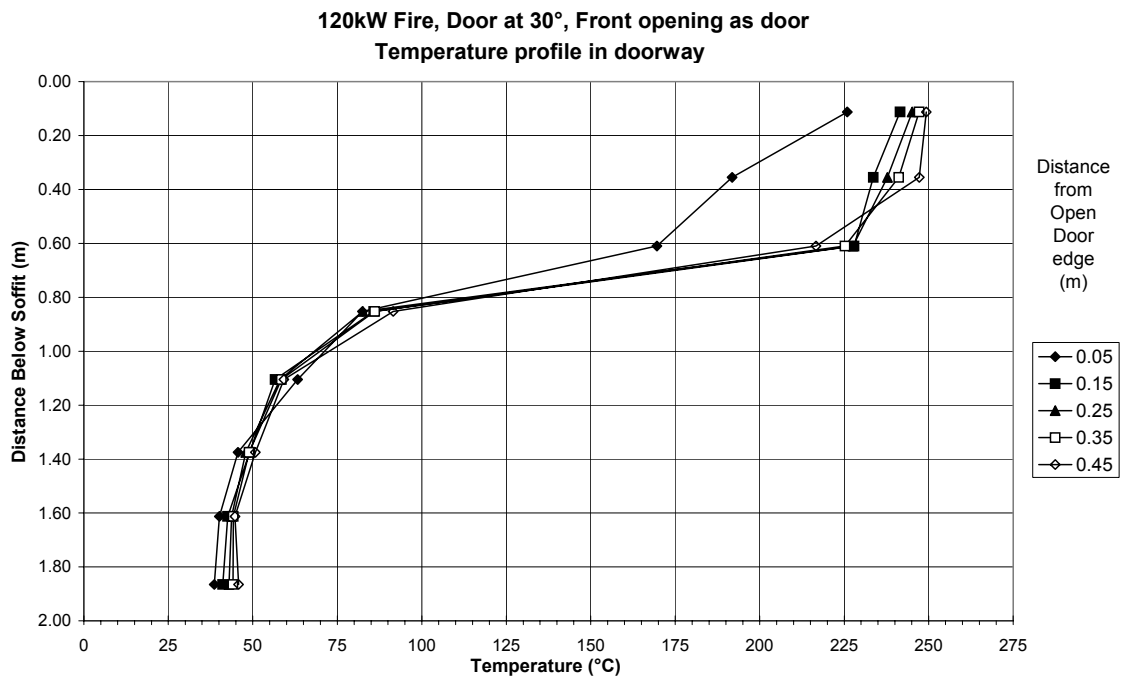


Figure 5.16 Temperature profile in doorway, 120kW fire, burner in centre of compartment, door at 30°, front opening as door

Again it can be seen that the distinction between the upper and lower layer is not as defined as for the runs where the front opening is fully open. The measurements taken at 0.05m from the open door edge differ from the behaviour from the rest of the data that agrees well across the width of the doorway.

The speed profile for the inflow section is shown in figure 5.17 below.

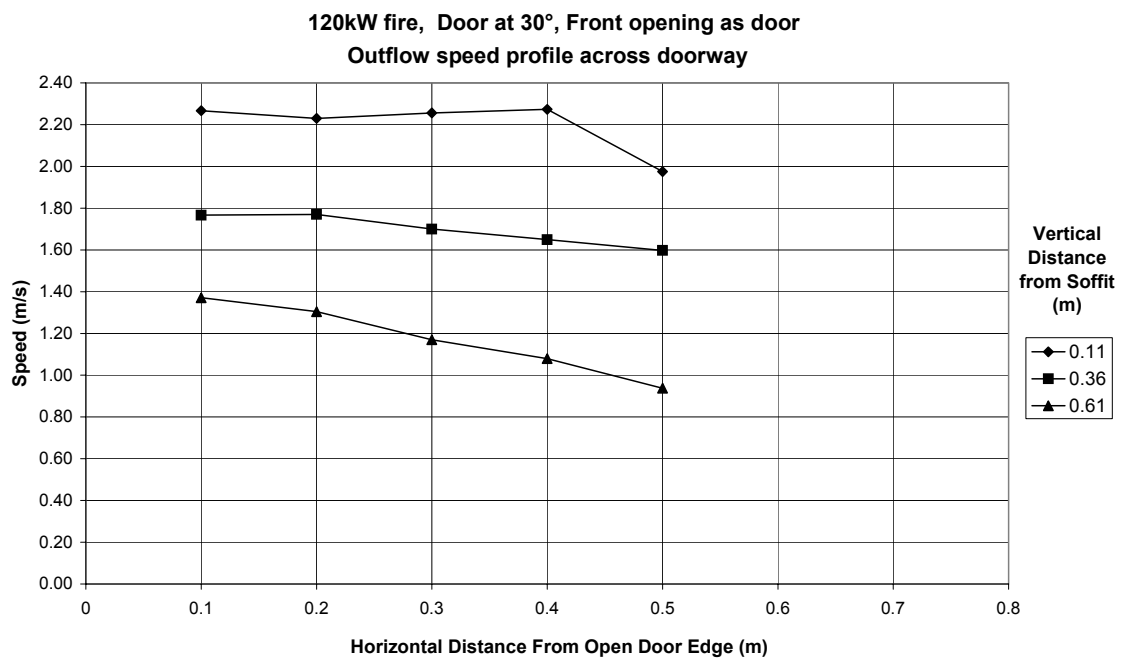


Figure 5.17 Doorway speed profile for outflow section, 120kW fire, burner in centre, 30° door angle, front opening as door

The general trend in this data is that the speed decreases with distance across the width of the doorway. Again however the speed increases with height above the neutral plane.

The speed profile for the outflow section is shown in figure 5.18 below. The general trend in this data is that speed decreases with distance across the width of the doorway. The measurements taken at 0.85m below the soffit however differ from this trend showing a parabolic profile across the width of the doorway.

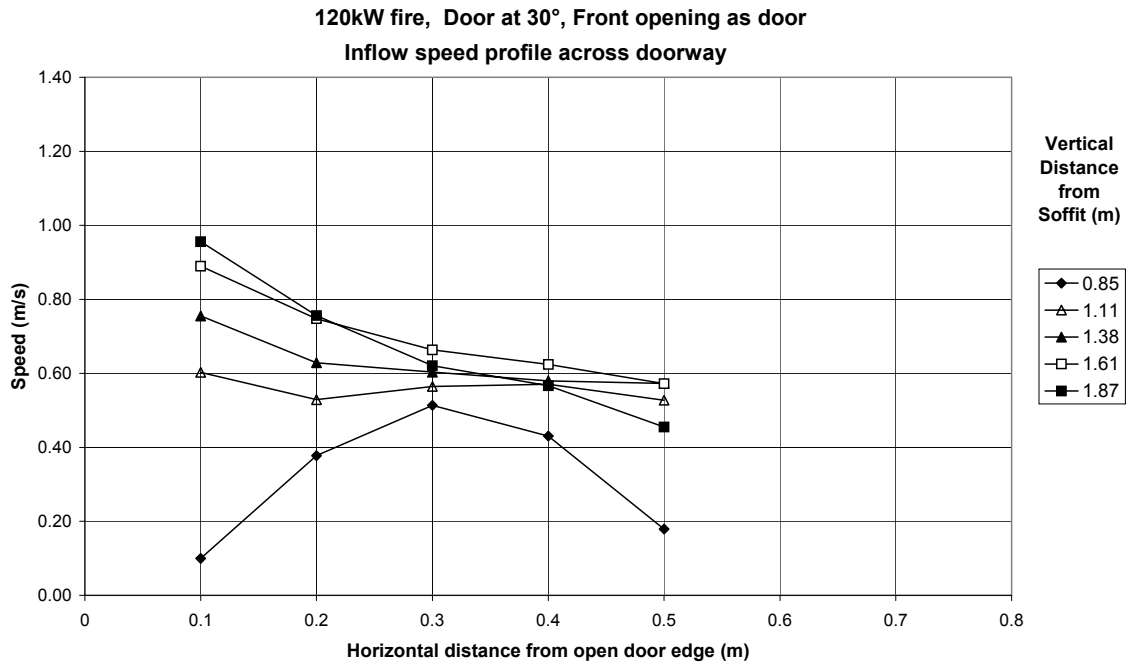


Figure 5.18 Doorway speed profile for inflow section, 120kW fire, burner in centre, 30° door angle, front opening as door

### 5.3.3 40° Open Door

The temperature distribution is shown in figure 5.19 below.

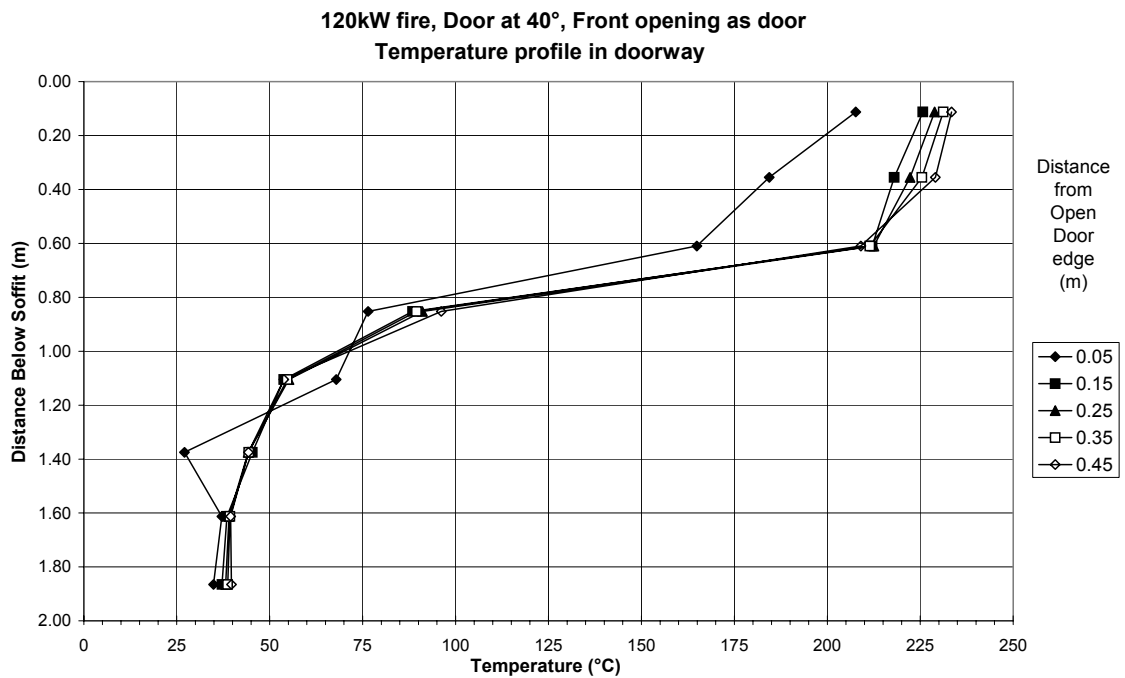


Figure 5.19 Temperature profile in doorway, 120kW fire, burner in centre of compartment, door at 40°, front opening as door

The temperature across the doorway is again constant for most of the width of the doorway with the exception of the measurement at 0.05m from the open door edge. Again the transition from the lower to upper layer in the doorway is not as defined as in the runs where the front opening was fully open.

The speed profile for the outflow section is shown in figure 5.20 below.

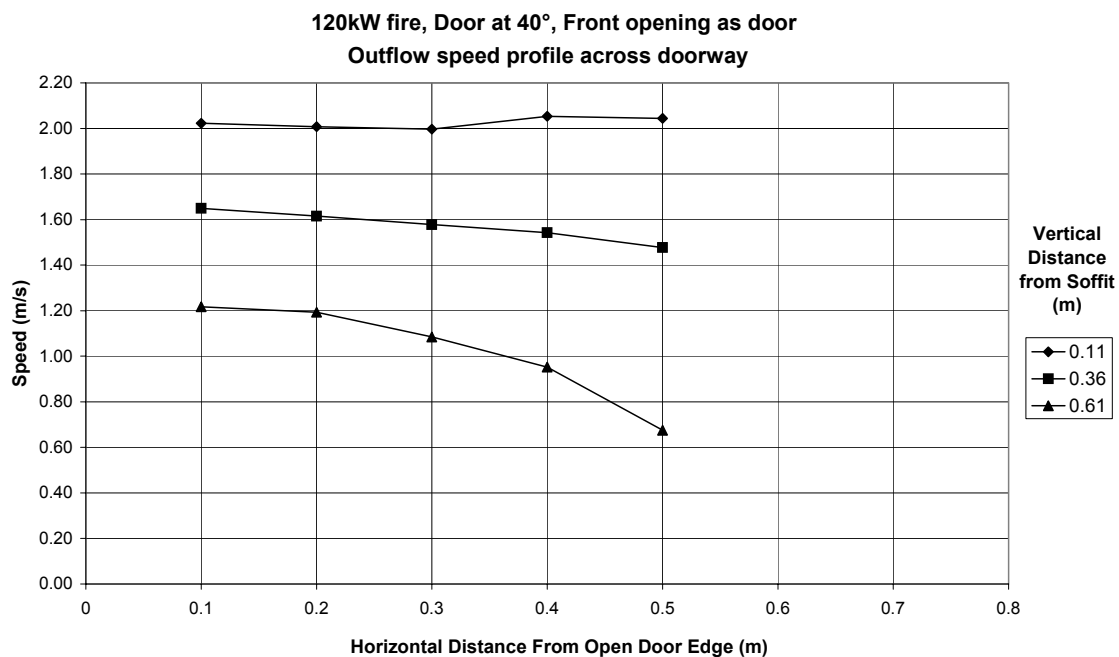


Figure 5.20 Doorway speed profile for outflow section, 120kW fire, burner in centre, 40° door angle, front opening as door

In general the speed decreases across the width of the doorway. The measurement at 0.11m below the soffit however is reasonably constant across the width of the doorway.

The speed profile for the inflow section is shown in figure 5.21 below. In this case the speed profile across the doorway is seen to be maximum at the door edge and fall to a near constant value in the centre of the doorway. The data recorded at 0.85m below the soffit does not display this trend but instead shows a parabolic shaped speed profile across the width of the doorway.

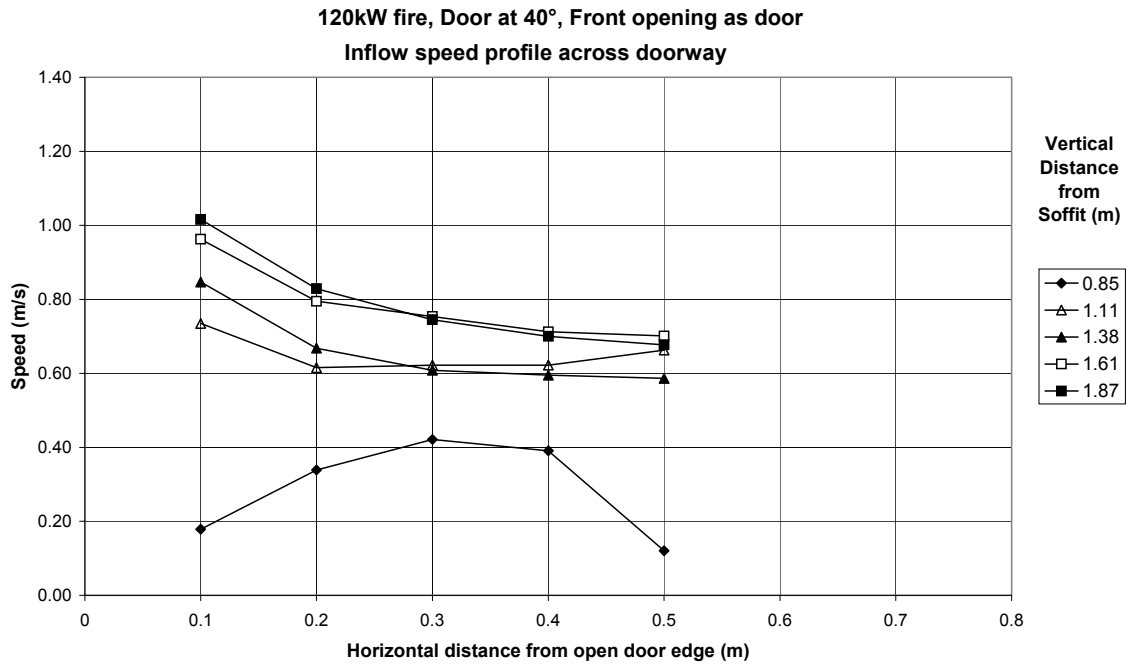


Figure 5.21 Doorway speed profile for inflow section, 120kW fire, burner in centre, 40° door angle, front opening as door

## 5.4 Aspirated Thermocouple comparison

A comparison between the temperature measurements taken with the aspirated and bare wire thermocouples for run 1 is shown in table 5.1 below. The comparison is made for the period where the bare wire thermocouples were 0.45m from the open door edge. The data for the remaining experiments are in Appenix B of this report.

Table 5.1 Comparison of temperature measurements for aspirated and bare wire thermocouples for run 1

<i>Height below Soffit (m)</i>	<i>Aspirated Thermocouple (°C)</i>	<i>Bare wire Thermocouple (°C)</i>	<i>Difference (°C)</i>	<i>% Difference</i>
0.11	270.1	249.3	20.8	8
0.36	239.8	231.3	13.0	4
0.61	36.6	75.7	39.3	-107
1.38	18.0	42.7	24.7	-137
1.61	18.5	35.4	16.9	-92
1.87	17.9	31.2	13.3	-75

Two trends can be seen in this data, for the first two readings the aspirated thermocouple provides the larger measurement. For the remaining four measurements the aspirated thermocouple reads a significantly lower value than the bare wire thermocouple.

## 5.5 Qualitative observations

### 5.5.1 Introduction

The purpose of this section is to discuss observations that were made during the experiments performed with the door in place which may not be shown in the physical data recorded but are thought to be significant.

### 5.5.2 Wind blown plume

During the experiments with the door in place the flame was seen to tilt towards the compartment wall. This consistently happened at all door angles but was not observed in any experiment when the door was not present in the compartment.

The flame was blown towards the wall of the compartment nearest the open door edge this situation is illustrated in figure 5.22 below.

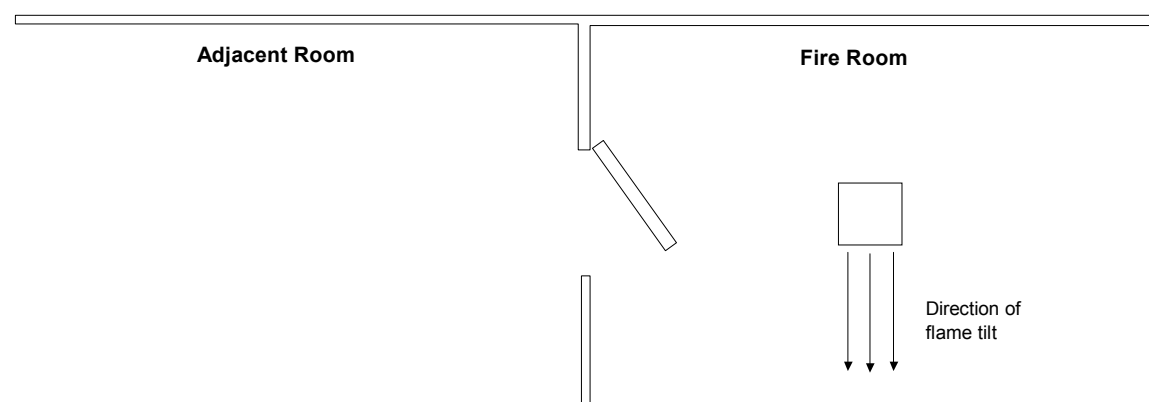


Figure 5.22 Direction of flame tilt observed in relation to fire compartment system

### 5.5.3 Flame behaviour

the flame also exhibited another interesting behaviour. It would periodically perform a slow rotation in tilt direction around the burner. This rotation was always in the same



direction and occurred at semi regular intervals. The flame during this rotation appeared to move in a spiral like motion.

## **5.6 Discussion**

### **5.6.1 Speed profiles**

It is clear through comparing the speed profiles across the doorway with the experiments performed with no door present, that the door is having a major effect on this part of the system.

One trend however remained the same, that is that the speed in the doorway increases with distance from the neutral plane. This is however expected behaviour and was discussed in the previous section.

Two other trends were of more interest. The first is the fact that the maximum speeds observed in the system increased with decreasing door angle. The second is that the observed speed decreased across the width of the doorway. These two observations can be explained by considering the effect that adding the doorway has on the system. The addition of the doorway acts as a throttling valve across the vent. This means that the area of the vent is dramatically decreased; this will lead to higher velocities being present in the system due to a similar volume of gas being required to flow out of a much smaller area. The speed is seen to decrease across the width of the doorway due to the door disrupting the symmetry of the system. Obviously the gases cannot flow through the doorway; therefore they are forced to flow through the remaining gap in the system. This will lead to the induced flows in the compartment being asymmetric around the doorway. This means that the majority of the flow will cross the doorway as close to the open door edge as possible. This will result in higher speeds being recorded in this section of the doorway.

### **5.6.2 Fire plume behaviour**

It is interesting to note that the tilting of the plume was only seen once the doorway was added to the compartment. Literature would suggest that flame tilt would be expected in

all of the experiments performed. A series of experiments were performed at the NBS to investigate this phenomenon (Quintere 1981). These experiments were performed in a compartment with one door-sized vent that was fully open to the ambient surroundings, a series of experiments were performed with fire sizes of 62.9 and 158kW. In these experiments the flame was seen to tilt to the wall opposite the open vent by 30 to 40 degrees. The room dimensions were similar in scale to those in this experiment at 2.8m x 2.8mx2.13m high.

The only major difference in this experiment is the addition of the second room, however the mass flow rates that were reported through the door are equivalent to what was measured in these experiments.

The flame tilt towards the wall can be partially explained by the looking at the speed behaviour within the fire compartment in the lower layer. The flow through the doorway will be directed towards the compartment wall on the open door edge side. The air in the lower layer on the other side will be relatively stagnant. If we look at Bernoulli's equation:

$$P_1 + \rho_1 \frac{u_1^2}{2} + \rho_1 g z_1 = P_2 + \rho_2 \frac{u_2^2}{2} + \rho_2 g z_2 \quad (5.1)$$

The we consider two discrete points in the lower layer of the compartment, point one near the wall on the open door edge side, point two on the other side of the compartment at the same height. This is illustrated in figure 5.23 below.

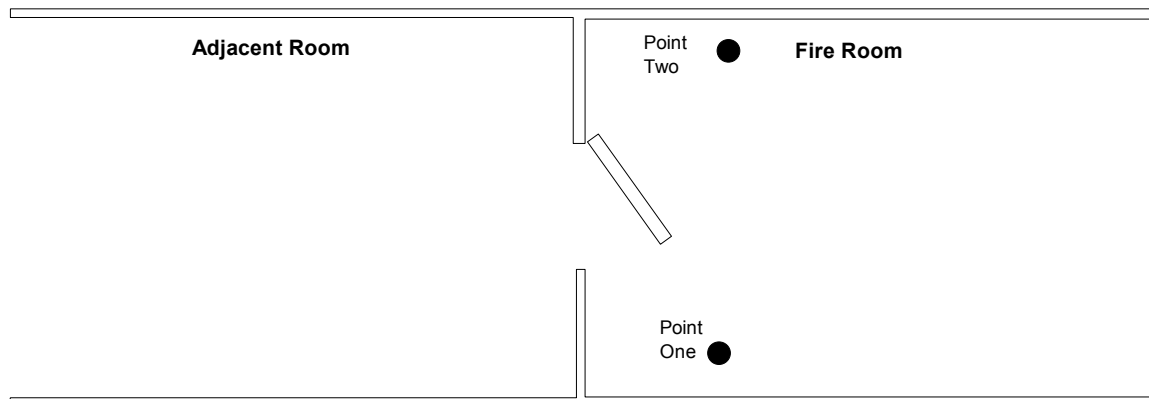


Figure 5.23 Points in compartment for Benoulli's analysis

As both points are at the same height and point two is stagnant in comparison to point one then equation 5.1 reduces to:

$$P_1 + \rho_1 \frac{u_1^2}{2} = P_2 \quad (5.2)$$

It can therefore be seen that there is a pressure gradient formed between the two points and that the pressure at point two will be larger than the pressure at point one. This situation would not last long as an induced velocity would be caused in the compartment to equalise the pressure. This would be in the direction of point two to point one and would lead to the flame tilt observed.

The two induced velocities in the compartment will lead to a rotational airflow being induced in the compartment as the flows hit the back wall and are forced to flow around the walls. This could account for the periodic flame spiral behaviour that was seen to exist.

### 5.6.3 Temperature Profiles

In general the temperature profiles observed in the compartment with the doorway show similar behaviour to those without the door. The same clear two layer behaviour is exhibited where the lower layer is characterised by a near constant temperature.

Two important differences are observed however, the first is that the temperatures in the compartment are hotter this is summarised in table 5.2 below. It should also be noted that the temperatures in the compartment increase as the door angle decreases. This is most likely due to a reduction in the radiative heat transfer from the fire compartment due to the decrease in effective door area. This will result in less heat loss from the upper layer and the resultant increased temperature.

Table 5.2 Comparison of maximum upper layer temperatures for fully open front opening experiments

<i>Door Angle</i>	<i>Maximum Upper layer Temperature</i>
(°)	(°C)
20°	260
30°	230
40°	215
60°	200
Fully open	180

The second difference is the temperature gradient that is observed at the measurements taken at 0.61m below the soffit. This is in the region that the neutral plane would be located. The fact that the temperature decreases across the width of the doorway suggests that the neutral plane height increases across the width of the doorway. This suggests that the neutral plane is tilted on an angle when a door is placed in position. Again it is observed that this behaviour is most severe when the door angle is minimised and that the behaviour tends to open door behaviour when the door angle is increased.

This phenomenon can also be seen in the comparison between the aspirated and bare wire thermocouple data. The measurement at 0.61m below the soffit shows a large discrepancy of 39.3°C, but it is important to note the position of each of the measurements. The bare wire thermocouple measurements were taken at 0.045m from the open door edge whereas the aspirated thermocouple readings were taken at 0.65m from the open door edge. This represents a significant difference in position across the doorway. For this reason it suggests that for this measurement the difference between the aspirated and bare wire thermocouple readings are at least partially due to an actual temperature gradient rather than error introduced by the method of measurement. This is supported by a comparison of this result with those presented for the case where the door is open. In both cases the aspirated thermocouple read a higher temperature in the upper layer and a lower temperature in the lower layer. The only significant difference between these data sets is the measurement at 0.61m below the soffit, where the aspirated thermocouple reading would be predicted to be higher it is actually significantly lower.

#### **5.6.4 Repeatability of results**

Due to time constraints there were no duplicate runs performed to assess the repeatability of results. In the case of the runs where the door leaf was added to the compartment there is the possibility of comparing the flow behaviour through the doorway due to runs being performed at the same door angle, fire placement and size but a different front opening configuration.

This makes some comparisons possible between these experiments. However it should be noted that the addition of the front opening will lead to some alteration in the driving force for the fire induced flows, this is due to the presence of a much deeper upper layer in the adjacent compartment. This leads to some differences that are consistent across all the experiments performed. The first is the temperature profile in the inflow section changes, when the front opening is fully open the profile shows a constant near ambient temperature and a sharp transition to the outflow section. When the front opening is a door however the temperature profile shows a gradual increase in the inflow section, which leads to a less clear transition to the outflow section. It should also be noted that the temperature gradient across the width of the doorway does not appear to occur in these experiments.

The second difference is that the maximum temperature in the doorway is slightly increased by the addition of the second doorway. This increase in temperature is fairly small however and consistently falls in the level of 25°C.

The third difference is that the maximum speeds observed in the outflow section are higher when the front opening is fully open. This is generally only by the order of 0.5m/s. This result can be explained by considering the pressure difference across the doorway. The closing of the front opening causes a deeper, hotter upper layer to form in the adjacent compartment. This results in the pressure difference in the upper layer to decrease and therefore reduces the induced flow through the doorway in this section.

If we ignore the differences in the data as noted above and concentrate on the shape of the speed distributions that are seen in each run, then we can see some close agreement between runs with identical door angles. For example, if we look at the speed

distribution for the outflow for the two 20° open experiments (Figures 5.2, 5.14). The same behaviour is seen, the measurements at 0.11m from the soffit are nearly constant until the measurement at 0.5m from the door edge where it falls in both cases, whereas the other two measurements fall across the whole width of the doorway. Again if we look at the speed distribution for the inflow section then in both cases the trend is for a consistent decrease in speed across the width of the doorway. This similarity in trends is seen to continue across the remaining two experiments. The only measurement that consistently differs between the two experiments is the speed measurements made at 0.85m below the soffit. These are seen to exhibit quite unpredictable behaviour in the majority of the experiments. This is most likely due to this measurements proximity to the neutral plane and the localised turbulence that is likely to exist in this region.

### **5.6.5 Mass flow rate predictions**

In these experiments, due to limitations in equipment speed and temperature, measurements were not taken across the whole width of the doorway. This prevents the mass flow rate from being calculated across the whole width of the doorway without some method to predict for the missing data points. This is a relatively simple process for the experiments where no door is present for two reasons. The first is that the flow through the doorway can be assumed to be symmetrical across the width of the doorway. This was shown in the experiments performed at the NBS (Steckler 1982) and the BRI in Japan (Nakaya 1986). The second is that the neutral plane is a constant height across the doorway. For this reason an adequate approximation for the mass flow rate through the doorway can be found by doubling the flow rate measured across half the doorway.

Problems arise in applying this method to the system when the door is in place. This is because these two assumptions have been shown to be no longer valid. The flow through the door way is seen to be asymmetrical and the neutral plane height varies across the width of the doorway. For this reason the missing readings must be found by extrapolating the speed and temperature profiles across the width of the doorway.

This process was not performed for the data shown in these experiments. The purpose of this experiment is to report the experimental findings of the effect of placing a

doorway into a fire compartment. The effect of performing the required extrapolations would mean that the results presented would no longer be classified as experimental results but would be the author's interpretation of the flow behaviour. This is due to the unknown nature of the flow patterns near the closed-door edge. This can be seen especially in the experiments performed with shallow door angles, for example run 1, where a 20° door angle was used. Examining Figure 5.3 it appears that if the current trend continues that the speeds will fall to below 0 m/s. The question is what happens at this point? Does the flow in this section reverse and flow out of the compartment? Is there a localised stagnation of flow at this point? Does the speed actually start to increase within this section? All of these scenarios are possible. To choose one over the other would require judgements of the flow behaviour in this situation. As there are previous experiments to draw experience from I feel that at this stage it would be premature to report such extrapolated data.

This shows however that there is a clear impetus to continue experiments along these lines with measurements being able to be taken across the full width of the doorway.

#### **5.6.5 Errors in speed measurements**

It is important to note that the bi-directional probes used in these experiments are said to be accurate if the air flow they are measuring is misaligned by no more than 50° from the probe head (Emmons 1997). In these experiments it is possible that more misalignment than this occurs. This could lead to substantial errors in the speed reported.

It is difficult to judge whether or not this has occurred, as visualisation of the flow patterns within the experiments is extremely difficult to achieve. This possible error is hard to eliminate, as the ability of the bi-directional probes to record speeds even when misaligned is their major advantage over other flow measurement devices in fire situations.





## 6 Conclusions

This experiment has confirmed the behaviour seen by other researchers for the fire-induced flow through an opening when the door is fully open. The most significant of these is the speed profile that is exhibited across the doorway. It was shown that this was at a maximum at the edge of the doorway and fell to a minimum in the centre of the doorway. It was also seen that the repositioning of the fire location from the centre of the compartment to the back wall leads to a reduction in the magnitude of the fire induced flow observed.

Two areas of turbulence through the doorway were observed, the first near the edges of the doorway, and the second in the proximity of the neutral plane. It was seen that this consistently affected the measurements that were made in these positions.

The introduction of a door leaf to the system was seen to have a large effect on the entire system. In the doorway itself the speed profile changed dramatically from that of the fully open case. The speed recorded across the doorway was now seen to fall across the width of the doorway. It was also seen that the neutral plane height was no longer constant across the width of the doorway. The effect of the door on the behaviour in the system was seen to decrease with increasing door angle.

The effect of the door on the system was not limited to the door however. The upper layer temperature in the compartment was seen to increase with the addition of the door due to a reduction in heat loss due to radiation. More dramatically the behaviour of the flame was effected. The flame developed a tilt that was not present in the experiments performed without the door in place. This suggests that there is an induced flow created within the fire compartment.

A comparison of temperature measurements made with bare wire and aspirated thermocouples was conducted. This was to estimate the level of error in temperature measurements made within the compartment. It was found that a significant discrepancy existed between the two measurements. This effect was most significant in measurements made in the lower layer where the aspirated thermocouples consistently provided a lower temperature reading.



## 7 Recommendations

The experiments performed at McLeans Island have indicated that the addition of a doorway into a fire compartment system leads to some interesting and major changes in the flow behaviour that is observed in the system. However this report has been hampered to some degree due to limitations in the experiments that were performed. This suggests that it would be beneficial to repeat some or all of the experiments discussed in this report but with the following additions.

- Speed measurements across the full width of the doorway. The number of probes in the doorway could also be increased to improve mass flow predictions.
- Aspirated thermocouples used for all temperature measurements
- Incorporate flow visualisation techniques to allow the flow patterns within the fire compartment and the neutral plane height to be observed
- Repetition of experiments to test consistency of results.

However it is recognised that the implementation of all of these changes is neither feasible nor practical.

It is recommended for the system to be modelled within a CFD package to investigate the ability of these systems to replicate the results of these experiments.

It is recommended that the results for the open door case be compared to published correlations for the induced mass flow rate. In particular it is recommended that the flow coefficients for this compartment system be investigated.



## References

EMMONS, H. W. (1975) Fire Induced Flow Through an Opening.. *Combustion and Flame*, **25**. 369-385

EMMONS, H. W. (1995) Vent Flows. Section 2-5 SFPE Handbook of Fire Protection Engineering. Society of Fire Protection Engineers, Massachusetts U.S.A

HALL, J. R. (2000) *Burns, toxic gases and other hazards associated with fires: Deaths and injuries in fire and non-fire situations*. Natonal Fire Protection Association Quincy Ma, U.S.A

ISO 9705 (1993) *Full Scale Room test for Surface Products*, International Standards Orginisation , Geneva Switzerland

KAWAGOE, K (1958) *Fire behaviour in Rooms*. Building Institute Institute report No. 27, University of Construction, Tokyo, Japan

LOU, M (1997) Effects of Radiation on Temperature Measurement in a Fire Enviroment. *Journal of Fire Sciences*. **15**, 443-461

NAKAYA, I. *et. al.* (1986) Doorway Flow Induced by a Propane Fire. *Fire Safety Journal*. **10**. 185-195

NEILSON, C. (2000) *An analysis of Pre-Flashover Fire experiments with Field Modelling Comparisons*. Fire Engineering Research Report 2000/10, Department of Civil Engineering, University of Canterbury

QUINTERE, J. G., RINKINEN, W. J., JONES, W. W. (1981) The Effect of Room Openings on Fire Plume Entrainment. *Combustion Science and Technology*. **26**, 193-201

ROCKETT, J. A. (1976) Fire Induced Gas Flow in an Enclosure. *Combustion Science and Technology*. **12**, 165-175

RUTHERFORD, L (2002), *Experimental Results for Pre-flashover Fire Experiments in Two Adjacent ISO Compartments* Fire Engineering Research Report 2002/?, Department of Civil Engineering, University of Canterbury

STECKLER, K. D., QUINTERE, J. G., RINKINEN W. J. (1982) Flow Induced by Fire in a Compartment. *Proc. 19th International Symposium on Combustion*. 913-920

STECKLER, K. D., BAUM, H. R., QUINTERE, J. G. (1986) Fire Induced Flow Through Room Openings – Flow Coefficients. *Proc. 20th International Symposium on Combustion*. 1591-1600

# Appendix A

This appendix contains the raw data for the experiments performed with the door fully open as discussed in section 4 of this report

## A.1 Burner in Centre of Compartment

### A.1.1 60kW Fire Size

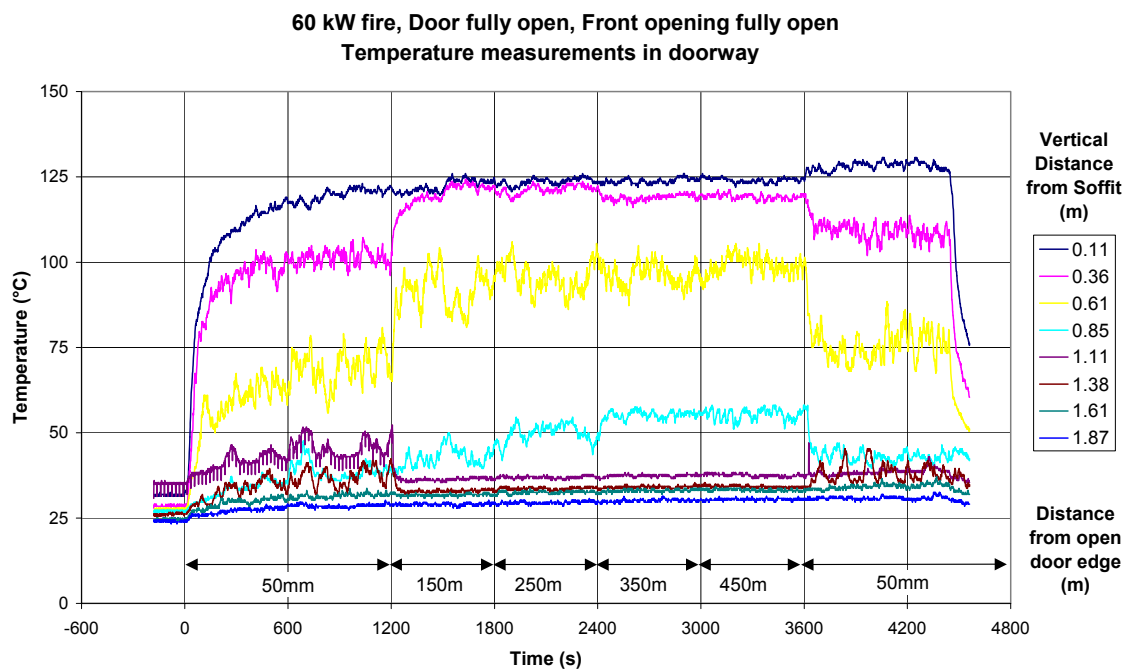


Figure A.1 Doorway temperature measurements for duration of experiment, 60kW fire in centre of compartment, fully open door, front opening fully open

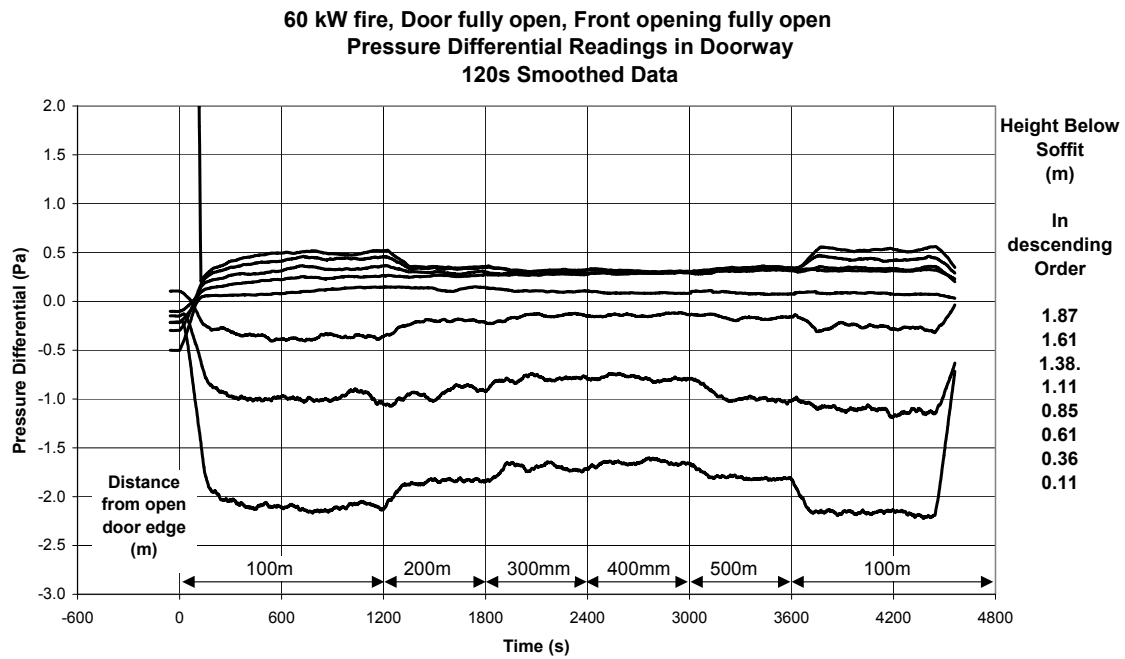


Figure A.2 Doorway pressure differential measurements for duration of experiment, 60kW fire in centre of compartment, fully open door, front opening fully open, 120s smoothed data

Table A.1 Comparison of temperature measurements for aspirated and bare wire thermocouples, 60kW fire in centre of compartment, fully open door, front opening fully open

<i>Height below Soffit (m)</i>	<i>Aspirated Thermocouple (°C)</i>	<i>Bare wire Thermocouple (°C)</i>	<i>Difference (°C)</i>	<i>% Difference</i>
0.11	129.0	128.1	1.1	1
0.36	127.8	109.9	17.8	14
0.61	102.1	76.1	26.1	26
1.38	23.6	43.7	20.1	-85
1.61	22.2	38.2	16.0	-72
1.87	22.4	38.0	15.6	-70



### A.1.2 120kW Fire Size

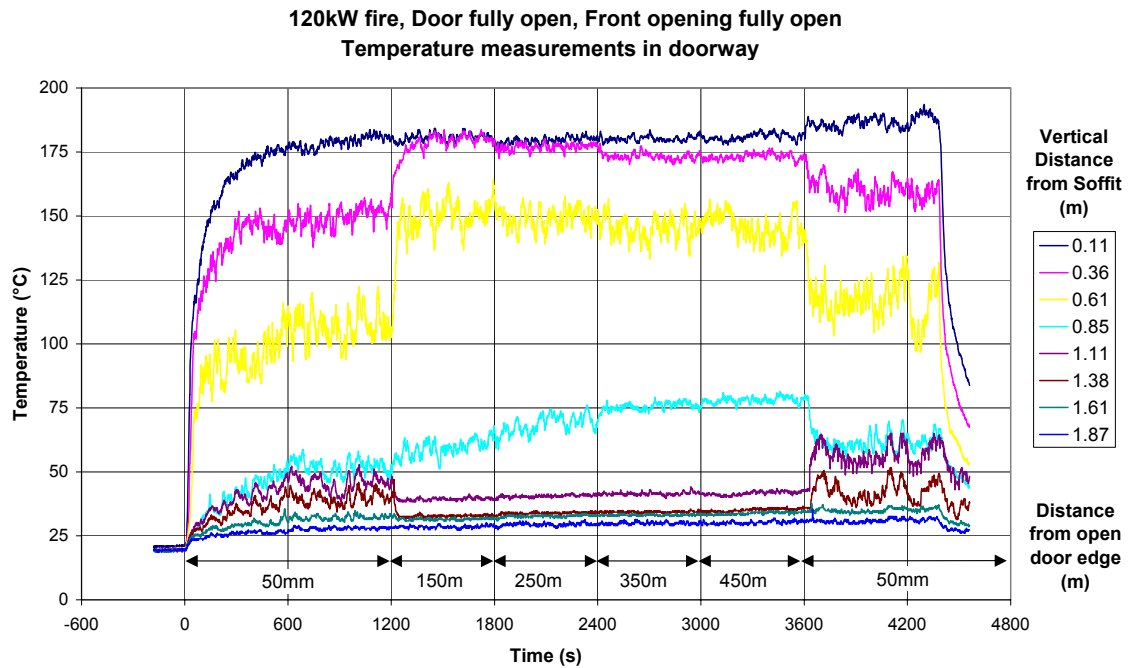


Figure A.3 Doorway temperature measurements for duration of experiment, 120kW fire in centre of compartment, fully open door, front opening fully open

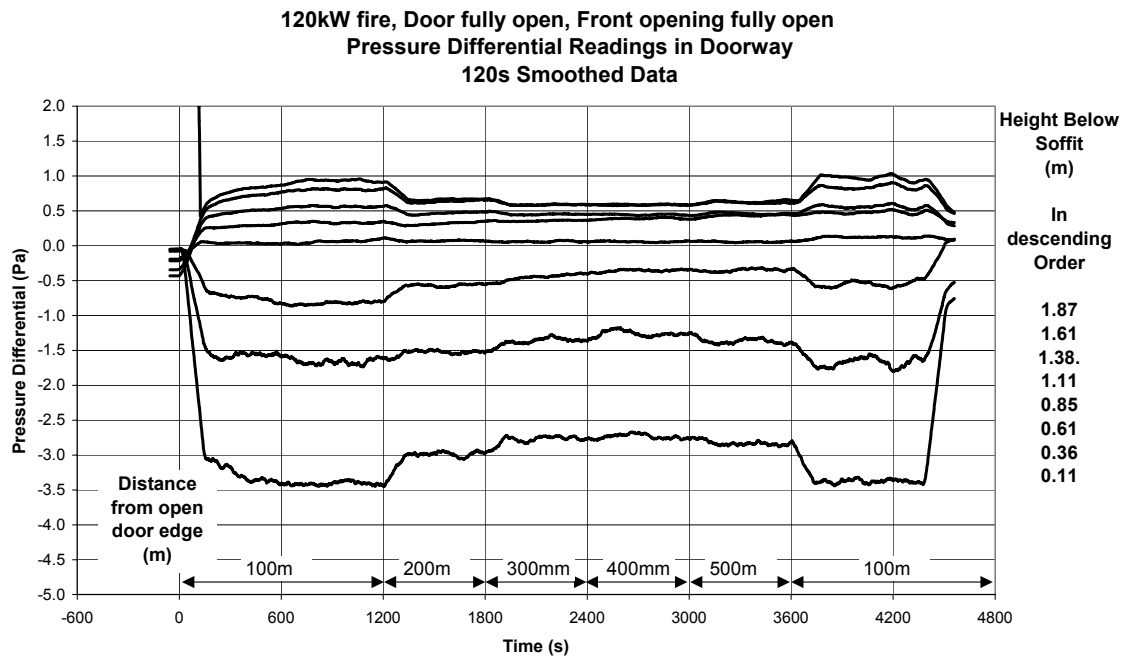


Figure A.4 Doorway pressure differential measurements for duration of experiment, 120kW fire in centre of compartment, fully open door, front opening fully open, 120s smoothed data

Table A.2 Comparison of temperature measurements for aspirated and bare wire thermocouples, 120kW fire in centre of compartment, fully open door, front opening fully open

<i>Height below Soffit (m)</i>	<i>Aspirated Thermocouple (°C)</i>	<i>Bare wire Thermocouple (°C)</i>	<i>Difference (°C)</i>	<i>% Difference</i>
0.11	193.0	186.1	6.9	4
0.36	192.2	160.9	31.3	16
0.61	159.1	118.5	40.6	25
1.38	20.8	62.5	41.7	-201
1.61	19.9	56.4	36.6	-184
1.87	20.4	42.3	21.9	-107

### A.1.3 180kW Fire Size

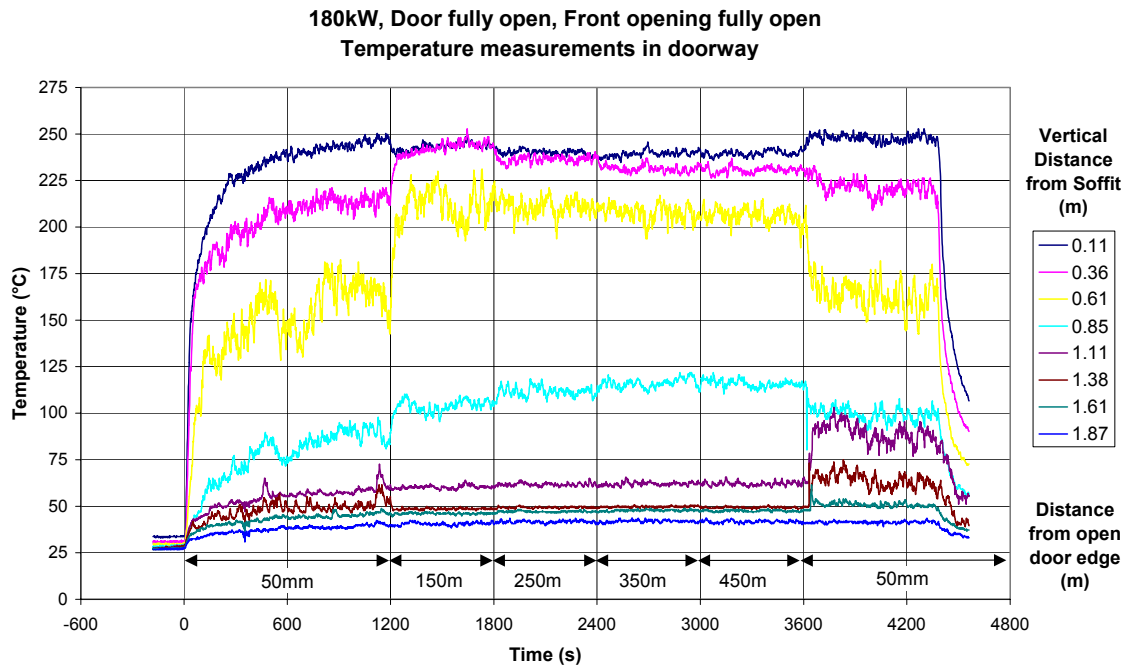


Figure A.5 Doorway temperature measurements for duration of experiment, 180kW fire in centre of compartment, fully open door, front opening fully open

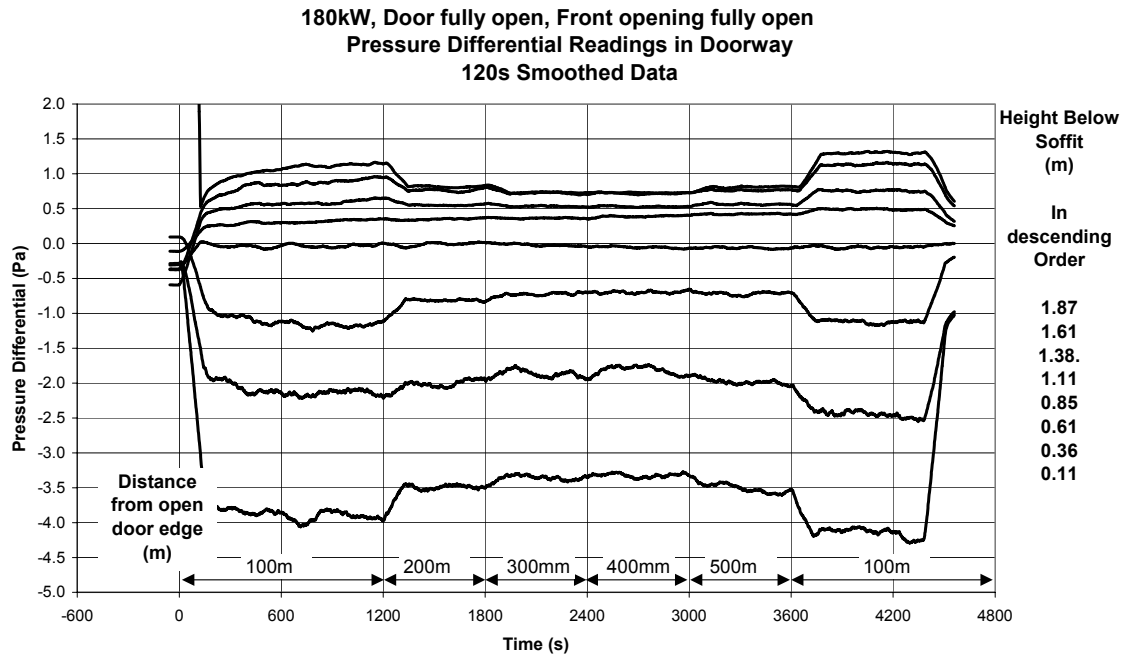


Figure A.6 Doorway pressure differential measurements for duration of experiment, 180kW fire in centre of compartment, fully open door, front opening fully open, 120s smoothed data

Table A.3 Comparison of temperature measurements for aspirated and bare wire thermocouples, 180kW fire in centre of compartment, fully open door, front opening fully open

<i>Height below Soffit (m)</i>	<i>Aspirated Thermocouple (°C)</i>	<i>Bare wire Thermocouple (°C)</i>	<i>Difference (°C)</i>	<i>% Difference</i>
0.11	256.0	247.6	8.3	3
0.36	253.1	221.8	31.3	12
0.61	224.4	165.9	58.5	26
1.38	27.2	100.3	73.1	-269
1.61	26.2	88.8	62.6	-239
1.87	26.3	63.6	37.4	-142

## A.2 Burner on Walls of Compartment

### A.2.1 Burner in Corner

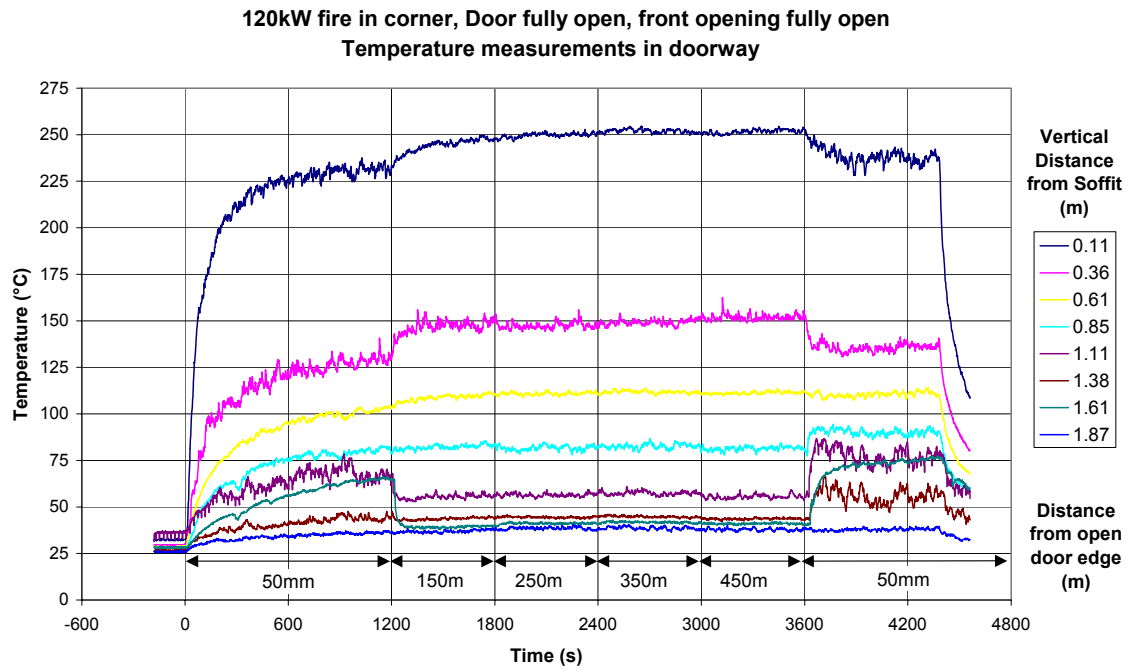


Figure A.7 Doorway temperature measurements for duration of experiment, 120kW fire in corner of compartment, fully open door, front opening fully open

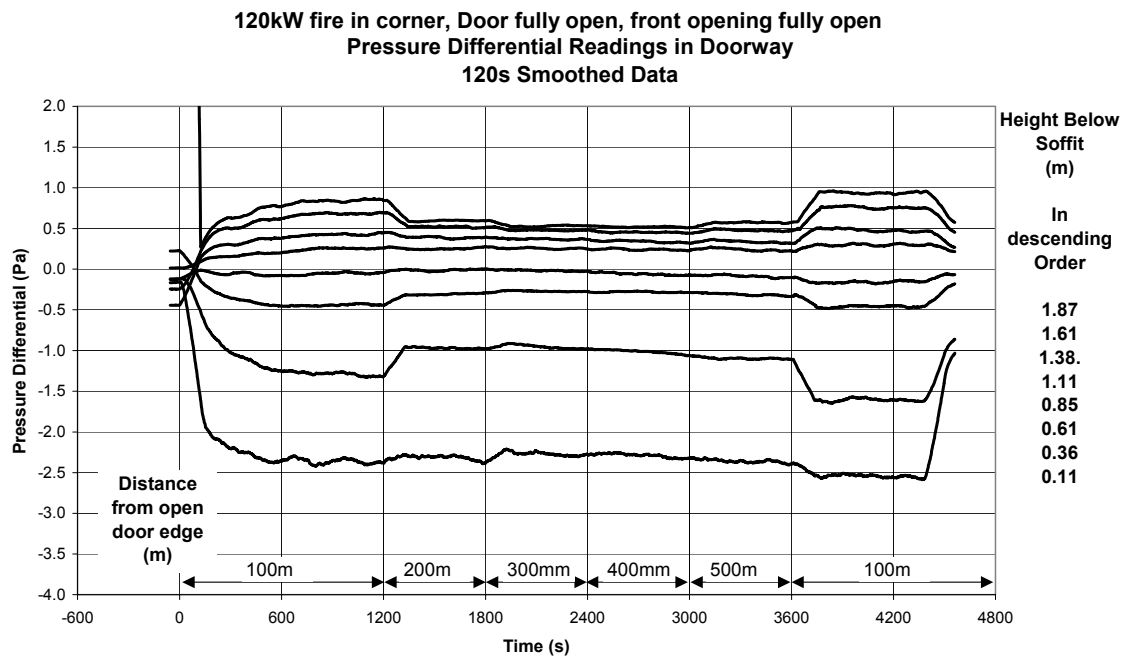


Figure A.8 Doorway pressure differential measurements for duration of experiment, 120kW fire in corner of compartment, fully open door, front opening fully open, 120s smoothed data

Table A.4 Comparison of temperature measurements for aspirated and bare wire thermocouples, 120kW fire in corner of compartment, fully open door, front opening fully open

<i>Height below Soffit (m)</i>	<i>Aspirated Thermocouple (°C)</i>	<i>Bare wire Thermocouple (°C)</i>	<i>Difference (°C)</i>	<i>% Difference</i>
0.11	281.8	239.4	42.4	15
0.36	153.3	135.9	17.4	11
0.61	80.0	110.2	30.2	-38
1.38	24.2	89.9	65.6	-271
1.61	23.4	77.5	54.1	-231
1.87	24.2	55.4	31.2	-129

### A.2.2 Burner on Back Wall

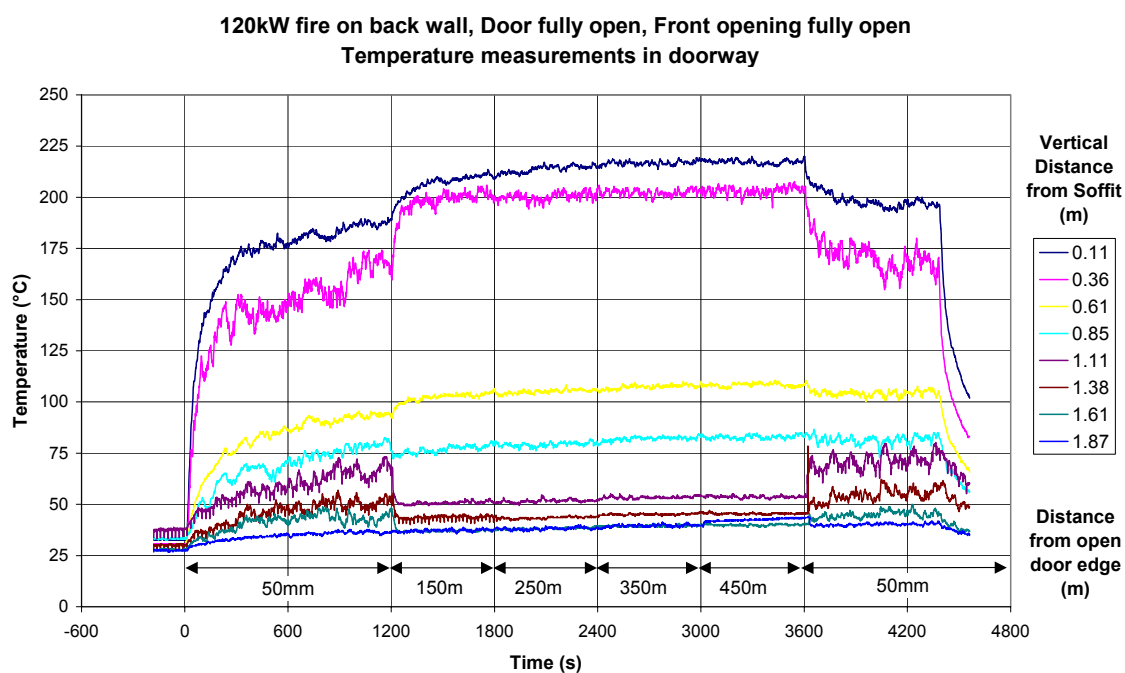


Figure A.9 Doorway temperature measurements for duration of experiment, 120kW fire on back wall, fully open door, front opening fully open

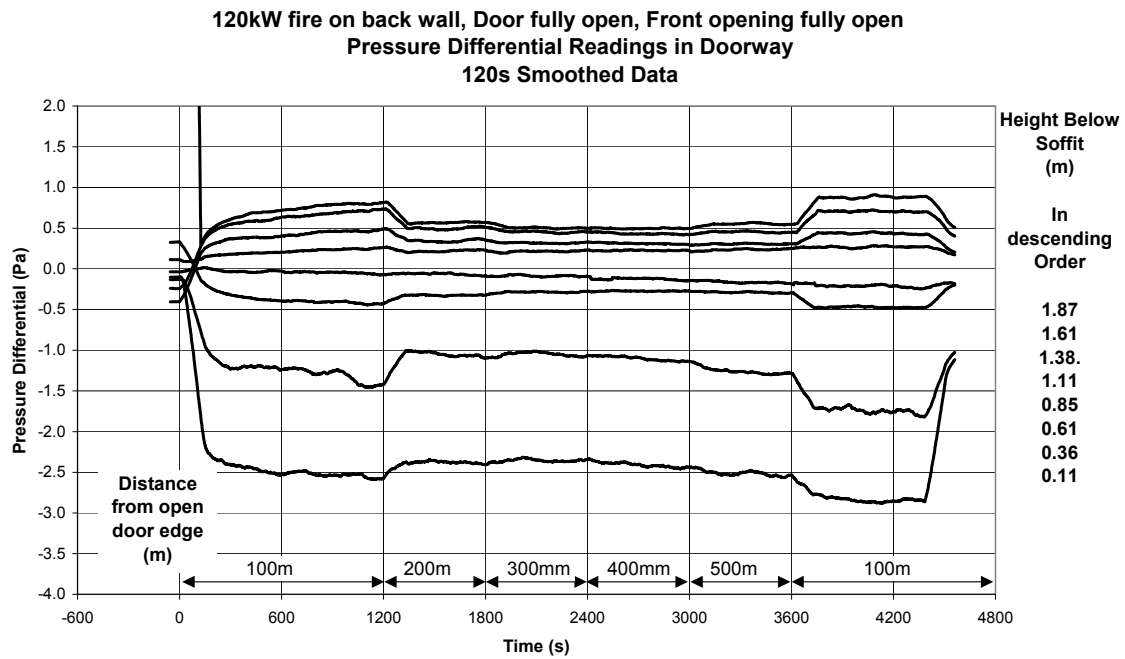


Figure A.10 Doorway pressure differential measurements for duration of experiment, 120kW fire on back wall, fully open door, front opening fully open, 120s smoothed data

Table A.5 Comparison of temperature measurements for aspirated and bare wire thermocouples, 120kW fire on back wall, fully open door, front opening fully open

<i>Height below Soffit (m)</i>	<i>Aspirated Thermocouple (°C)</i>	<i>Bare wire Thermocouple (°C)</i>	<i>Difference (°C)</i>	<i>% Difference</i>
0.11	239.7	199.3	40.3	17
0.36	217.4	173.0	44.5	20
0.61	83.5	104.3	20.8	-25
1.38	28.9	81.4	52.5	-181
1.61	27.1	70.2	43.0	-158
1.87	26.9	53.6	26.7	-99

## Appendix B

This appendix contains the raw data for the experiments performed with the door partially open as discussed in section 5 of this report

### B.1 Front opening fully open

#### B.1.1 Door at 20°

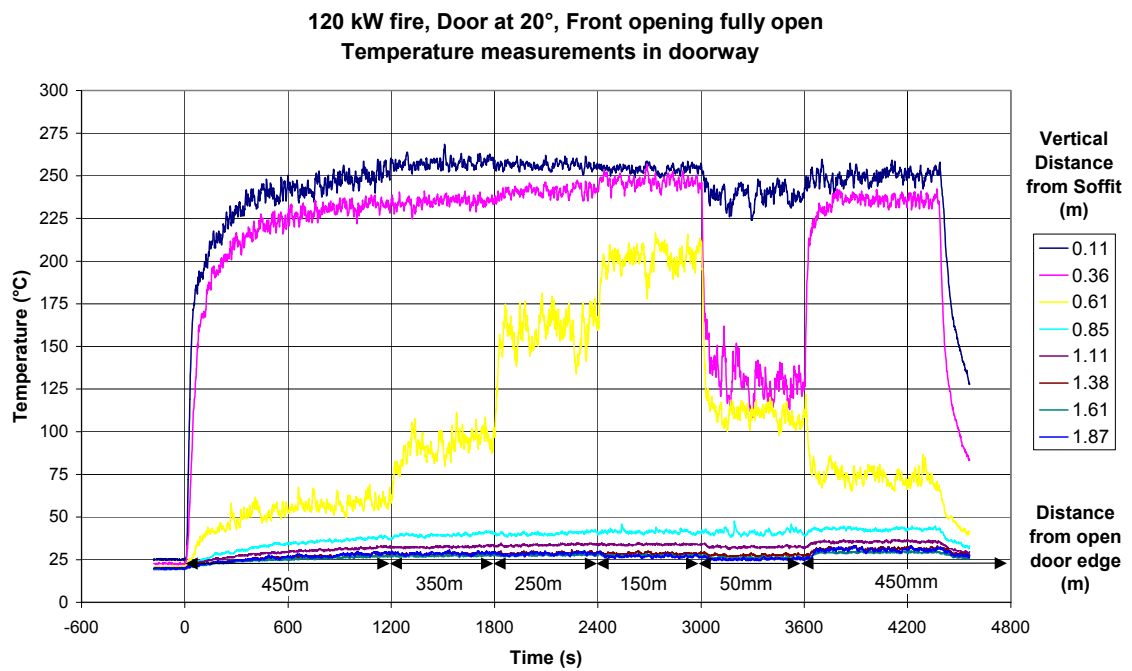


Figure B.1 Doorway temperature measurements for duration of experiment, 120kW fire in centre of compartment, door at 20°, front opening fully open

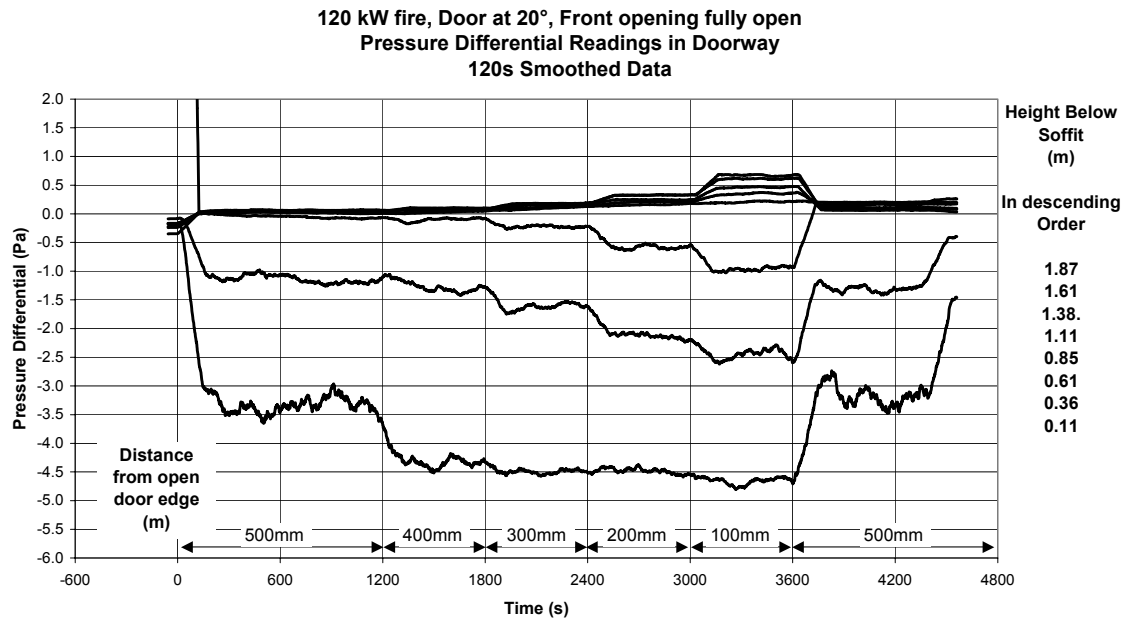


Figure B.2 Doorway pressure differential measurements for duration of experiment, 120kW fire in centre of compartment, door 20° open, front opening fully open, 120s smoothed data

Table B.1 Comparison of temperature measurements for aspirated and bare wire thermocouples, 120kW fire in centre of compartment, door 20° open, front opening fully open

<i>Height below Soffit (m)</i>	<i>Aspirated Thermocouple (°C)</i>	<i>Bare wire Thermocouple (°C)</i>	<i>Difference (°C)</i>	<i>% Difference</i>
0.11	270.1	249.3	20.8	8
0.36	239.8	231.3	13.0	4
0.61	36.6	75.7	39.3	-107
1.38	18.0	42.7	24.7	-137
1.61	18.5	35.4	16.9	-92
1.87	17.9	31.2	13.3	-75



### B.1.2 Door at 30°

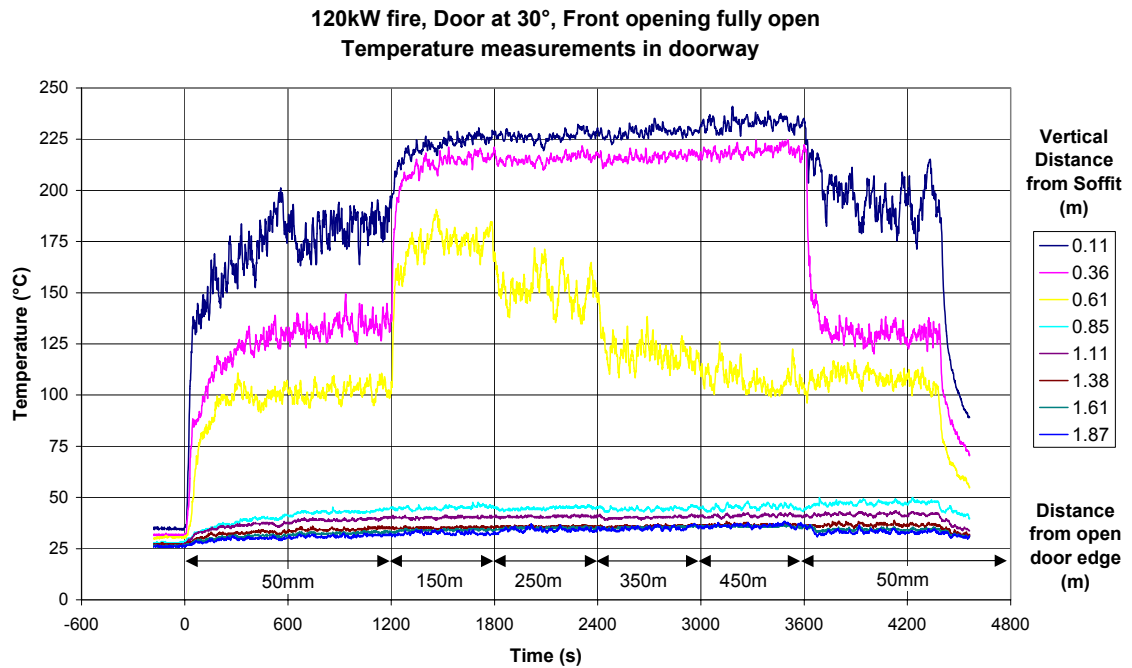


Figure B.3 Doorway temperature measurements for duration of experiment, 120kW fire in centre of compartment, door at 30°, front opening fully open

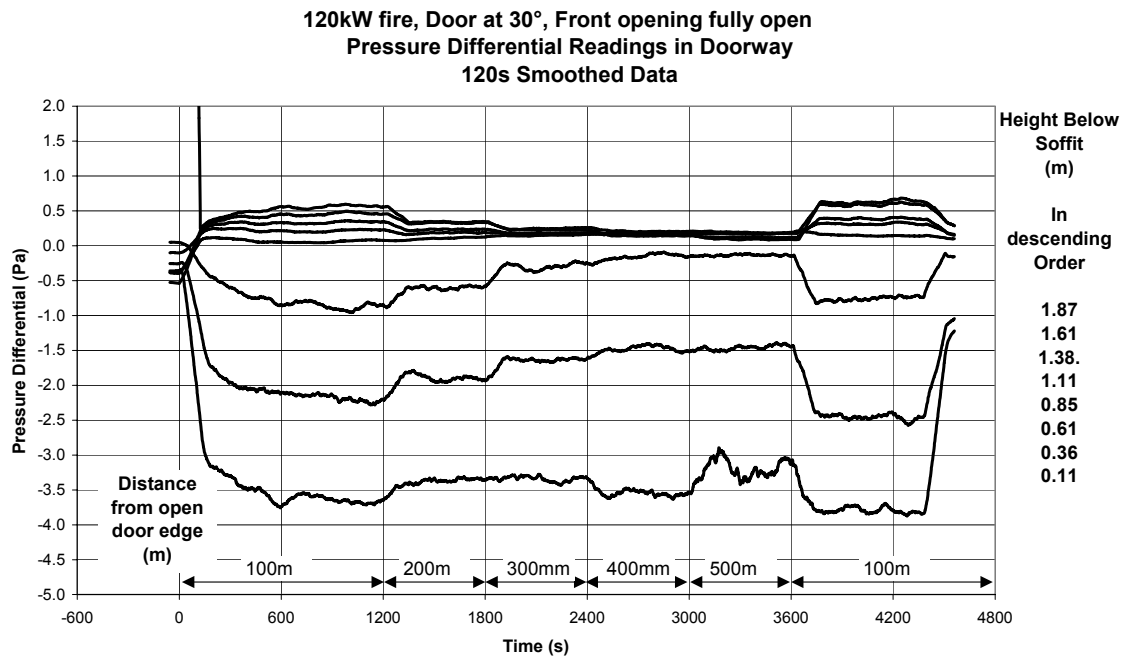


Figure B.4 Doorway pressure differential measurements for duration of experiment, 120kW fire in centre of compartment, door 30° open, front opening fully open, 120s smoothed data

Table B.2 Comparison of temperature measurements for aspirated and bare wire thermocouples, 120kW fire in centre of compartment, door 30° open, front opening fully open

<i>Height below Soffit (m)</i>	<i>Aspirated Thermocouple (°C)</i>	<i>Bare wire Thermocouple (°C)</i>	<i>Difference (°C)</i>	<i>% Difference</i>
0.11	244.1	198.8	45.3	19
0.36	241.1	135.3	105.7	44
0.61	133.0	108.6	25.1	18
1.38	25.7	47.0	21.3	-83
1.61	24.2	41.7	17.4	-72
1.87	23.5	36.6	13.1	-55

### B.1.3 Door at 40°

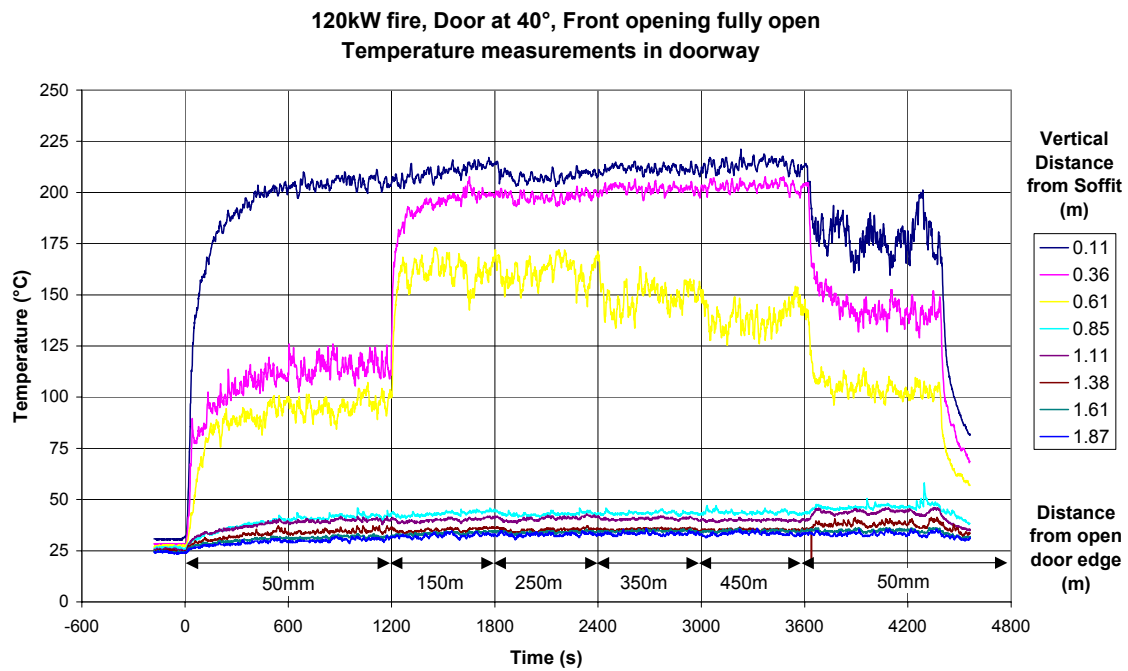


Figure B.5 Doorway temperature measurements for duration of experiment, 120kW fire in centre of compartment, door at 40°, front opening fully open

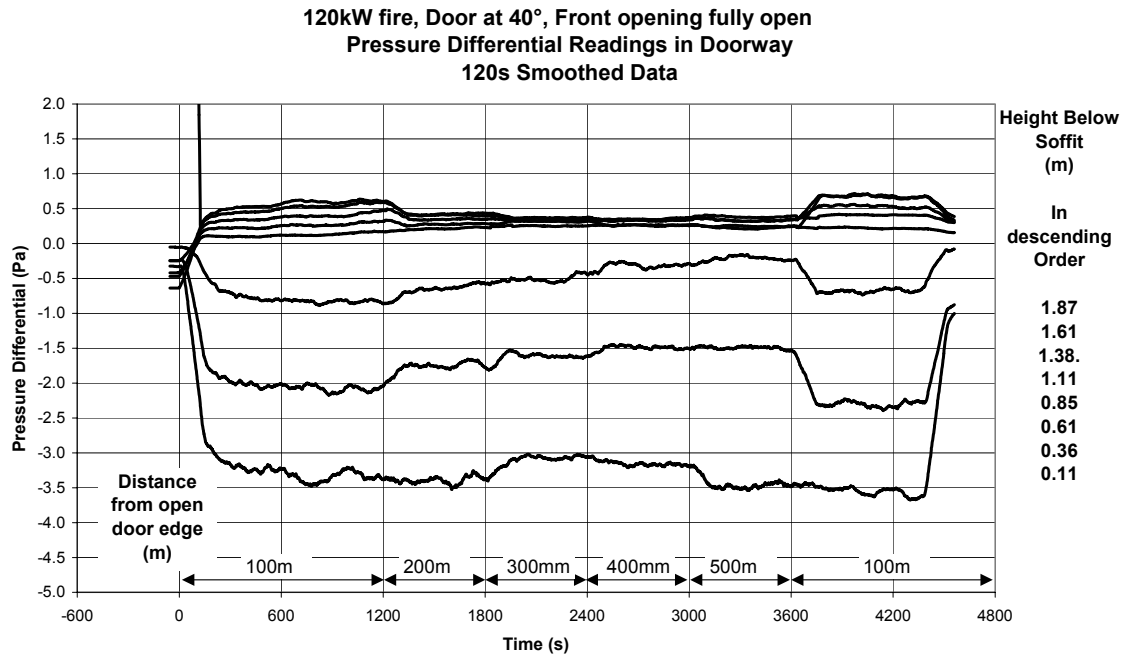


Figure B.6 Doorway pressure differential measurements for duration of experiment, 120kW fire in centre of compartment, door 40° open, front opening fully open, 120s smoothed data

Table B.3 Comparison of temperature measurements for aspirated and bare wire thermocouples, 120kW fire in centre of compartment, door 40° open, front opening fully open

<i>Height below Soffit (m)</i>	<i>Aspirated Thermocouple (°C)</i>	<i>Bare wire Thermocouple (°C)</i>	<i>Difference (°C)</i>	<i>% Difference</i>
0.11	222.4	179.5	42.9	19
0.36	222.6	148.3	74.3	33
0.61	154.6	107.0	47.9	31
1.38	24.4	46.1	21.7	-89
1.61	23.5	43.8	20.3	-87
1.87	23.2	38.0	14.8	-63

## B.1.4 Door at 60°

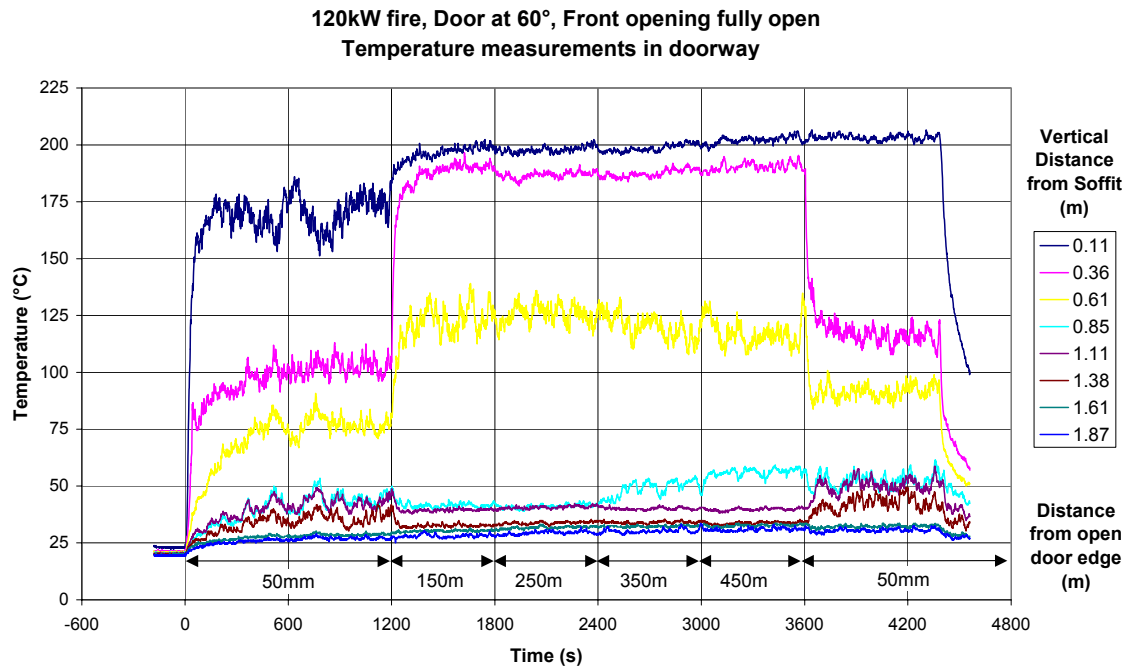


Figure B.7 Doorway temperature measurements for duration of experiment, 120kW fire in centre of compartment, door at 60°, front opening fully open

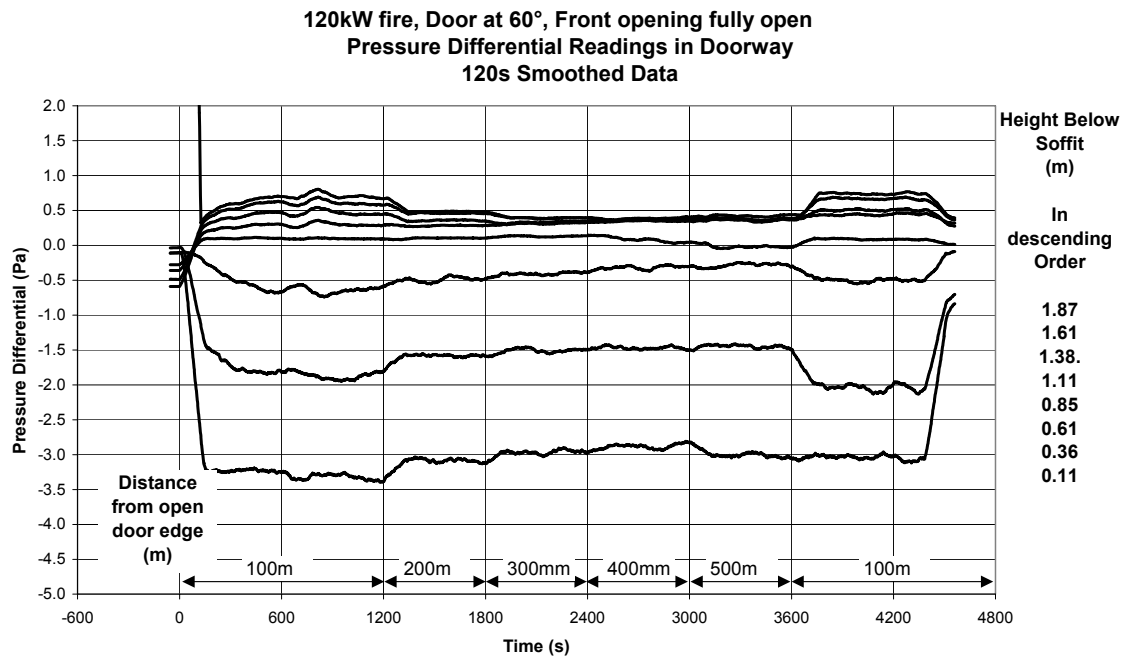


Figure B.8 Doorway pressure differential measurements for duration of experiment, 120kW fire in centre of compartment, door 60° open, front opening fully open, 120s smoothed data

Table B.4 Comparison of temperature measurements for aspirated and bare wire thermocouples, 120kW fire in centre of compartment, door 60° open, front opening fully open

<i>Height below Soffit (m)</i>	<i>Aspirated Thermocouple (°C)</i>	<i>Bare wire Thermocouple (°C)</i>	<i>Difference (°C)</i>	<i>% Difference</i>
0.11	216.0	203.3	12.8	6
0.36	204.0	120.0	84.0	41
0.61	108.2	91.7	17.0	15
1.38	21.6	52.0	30.4	-140
1.61	20.8	49.5	28.7	-138
1.87	20.8	42.1	21.2	-102

## B.2 Front opening as door

### B.2.1 Door at 20°

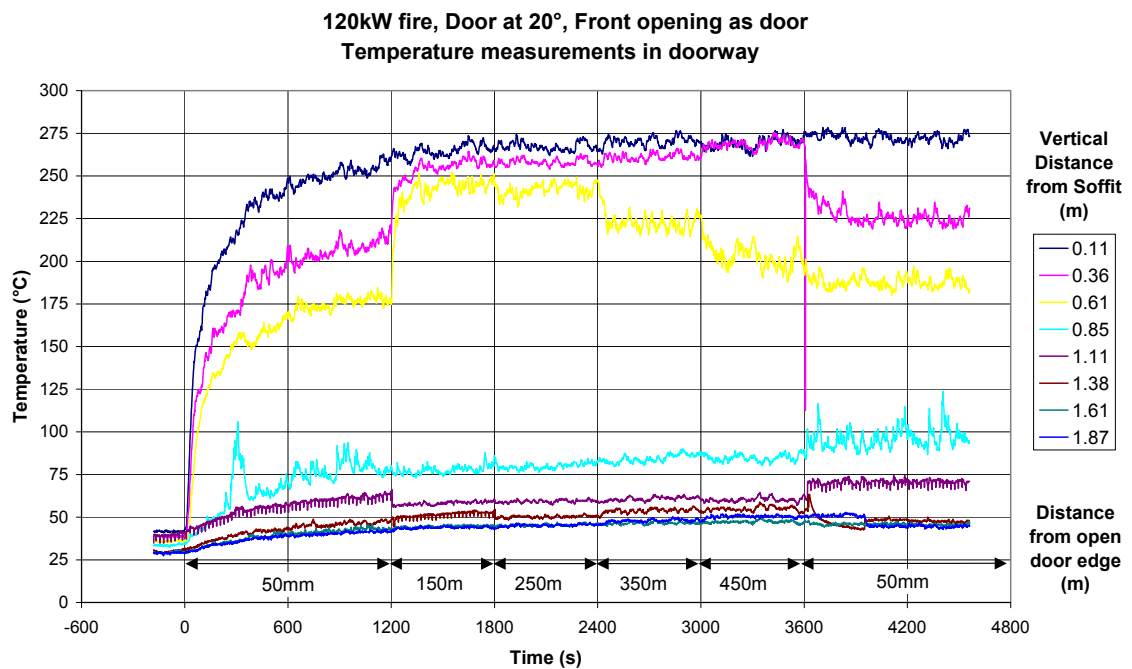


Figure B.9 Doorway temperature measurements for duration of experiment, 120kW fire in centre of compartment, door at 20°, front opening as door

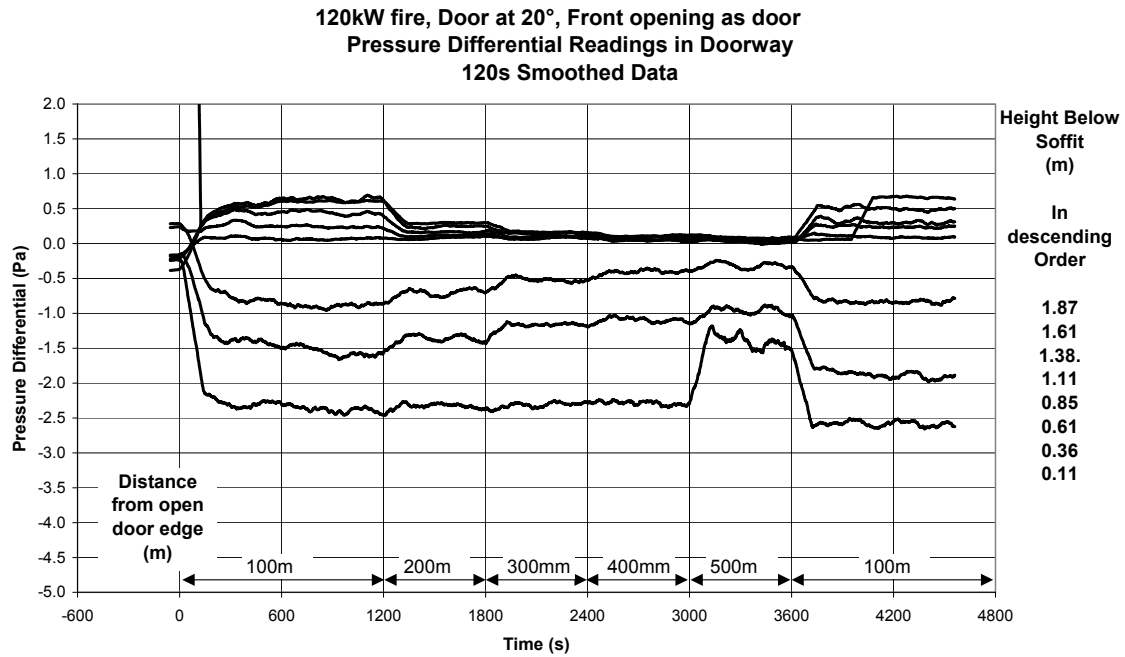


Figure B.10 Doorway pressure differential measurements for duration of experiment, 120kW fire in centre of compartment, door 20° open, front opening as door, 120s smoothed data

Table B.5 Comparison of temperature measurements for aspirated and bare wire thermocouples, 120kW fire in centre of compartment, door 20° open, front opening as door

<i>Height below Soffit (m)</i>	<i>Aspirated Thermocouple (°C)</i>	<i>Bare wire Thermocouple (°C)</i>	<i>Difference (°C)</i>	<i>% Difference</i>
0.11	286.0	273.0	13.1	5
0.36	291.1	228.6	62.5	21
0.61	246.4	188.0	58.4	24
1.38	38.7	95.2	56.5	-146
1.61	36.5	70.4	33.9	-93
1.87	35.4	47.9	12.5	-35

## B.2.2 Door at 30°

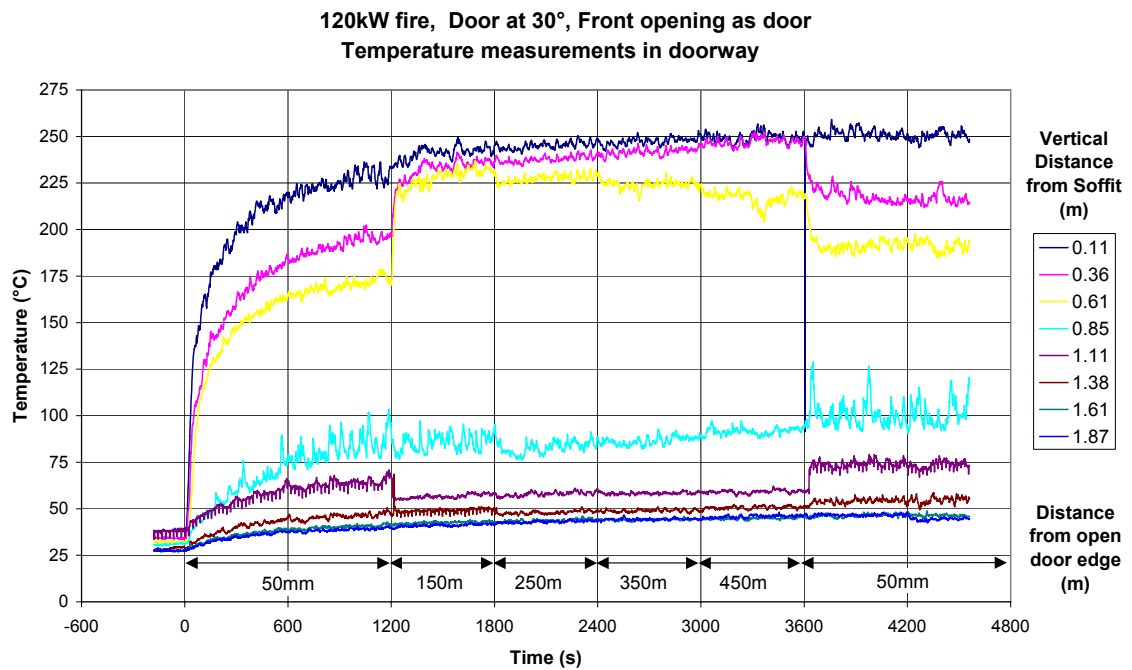


Figure B.11 Doorway temperature measurements for duration of experiment, 120kW fire in centre of compartment, door at 30°, front opening as door

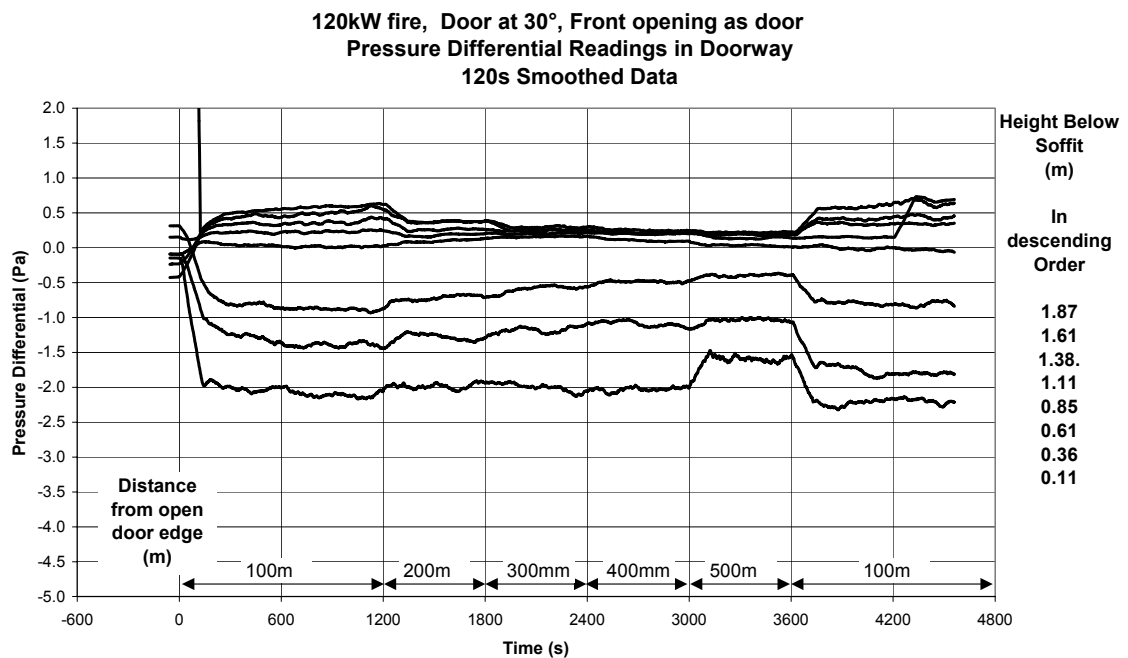


Figure B.12 Doorway pressure differential measurements for duration of experiment, 120kW fire in centre of compartment, door 30° open, front opening as door, 120s smoothed data

Table B.6 Comparison of temperature measurements for aspirated and bare wire thermocouples, 120kW fire in centre of compartment, door 30° open, front opening as door

<i>Height below Soffit (m)</i>	<i>Aspirated Thermocouple (°C)</i>	<i>Bare wire Thermocouple (°C)</i>	<i>Difference (°C)</i>	<i>% Difference</i>
0.11	259.0	250.9	8.1	3
0.36	268.2	219.2	49.0	18
0.61	252.7	192.4	60.3	24
1.38	37.8	100.7	62.9	-167
1.61	33.9	73.4	39.6	-117
1.87	33.0	54.0	21.0	-64

### B.2.3 Door at 40°

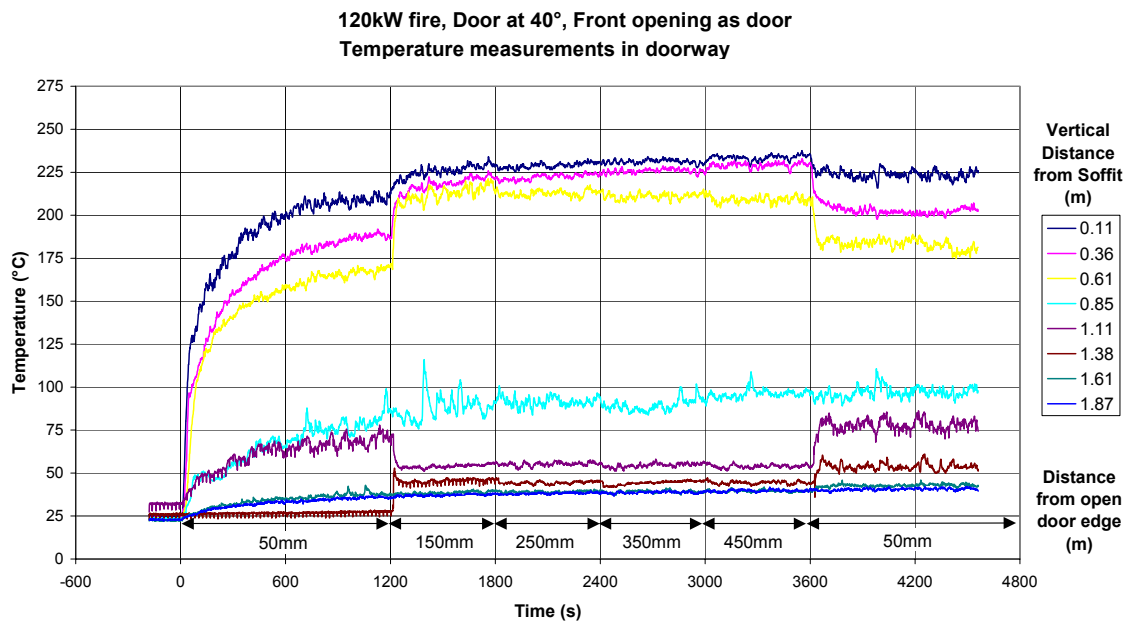


Figure B.13 Doorway temperature measurements for duration of experiment, 120kW fire in centre of compartment, door at 40°, front opening as door



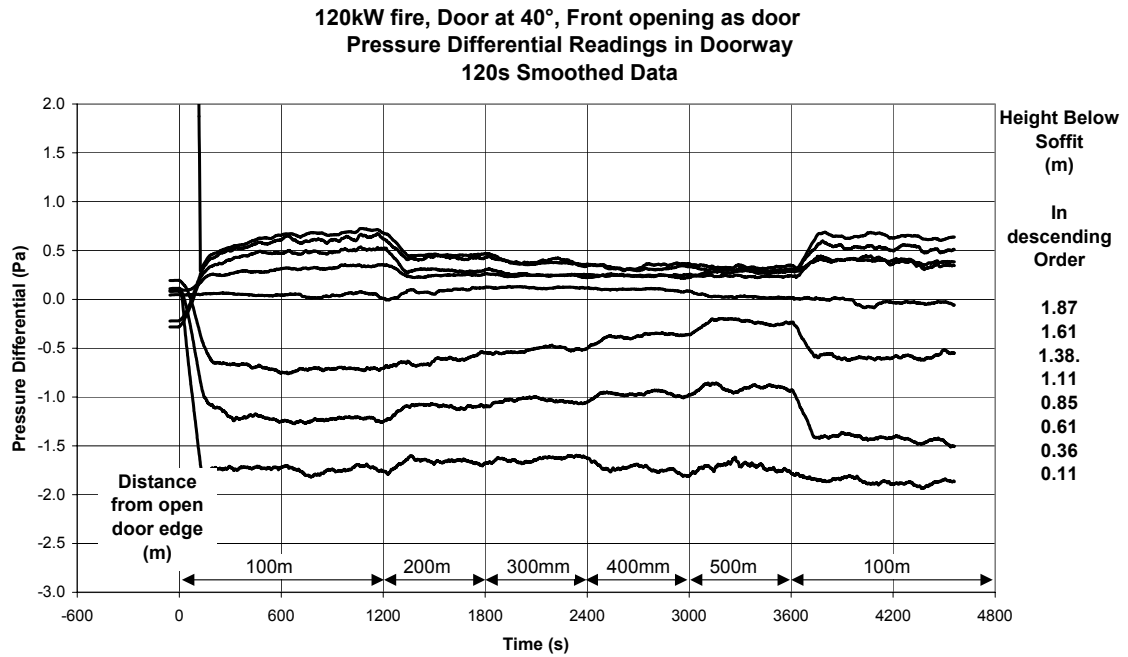


Figure B.14 Doorway pressure differential measurements for duration of experiment, 120kW fire in centre of compartment, door 40° open, front opening as door, 120s smoothed data

Table B.7 Comparison of temperature measurements for aspirated and bare wire thermocouples, 120kW fire in centre of compartment, door 40° open, front opening as door

<i>Height below Soffit (m)</i>	<i>Aspirated Thermocouple (°C)</i>	<i>Bare wire Thermocouple (°C)</i>	<i>Difference (°C)</i>	<i>% Difference</i>
0.11	239.1	224.2	15.0	6
0.36	250.5	204.1	46.4	19
0.61	236.9	185.2	51.7	22
1.38	33.0	96.6	63.6	-193
1.61	28.2	76.9	48.7	-172
1.87	27.9	53.2	25.3	-90